

50X1-HUM

Page Denied

Next 7 Page(s) In Document Denied

THE AURORA AND THE AIRGLOW

V.I. KRASCOVSKY

Institute of atmospheric Physics, Academy of
Sciences, USSR, Moscow

Principal facts on the aurora and related airglow are described. The paper contains some critical remarks and outlines the necessary objectives of further research.

It is generally recognized that emissions of upper atmosphere are caused mainly by three factors. Firstly, by various chemical reactions. Secondly, by the excitation of molecules and atoms of atmosphere in the process of colliding with other energetic neutral and charged particles. And thirdly, by fluorescence of some atoms and molecules of atmosphere, including metastable particles, in sun's irradiation. The most intensive emissions of upper atmosphere are observed during the aurora. High sensitivity of modern spectrographic and electro-photometric apparatus makes it possible to register typical emissions of very weak auroras which can be neither observed visually nor photographed. The number of such auroras is much greater compared with those detectable visually or photographically. They are observed not only in high-latitude areas but in low-latitude and equatorial areas as well [1, 2, 3, 4]. It is not improbable that the introduction of electrophotometric and spectrographic apparatus of higher resolving power sensitivity

- 2 -

will make aurores a usual phenomenon easily observed in all regions, and the attribute "polar" is then certain to lose its absolute meaning.

So far the main data on aurora have been obtained by means of ground observations at night in visible and near ultraviolet and infrared areas of the spectrum

[4, 5, 6, 7]. Highly desirable data on emissions which do not penetrate the earth's atmosphere could be obtained with the help of rockets and sputniks. Unfortunately, little has been done in this respect. The absence of regular data on aurores in the day-time is also a considerable disadvantage. The prospects for the use of rockets and sputniks in order to eliminate the masking background of diffuse atmospheric light are very attractive. However, these possibilities remain absolutely unexploited.

The phenomenon of aurora is associated with additional ionization of upper atmosphere. If the energy level of the exciting agent is higher than the ionization potential of atmospheric molecules and atoms, the optical excitation is always accompanied by ionization. This ionization can be detected with the help of ground radiolocation of aurora [8, 9].

The picture of the distribution of ionization and radiance is in general rather consistent especially if we have in mind the geometrical conditions of radioreflections and the fact that the average life of excited atoms and molecules responsible for radiance is much shorter than

- 3 -

the average life of ionization which ensures the diffusion of electrons and ions from the place of their origin to the neighbouring regions of the space. If an exciting agent which is able to penetrate below the 100 km level appears during aurora, the ionization of this area is accompanied by additional absorption of radiowaves both from terrestrial and space sources [4, 5, 10].

The ground observations have shown that spectra of aurora, apart from absolute intensity, are characterized in the first place by the relative content of atomic and molecular emissions. This ratio is highly variable and evidently reflects the depth of penetration of the exciting agents into the earth's atmosphere. The deeper is this penetration, the more intensive are the molecular bands and the weaker are atomic emissions, especially from metastable states. The energy of the highest levels of radiating particles is another characteristic feature of emissions of aurora. During many aurores high levels are excited with an energy of tens of ev. It is natural that such excitation is accompanied by intensive ionization of the atmosphere. It happens, however, that spectra of aurora display abnormally intensified metastable emissions of atomic oxygen and nitrogen 6300 Å and 5200 Å (excitation energy 1.96 and 2.35 ev respectively), sometimes even without traces of other emissions from higher excited levels,

- 4 -

for example, even without increased metastable emission of oxygen 5577 Å (excitation energy 4.06 ev). And finally, the most remarkable feature of the spectra of aurora is the presence or absence of hydrogen emission with a wide spectral contour. Whenever the radiation proceeds from the magnetic zenith the contour of such emission is always shifted to the short-wave part of the spectrum. The wide contour of hydrogen emission can be most easily explained by the penetration into atmosphere of comparatively soft protons with a rather stable wide interval of velocity. The most frequently encountered velocity corresponds to an energy of about several hundreds ev [7, 11]. Only in several cases has a contour corresponding to about 100 ev been observed [12, 13]. The most intensive hydrogen emission with a wide contour is more often observed in spectra of atomic type though very often it is not observed there at all. It is necessary to point out, however, that radiation of the night sky is always accompanied by weak hydrogen emission H λ with a very narrow contour which corresponds to hydrogen atoms with an energy which does not exceed several tens of ev [4]. The origin of this emission is not completely understood yet. When aurora appear in a sunlit area they are supplemented with fluorescent emissions of the ionized nitrogen molecule and metastable orthohelium atoms [4, 14].

- 5 -

These peculiarities of spectra of aurores enable the conclusion to be made that in some cases, but by no means always, emissions of aurores can be excited by fast protons. It is interesting to note that at this time some relative weakening of the Meinel system of the ionized nitrogen molecule and some relative intensification of the emission of ionized nitrogen about 5004 Å are observed. The same peculiarities are observed in experimentally produced spectra with similar exciting agents. When very fast protons are able to penetrate into lower areas of atmosphere with molecular composition, hydrogen emission may be hidden from observation because of intensive blinding with bands of neutral and ionized nitrogen molecules. When hydrogen emission with a wide contour is absent aurora can be excited by fast electrons. The energy of primary protons and electrons responsible for aurora can be determined approximately by the lower margin of glow. In order to penetrate into the atmosphere below 200 km the primary proton should have an energy exceeding 0,5 kev, the primary electron only above 20 ev. In order to penetrate below 100 km the energy thresholds exceed 200 kev and 10 kev respectively. Emissions of atomic type are usually observed at heights exceeding 200 km. The lower border of some aurores lies lower than 100 km.

Some American scientists have used rockets to

- 6 -

investigate corpuscles which cause aurora at heights below 200 km [15, 16, 17, 18]. They have discovered electrons with energies of several kev and protons with energies of hundreds of kev. As far as electrons are concerned these energy data agree with the results of ground observations. As to protons, however, their energy estimates are much higher than the low ones which were expected according to the observed Doppler shift towards the short-wave part of the spectrum. It is quite possible that the observed protons did not cause aurora; the latter were then excited by protons with energies of several hundred ev which were not registered by the apparatus used. Apparently additional investigations should be undertaken to collect more reliable data.

The above-mentioned investigations have made it possible to establish a certain relationship between the radiance of aurora and primary corpuscles [18]. Thus it has been estimated that about 0,1 % of the primary energy of corpuscles turn into visible radiation. It is desirable, however, to know this value more exactly as a function of the height of radiance taking into account the back flux of corpuscles reflected from the geomagnetic field. It is very important to investigate simultaneously the energy lost on ionization, and the radiation in spectrum regions inaccessible for ground observations.

- 7 -

It is necessary to note, however, that the investigations which have been accomplished, are not sufficient for conclusive determination of the nature of the initial exciting agent of polar lights. Since various mechanisms of the generation of corpuscles in the earth's exosphere itself are being discussed, it is impossible to deny unconditionally the existence of a corpuscular flux consisting of atmospheric ions (N_2^+ , N^+ , O_2^+ , O^+ , NO^+ , Ar^+ , He^+). Besides Shklovsky admits the penetration into the Earth's atmosphere of neutral hydrogen atoms which are formed in the interplanetary space during the re-charge and neutralization of protons of primary corpuscular fluxes [19]. This process should augment in a medium filled with micrometeorites. As to electrons with an energy of several kev the excitation of radiance should not be attributed only to primary electrons. It can be caused by secondary electrons which appear during atmosphere ionization by primary electrons. Secondary electrons may possess an energy of several tens of ev and, mixing with thermal electrons of the upper atmosphere, form a surplus of primary electrons as compared with the value which follows from purely Maxwell distribution.

It is necessary to note that the energy of corpuscles (protons and electrons) found in the upper atmosphere does not correlate with the delay time of the beginning of geomagnetic storms in relation to the appearance of

- 8 -

active formation in the Sun. This is a convincing proof that corpuscles which cause aurora are not primary solar corpuscles but originate in the terrestrial exosphere as a result of some complex processes of interaction with corpuscular fluxes of the Sun. Of great interest is the abnormal intensification of metastable emissions of oxygen and nitrogen atoms 6300 \AA and 5200 \AA with a low excitation potential (1.96 and 2.35 ev respectively) without any significant intensification of the metastable emission of atomic oxygen (5577 \AA) with a slightly higher excitation potential (4.06 ev). Two mechanisms of such selective excitation of the abovementioned emission are possible in principle. First of all, it is excited by thermal electrons at a temperature of several thousand degrees K, which is insufficient for simultaneous excitation of the green emission of atomic oxygen. This temperature, however, is higher than the temperature of $1000\text{-}1200^\circ \text{ K}$ which is usually expected in the region of aurora. Another possibility is selective origination of these emissions resulting from chemical reactions, for example, in the process of dissociative recombination of ionized molecules of oxygen, nitrogen and nitrogen oxide [7]. However, when molecular emissions are absent and the intensity of the red emission of atomic oxygen is too high such a mechanism does not seem probable, for it is difficult to admit that there is a swift

- 9 -

and abundant upward entrainment of molecular ions formed below without the excitation of molecular emissions.

It is important to underline that corpuscles with energies above several ev cannot be agents of abnormal red emission of atomic oxygen 6300 Å . If these corpuscles were excitors of the above emission it would have inevitably resulted in other emissions corresponding to higher excitation. This is not observed, however.

To conclude our review of emissions of aurora we must point out that it is only the red emission of oxygen that can be somehow explained by chemical reactions, for example, in the process of dissociative recombinations of molecular ions. Such a mechanism, however, is of no use for explaining other emissions with a higher excitation potential. During the coruscation of aurora, in a period of time less than a second all the principal emissions, except the red oxygen one 6300 Å , have a synchronous development and equal relative depth of modulation. Since the time of ion recombination greatly exceeds a second this is possible only when the excitation of emissions is the result of either a direct impact of primary corpuscles or short-lived secondary electrons which have originated from them [4, 27].

We have suggested the idea of sporadic ionization and heating of the upper atmosphere with corpuscular fluxes and systems of ionospheric currents, assuming expansion of

- 10 -

the upper atmosphere as a result of heating [20, 21, 22, 23]. Some authors believe the heating to be the result of magnetic-hydrodynamic waves [24, 25]. It has already been found with the help of interferometers that during intensive aurores with abnormally intensified red emission of oxygen the width of its Doppler contour testifies to the rise in temperature. Temperatures reaching 3500° K [26] have been registered.

The heating is accompanied by an increase in the height of uniform atmosphere and by circulation and mixing. All this are satisfactorily confirmed with observations of intensive aurores. The upward movement of a great mass of nitrogen molecules results in an increase in the number of their ions there. They are easily observed beyond the Earth's shadow due to fluorescence which is sharply clearly seen thanks to well-developed bands from high vibrational levels of ions of molecular nitrogen. Thus, for example, on the 11th of February, 1958, when aurora were studied in Zvenigorod, at 30° to northern horizon, at altitudes of over 300 km there were about $5 \cdot 10^{11}$ ions of molecular nitrogen in the line of vision with the scale height of about 10^7 cm approximately corresponded to several thousand N_2^+ in cm^{-3} . It is necessary to remember that the detection threshold was about $5 \cdot 10^8$ ions of $N_2^+ cm^{-2}$

- 11 -

in the line of vision and that under usual conditions these ions could not be detected. During the aurora on the night from the 4th to the 5th of November, 1958, N_2^+ ions about two orders less in number were observed above the 500 km level.

Additional ionization and heating of the upper atmosphere can be attributed even to weak corpuscular fluxes and systems of ionospheric currents. The additional ionization, which was expected by us, could be the cause of disturbance of the uniformity of ionosphere and appearance of sporadic layers. Later some authors argues in favour of a more significant role of these processes [28, 29]. But such trend in the development of this idea encounters a very serious obstacle, i.e. the absence of significant emissions above 100 km. Some non-uniformities of radiation fields of the night sky may also be suspected as traces of corpuscular excitation. However, the final solution of the problem requires an accurate determination of heights of these additional radiations. It is highly important to carry out regular observations of the height of the initiation of emissions in ionosphere at different latitudes and in different parts of the day.

Systems of ionospheric currents are naturally associated with the existence of systems of electromotive forces. These systems must change movements and locations of the trapped corpuscles, especially, when energy of these corpuscles is small. The circulation of the ionized upper atmosphere

- 12 -

in the geomagnetic field may be one of the causes of the existence of systems of electromotive forces. When vertical electromotive forces of a definite direction develop, upward diffusion of molecular ions is possible. This phenomenon as well as the expansion of the upper atmosphere upon heating may lead to an extension of aurora in height. We have noticed that the development of aurora is accompanied at high altitudes not only by fluorescent emissions of ionized hydrogen molecules but also by emissions of metastable atoms orthohelium [4, 14]. In this connection it is interesting to note that as far back as 1952, Gartlein

[30] found that the appearance of nitrogen molecular emission originates somewhat later than the initiation of polar lights. And what is more, already in 1956 Gartlein explained the well-known phenomenon of the shrinking of the lower boundary and extent of aurora in height in the years of minimum solar activity as compared with active periods due to the diminution of the extent of the Earth's atmosphere in this period. [31].

The nature of polar ~~xx~~ lights varies considerably at different geomagnetic latitudes. We distinguish three principal types of polar lights with regard to latitudes :

- 1) polar area lights ;
- 2) usual high-latitude aurores;
- 3) low-intensity visually-unobservable lights of middle and equatorial latitudes.

- 13 -

Typical polar area lights are caused by protons of solar origin with an energy of several tens of Mev [32, 33, 34]. They reach the Earth in several tens of minutes to several hours after some chromospheric flares preceding the geomagnetic storm. These protons freely penetrate into polar areas approximately along Stoermer's trajectories and produce above them almost uniform scintillation of great extent. Since hard protons penetrate below the 100 km level the ionization which they create is accompanied by an intensive absorption of radiowaves, and the radiation contains intensive molecular bands which mask the hydrogen emission. Polar areas are very convenient for observing hard solar protons. Ground observations and those with the help of rockets and sputniks, even at short distances from the Earth, can provide extremely valuable data. Since it is sometimes conjectured that hard solar protons reach the Earth along magnetic lines of force which originate in the Sun some insignificant variations may be expected in latitudinal boundaries of lights due to different configuration of the cumulative magnetic field and corpuscular fluxes above the northern and southern polar areas.

Ordinary aurora are known to have the form of a halo around the geomagnetic poles at an average distance of about 23° . During geomagnetic storms zones of auroras extend and their center shifts toward low latitudes. A similar shift of a smaller extent is observed at evening

- 14 -

hours, reaching its peak at local midnight, whereas toward morning the motion is reversed. Radiance is highly non uniform with regard to latitude and longitude. The low-intensity diffuse glow usually spreads over vast surfaces, where sometimes additional sharply-outlined formations appear, such as arcs, strips, loops, spots, rays. The more concentrated, contrasted and less extended are these formations, the less stable they are. The sharply-outlined formations contain the smaller part of the auroral radiation, the greater part of which occurs in vast diffuse fields poorly visible because of the low contrast sensitivity of the human eye at low illumination [4, 35].

We wish to lay special emphasis on the above-mentioned facts for they are of great importance for general energetics of aurora because during recent years paramount importance has been attached only to visual and photographic observations of the most intensive, shortly defined areas of aurores.

Ray-like formations are especially interesting among the sharply-outlined forms. They appear from arcs and strips which become thinner and break up into separate elements. Separate little rays have different degrees of focusing. Some of them are only hundreds of meters in diameter. Such separate rays are very short-lived formations which exist less than one tenth of a second. When these thin rays are especially sharply focused they

- 15 -

usually flare at certain points forming sheaves (accumulation of thin rays) along some straight or curved lines the majority of which coincide with the geomagnetic parallel. When such rays are focused poorly their sheaves merge into one, practically non-scintillating column. Sheaves of sharply-outlined rays or solid columns are drifting along the geomagnetic parallel at colossal velocity both in the western and the eastern directions.

We observe drifts at 100 km height which sometimes reached a velocity of several km sec^{-1} [4]. Some authors, however, noted velocities reaching 20 km sec^{-1} [36]. The formations extending along the parallel sometimes have a wavy structure and form loops and little horseshoes. The latter, as a rule, are turned with their convex side eastward.

When we see ascafilms moving at a high speed vortical movements of radiant formations are observed [4, 37]. The pattern on aurores sometimes consists of numerous and diverse structural details and coruscates with very short periods from fractions of a second to several tens of seconds. Calm forms are usual at evening and morning hours, eruptive forms - at midnight. Some past observations of the minimums of solar activity showed that calm forms predominate at such periods. Mobile, sharply-outlined ray-like formations are sometimes accompanied by the so-called "weather-vane effect" [4]. As a result of the relative motion of the ray of the exciting agent and the atmosphere the front of the ray has

- 16 -

colours of low-inertia emissions, and areas behind the moving ray have colours of inertial emissions.

It was already shown in Strömer's classical works [6] that, in the sunlit zone, rays appear on the extension of geomagnetic lines which cross rays in unlit atmosphere. Thus the ray weakens, as it were, beginning with its lower boundary, and then dies out, but begins to glow again on the boundary of the night shade. This additional glow can be explained by fluorescence in solar radiation of ionized nitrogen molecules which reach very great heights along geomagnetic lines. We succeeded, however, in discovering a somewhat different phenomenon [4.] It consists in the fact that a ray in full darkness at some distance from the lower boundary almost suddenly decreases its brightness several times and sometimes even more than by one order. Sometimes rapidly moving sharply intensified clots appear in the ray. It appears that such luminiscence details are due to streams or currents of the gas which rich in effectively excited molecules and flow in the dissociated area of the upper atmosphere. This presents an extensive field of investigation by direct sounding of the upper atmosphere.

During the development of ray structures the absorption of radiowaves in the layer D below these structures increases drastically. This shows that either harder cor-

- 17 -

puscles or X-rays develop at this time (which penetrate into the lower areas of the atmosphere) due to harder electrons appearing in the area of lights [4, 38, 59].

During geomagnetic storms the width of the band of polar lights becomes much greater. Emissions of polar lights can be detected even visually at a distance of thousands, sometimes even several thousand kilometers from the most intensive areas. Fields of hydrogen emission are more diffusive and uniform than emission fields without hydrogen emission. Maximum intensity of the former lies in more low-latitude areas than maximum intensity of the latter. However, the fields of the latter penetrate into low latitudes much deeper than those of the former. Thus, as a rule, the former are generally framed with the latter on the side of both high and low latitudes. In sharply-outlined forms of aurora, including ray-like ones, no intensification of hydrogen emission is observed [4, 39]. Some investigators point out that fields of hydrogen emission even avoid locations of sharply-outlined forms [40]. It must be noted too that beyond the area of maximum intensity atomic emissions predominate, this fact showing that either the corpuscles are more short-range or the atmosphere height in the area of maximum intensity becomes greater due to intensive heating. Aurora and hydrogen

- 18 -

emission often appear in usual polar zones even on magnetically calm days with high and zero K-indices, including years of minimum solar activity.

During geomagnetic perturbations only the development of intensive emissions over greater Earth's areas becomes more probable. Low-intensity visually-observed arc-shaped radiances have been recently observed by Barbier and Roch [1,2] at low latitudes. They result from insignificant intensification of the red forbidden emission of oxygen 6300 Å. Recently Trutze [3] has been trying to find such formations in the Ashkhabad region (Turkmenian SSR). He has not found solid arcs, but observed separate spots in the red and green forbidden emissions of oxygen, which do not coincide. Low-latitude red arcs and spots are a new and little-known phenomenon. The sporadic non-uniformity of additional ionization of the upper atmosphere should probably be included in similar phenomena.

We have dealt, hitherto, mainly with processes within the area of the observed aurores. It is not less interesting, however, to investigate higher areas of the upper atmosphere from which corpuscles causing lights penetrate downwards. In May, 1958, we made an attempt, with the help of the third Sputnik, to find fluxes of geomagnetic corpuscles slightly above the area of aurores [21, 22, 23, 24]. This attempt was successful. It was for

- 19 -

the first time that at an altitude of 1000 - 2000 km fluxes of electrons were discovered with an energy of about 10 kev. Namely, they were electrons which are the most responsible for aurores. But they were not hard corpuscles of radiation belts. Their flux exceeded $10^{10} - 10^{12}$ particles $\text{cm}^{-2} \text{ sec}^{-1}$. It was found that though the direction of most electrons of such fluxes is nearly perpendicular to geomagnetic lines, the direction of some of them coincides with these lines. Similar fluxes were later observed by other scientists [41, 42, 43, 44]. It is especially interesting that O'Brien and Laughlin, having found such intensive fluxes at an altitude of 1000 km, did not find them in the equatorial plane at a distance of several terrestrial radii [44]. According to ground observations, corpuscles which are responsible for aurora, as we have pointed out many times, have moderate energies. Since the period of drift of such particles around the Earth is long as compared with their lifetime, we expected that they would form only separate fibres around geomagnetic lines [5, - 20]. However, we did not admit that such particles form radiative zones.

It is difficult to interpret the drift of rayed structures as a drift of compact clots of corpuscles in a geomagnetic field because of the enormous velocity and different directions of the drift. This requires rejection

- 20 -

of the dipole field and assumption that in the equatorial plane at a distance of several terrestrial radii there are very complex magnetic fields of varying intensity. Besides, though aurora around the northern and southern poles are generally more or less simultaneous and conjugated, the similarity of their detailed structure is not yet proved [45, 46].

Outwardly separate thin rays rather resemble some discharge along geomagnetic lines. It is not surprising that only recently aurora were generally interpreted as a gas discharge. It was also suggested that the drift of electrons and protons in different directions results in the development in the exosphere of electric fields which affect the structure of aurora [60].

Since 1957, at first with the help of Geiger counters, an accumulation of hard charged particles which formed stable radiative zones was found in the geomagnetic field [47, 48]. Though, in contradistinction to our experiment, it was impossible to ascertain unambiguously the presence of kev electrons with the help of Geiger counters, nevertheless, the data obtained with such counters were interpreted as the result of the effect of X-rays from electrons with energies of tens of kev upon Geiger counters enclosed in sputnik shells. It was also assumed that fluxes of such electrons reached $10^{11} - 10^{12}$ particles $\text{cm}^{-2} \text{ sec}^{-1}$. Later Gringaus, Kurt, Morez and Shklovsky 49

- 21 -

on the basis of data obtained by means of ion traps, found that near the equatorial plane, at a distance of several radii of the Earth, the intensity of electron fluxes was about 3 orders less than had been expected. Later this fact was confirmed by O'Brien, Van Allen and Frank [50]. At the same time Gringaus, Kurt, Moroz and Shklovsky found small electron fluxes with individual electron energies exceeding 200 ev near the equatorial plane at a distance of about 10 Earth radii. The registered flux did not exceed 10^8 particles $\text{cm}^{-2} \text{ sec}^{-1}$. The authors thought that they had found a new radiation belt. Not so long ago Davis discovered in the geomagnetic field an intensive accumulation of protons with energies of 0.1 to 4 Mev [51]. In the end it became evident that the entire space in the geomagnetic field is filled with various charged particles with different energies. Confident distinction of separate radiation belts there becomes conditional. Instead of the former "belt" the terms "inner" and "outer" zones become more and more popular for they reflect the nature of the fact more exactly.

Radiation belts appear as continuous, non-discrete in longitude accumulations of charged particles trapped by the geomagnetic field, whose lifetime greatly exceed one circular drift around the Earth. According to these notions,

- 22 -

particles with a pitch-angle of about 90° located near the equatorial plane are the most stable ones. As these angles decrease, particles undergo deeper oscillations along the geomagnetic lines, their lifetime becoming much shorter. As a result of this, the density of particles near the equatorial plane is much higher than near polar areas. When such conjecture became widely popularised it was hoped that aurora are a stage in the disintegration of radiation belts. The present factual data, however, make such hopes rather doubtful.

The intensity of the hard particle flux in radiation belts near the equatorial plane during the maximum radiance of intensive aurora, which accompany geomagnetic storms, is decreased and is restored only after this aurora cease to exist [52].

However, the energy content in radiation belt cannot provide for auroral lights even if they take place at a magnetically - calm period. All this is redebuted during the existence of ray-shaped structures with a sharply increased lights density.

We shall cite some examples characterising the intensity of aurores. When determining the intensity of aurora we assume that about $3 \cdot 10^{-3}$ parts of the total energy of corpuscles having individual energies of about 10^{-8} erg turn into visible radiation of aurora. On the

- 23 -

5th of November, 1956, in Murmansk, at 18 hours universal time, we observed the aurora for half an hour, the universal index K being about 1, which had the form of a spiral with numerous twists and diffuse radiance which covered an area from 10^{16} cm² from the western horizon to 45° of the eastern zenith distance. The westward extent of the aurora beyond the horizon is not known. This aurora produced illumination of the Earth's surface which exceeded the illumination of the full Moon, i.e. not less than 0.1 erg cm⁻² sec⁻¹. Thus, an energy exceeding $5 \cdot 10^{20}$ erg was released during half an hour. Such aurorae could be produced by a flux of electrons with an individual energy of 10 kev, exceeding $5 \cdot 10^9$ particles cm⁻² sec⁻¹. On the 11th of February, 1958, after midnight universal time, one of most spectacular polar lights in recent times were observed. The universal index K reached 9. The lights spread probably over at least 50 % of the Earth's surface. The intensity of visible illumination on the Earth's surface was not less than 1 erg cm⁻² sec⁻¹. These lights continued for several hours. They were observed above America longer than in our country, with an intensity two orders higher than the one mentioned above. Thus, during this event energy release in the Earth's atmosphere only during 1 sec would exceed 10^{21} erg. It means that an electron

- 24 -

flux with an energy of 10 kev on an average could reach $5 \cdot 10^{10}$ particles $\text{cm}^{-2} \text{ sec}^{-1}$. Even assuming that our estimate is exaggerated and should be decreased by several orders, it is all the same evident that the energy content in radiation belts is not sufficient for such immense energy releases.

O'Brien, Van Allen, Roch and Gartlein found increased intensity of hard particles above red low-latitude arcs [53]. Such discovery, however, cannot be considered as the proof that red arcs are provoked by hard particles dumping from the radiation belt. If these arcs were provoked by such particles, then, as has already been mentioned, the red emission of atomic oxygen would, no doubt, be supplemented by other emissions corresponding to a higher excitation potential. The peculiarities of the irradiation of red arcs show that it is the result of either the high temperature of ionosphere or selective chemical reactions of ions which are carried up with the upward current of air. So in both cases the swelling of the atmosphere in the red arc area is postulated. In addition to this, the above processes may induce an electromotive force. All this taken separately and in combination, may stimulate dumping of hard particles from the radiation belt. It is interesting to note that King and Roch [54] report lower density of electrons within the red arc area which probably proves that there ionosphere

is higher.

The same considerations as affect the inner belts show that the new, outermost radiation belt suggested by Gringaus, Kirt, Morez and Shklovsky cannot be the cause of aurora either. This belt is supposed to lie in the zone of the interaction of interplanetary plasma or "solar wind" and the Earth's geomagnetic field where the geomagnetic dipole field is seriously distorted [55, 56]. Therefore it is far from clear whether the drift of charged particles around the Earth exists and whether they surround the Earth with a continuous belt. It cannot be doubted that the appearance of energetic particles in this area is unambiguous evidence of the interaction of the interplanetary plasma or "solar wind" with the geomagnetic field. But this accumulation of energetic charged particles may belong not to the terrestrial exosphere but to interplanetary plasma or "solar wind" which flows round the geomagnetic field, i.e. the above accumulation of energetic charged particles is not the Earth's radiation belt. All this can be determined only by data on the deflections of magnetic fields, which exist there, from the dipole geomagnetic field and by distributions of pitch-angles of registered particles. This is, however, a subject for future investigations. It would be also especially illustrative to inject artificially into this area charged corpuscles which are not present in the natural medium, and to observe their

lifetime and distribution round the Earth.

The essential role of radiation belts in aurora can be rehabilitated by finding compact clots of corpuscles in the equatorial plane with the help of apparatus of high time resolution. The analogy with the appearance of discrete corpuscular fluxes in rayed aurora allows us to suppose in principle a similar process in the equatorial plane. Very dense corpuscular clots may remain unobserved because of the low resolution of the recording apparatus. We noticed something of the kind in our above-mentioned experiment on the third sputnik at moderate altitudes. Further studies should probably take into consideration such a possibility.

Presently we have no exhaustive data on all the details of aurora and accompanying phenomena. There is no conclusive theory in this respect either. We are not going to review the relevant modern conceptions (see, for example, [57, 58]). However, it is beyond doubt that aurora is one of the most essential chain in the interaction of the geomagnetic field with the interplanetary plasma (or "solar wind") on the one hand and of the whole electroconducting ionized upper atmosphere with interplanetary magnetic fields as well as with the geomagnetic field during its own circulation, on the other [21]. The effect of the direct action of primary solar corpuscles for which

- 27 -

only polar areas are open is of little importance from the energetic point of view. The change of the intensity of the geomagnetic field in any place of the circumterrestrial space is a cumulative effect of the interacting complex current systems of the surrounding space. It is difficult, therefore, to expect an exact correlation of the local energy release of aurora and the data which characterise the disturbance of the magnetic field. Chapman [57] assumes that the ring current of radiation belts during the geomagnetic storms can provoke in the equatorial plane lines with zero value of the geomagnetic field which result in concentrated formations of aurora. This idea is very attractive. But concentrated formations develop during aurora at magnetically calm periods as well. Besides during geomagnetic storms the intensity of the particle flux in radiation belts during polar lights becomes lower which indicates that storm-time variations depend not only on the drift current in radiation belts but on other systems of currents near the Earth as well. Further observations are necessary to draw more convincing conclusions.

Setting aside the less important phenomenon of radiation belts is necessary to make a special stress on the fact that huge planetary energy releases which accompany some aurores are sometimes even greater than the energies

- 28 -

which are usually thought to be released by the accompanying geomagnetic storms. A satisfactory correlation of all these facts is very important for complete understanding of the phenomena of aurores and geomagnetic perturbations.

Since the phenomenon of aurora is associated with the intrusion of intensive corpuscular fluxes of a considerable energy into the Earth's atmosphere, especially in the polar areas, it is natural to expect corpuscular dissociation of the atmosphere's molecules. This process may lead to a considerable increase of the reserves of active atoms which cause the formation of ozone and usual emissions of the upper atmosphere. The heating of the upper atmosphere during aurora may increase the dissipation of hydrogen which must of course affect the intensity of hydroxyl radiation. Besides, metastable atoms and molecules may appear in the upper atmosphere under the action of corpuscles. It must be remembered that fluorescence of metastable atoms of ortho-helium has already been found in polar lights 14. Effective excitation of these atoms requires electrons with energies of about 25 ev. Thus fluorescent emission of helium is a direct evidence of the existence of a great number of such geoactive electrons in the upper atmosphere. All the problems mentioned are still insufficiently understood and also deserve attention.

REFERENCES

- 1.D.Barbier. Ann.Geophys., 16, 544,1960.
- 2.F.E.Roach,Z.A.Karevich,Journ.Res.Nat.Bur.Stand.
D63, 297,1959.
- 3.Yu.L.Truttse,Pl. Sp.Sci., 9,993,1962.
- 4.V.I.Krassovsky.Pl.Sp.Sci., 8, 125,1961.
- 5.V.I.Krassovsky.Report to Symposium of Aurora and Airglow
5 General Assembly of C.S.A.G.I.,Moscow,July 1958.
Transl.:Pl.Sp.Sci., 1, 57,1959.
- 6.C.Störmer.The polar Aurora. At the Clarendon Press.
Oxford,1955.
- 7.J.W.Chamberlain.Physics of the Aurora and Airglow.
Academic Press.New York and London,1961.
- 8.P.A.Forsith.Pl.Sp.Sci., 10, 179,1963.
- 9.B.A.Bagaryatsky.Coll."Spect., Electrophot.and Rad.Invest.
of Aurorae and Night Airglow" published by Ac.Sci.USSR
No. 2-3,11, 1960..
- 10.Y.Hakura. Rep.Ion.Res.Japan, 12,459,1958.
- 11.Yu.I.Galperin.Pl.Sp.Sci. 10, 187,1963.
- 12.R.Montalbetti.Journ.Atm.Terr.Phys., 14,200,1959.
- 13.J.M.Malville , Pl.Sp.Sci., 2, 130,1960.
- 14.N.N.Shevov.Pl.Sp.Sci., 10,73,1963.
- 15.J.A.Van Allen.IGY Rocket Series USA, No.1, 159,
30 July 1958. Report
- 16.C.E.McIlwain, IGY Rocket Report Series USA, No.1,164,
30 July 1958.
- 17.L.H.Meredith,L.R.Davis,J.P.Heppner,O.S.Berg. IGY Rocket
Report Series USA, No.1,169,30 July 1958.

2.

18. C.S.McIlwain. Journ.Geophys.Res., 65, No. 9, 1960.
19. I.S.Shklovsky. Ann.Geophys., 14, 414, 1958.
20. V.I.Krassovsky. Report to Symposium of satellites rockets and balloons, 5 General Assembly of C.S.A.G.I. Moscow, July 1958. Transl.; Pl.Sp.Sci., 5, 233, 1961.
21. V.I.Krassovsky. Report to Symposium of satellites, rockets and balloons, 13 August 1958. Trans. Intern. Astron. Union, 10, 716, 1960.
22. V.I.Krassovsky, I.S.Shklovsky, Yu.I.Galperin, S.M. Svetlitsky. Proceedings of the Moscow Cosmic Ray Conference, July 1959, published Ac.Sci.USSR, 2, 59, 1960.
23. V.I.Krassovsky, I.S.Shklovsky, Yu.I.Galperin, S.M.Svetlitsky, Yu.K.Rushnir, G.A.Bordovsky. Isk.Sput.Zemli, Ac.Sci.USSR, No. 6, 113, 1961. Transl.: Pl. Sp. Sci., 9, 77, 1962.
24. A.J.Bessler. Journ.Geophys.Res., 64, 397, 1959.
25. H.Sugiura. Journ.Geophys.Res., 66, 4037, 1961.
26. T.M.Mulyarchik, P.V.Scheglov. Pl.Sp.Sci., 10, 215, 1963.
27. N.V.Dorjio. Izv.Ac.Sci.USSR, ser.Geofiz., No 5, 714, 1960.
28. R.Jastrow. Journ.Geophys.Res., 64, 1789, 1959.
29. G.S.Ivanov-Kholodny. Pl.Sp.Sci., 10, 219, 1963.
30. C.v.Gartlein, G.Sprage. Mém.Soc.Roy.Sci., Liège, 12, 1952.
31. C.v.Gartlein, G.Sprage. Journ.Geophys.Res. 521, 1957.
32. T.Obayashi, T.Nakura. Pl.Sp.Sci., 5, 59, 1961.
33. B.P.Sandford. Journ.Atm.Terr.Phys., 29, 152, 1962.

3.

34. B.P.Sandford. Pl.Sp.Sci., 10, 195, 1963.
35. N.V.Jorjic. Coll. "Spect., Electrophot. and Rad. Invest. of Aurora and Night Airglow" published by Ac.Sci.USSR, No.1, 30, 1959.
36. A.Omholt. Pl.Sp.Sci., 9, 285, 1962.
37. K.D.Cole. Pl.Sp.Sci., 10, 129, 1963.
38. B.F.Potapov, Z.Ts.Rapoport, T.B.Borsuk. Coll. "Spect., Electrophot. and Rad. Invest. of Aurora and Night Airglow" published by Ac.Sci.USSR, No.2-3, 42, 1960.
39. G.L.Vaisberg. Coll. "Aurorae and Airglow" published Ac.Sci.USSR, No.8, 35, 1962.
40. L.S. Svlashin. Geomag. Aeron. USSR, 1, 54, 1961.
41. L.A.Antonova, G.S.Ivanov-Kholodny. Izv.Ac.Sci.USSR, ser.geofiz., No.5, 756, 1960.
42. L.A.Antonova. Izv.Ac.Sci.USSR, ser.geofiz., No.9, 1437. 1961.
43. I.A.Savenko, P.I.Shavrin, N.F.Pisarenko. Isk.Sput.Zemli, Ac.Sci.USSR, No.13, 75, 1962.
44. B.J.O'Brien, C.D.Langhlin. Journ.Geophys.Res. 67, 2257 1962.
45. R.Hultqvist. Pl.Sp.Sci., 8, 142, 1961.
46. J.Paton. Observatory, 82, 173, 1962.
47. S.N.Vernov, A.I.K.Chudakov. Proceedings of the Moscow Cosmic Ray Conference. July 1959, published Ac.Sci.USSR 3, 19, 1960.

48. J.A. Van Allen. Proceedings of the Moscow Cosmic Ray Conference, July 1959, published Ac.Sci.USSR, 3,7,1960.
49. K.I. Gringaus, V.G. Kurt, V.I. Moroz, I.S. Chklovsky. Isk. Sput. Zemli Ac.Sci.USSR, No.3, 1961, Transl. Pl.Sp.Sci., 2, 21, 1962.
50. B.J.O'Brien, J.A. Van Allen, C.D.x Laughlin, L.A. Frank. Journ.Geophys.Res., 67, 397, 1962.
51. Suin-Ishi Asasofu, J.C. Cain, S.Chapman. Journ.Geophys. Res., 67, 2649, 1962.
52. R.A. Hoffman, R.Y. Arnoldy, J.d. Winckler. Journ-Geophys. Res., 67, 4543, 1962.
53. B.J.O'Brien, J.A. Van Allen, F.S. Roach, C.W. Cartlein. Journ.Geophys.Res., 65, 2759, 1960.
54. D.A.M. King, F. A. Roach. Journ. Res.Nat.Bur.Stand., D65, 129, 1961.
55. P.J. Coleman. The boundary region of geomagnetic field. 13' Inter.Astronautics Cong., Varna, Bulgaria, Sep.1962.
56. J.P. Heppner, N.F. Ness, C.S. Scearce, T.Z. Skillman. Journ.Geoph. Res., 66, No.1, 1963.
57. S.Chapman, American Scientist, 49, No.4, 249, 1961.
58. J.H. Piddington, Pl.Sp.Sci., 2, 947, 1962.
59. K.A. Anderson. Journ.Phys.Soc.Japan, 17, Suppl. A-I, 237, 1961.
60. J.W. Chamberlain. Ap.J., 174, 401, 1961.

UPPER ATMOSPHERE RESEARCH BY USING
ARTIFICIAL EARTH SATELLITES
"COSMOS 3" and "COSMOS 5"

I. Equipment

Yu.I.Galperin, V.I.Krassovsky

Institute of Atmospheric Physics

of the USSR Academy of Sciences, Moscow.

To continue the research of geoactive corpuscles begun in May of 1958 by means of the Third Soviet Sputnik 1958 δ₂ (1, 2, 3), a perfected equipment installed in satellites COSMOS 3 and COSMOS 5 was used. These satellites were long-lived geophysics stations. They functioned in latitude ± 49° at altitudes ranging from 200 to 1600 km. (4). Each of these satellites carried two charged fast particle traps, five fast electron indicators with fluorescent screens and a G-M counter shielded with lead and intended for registering most hard particles. The traps and the indicators were located outside the satellite and had different aperture and mutual orientation. The orientation of the traps and indicators is shown in Fig.1. The arrow indicates the axis direction of the viewing apertures of the traps and the indicators.

ION TRAP → The charged particle traps registered the total current of ion fluxes and electron fluxes of energies exceeding certain thresholds. The principle of operation of one of the traps is illustrated in Fig.2. Metal grids 2 are coupled to

- 2 -

body 1. A potential of ~ 40 V preventing thermal electrons of the ionosphere from penetration into the trap was applied to grid 3. Variable voltage which retarded positive ions was fed to grid 4. As a result of that, admission of ions of energies below 0.15 - 3.0 - 6.0 - 11 keV is stopped by turns. Within a part of the time spent the grid was deenergized and its potential relative to the body equaled zero. The variable voltage mentioned above does not influence practically the electron fluxes under research. Ring collector 5 was placed in an intensive field of permanent magnet 6. The magnetic field sharply reduced the sensitivity of the traps for electrons of energies below 5 keV. This magnetic field similarly influences ions of the same Larmor radius which approximately corresponds to the energy of 30 eV for ions of atomic oxygen O^+ . Besides, the magnetic field, which was almost parallel to the surface of the ring collector, restricted leakage of secondary electrons and photoelectrons of low energies from the latter which arose as a result of irradiation of the collector by the sunlight and corpuscles. When the trap was directed to the sun, its current value from the silvercovered collector with the area of 43 cm^2 reached approximately 10^{-11} A . It means that the configuration of the magnetic field applied reduces the photocurrent from the collector to the body by not less than 4 orders of magnitude. On the other hand, the photocurrent values registered were caused by photoelectrons of comparatively high energy. Their

- 3 -

analysis will permit to obtain information of the ultraviolet radiation of the Sun.

The effective solid angle of the trap for ions and electrons of high energy equaled approximately 1 steradian. With respect to particles moving at an angle of 30° relative to the axis of the trap its sensitivity is only twice as low as for axial ones. This smoothed over the effect of rotation of the satellite when anisotropic fluxes of corpuscles were registered. The scale of the trap current amplifier permitted to register positive isotropic currents inside a solid angle of about 1 steradian within the limits of $3 \cdot 10^5$ to $5 \cdot 10^6$ ion $\text{cm}^{-2} \text{ sec}^{-1} \text{ ster}^{-1}$ and anisotropic currents with a narrow disk-shaped distribution within the limits of $3 \cdot 10^6$ to $5 \cdot 10^7$ ion $\text{cm}^{-2} \text{ sec}^{-1} \text{ ster}^{-1}$ (provided their speed is high enough to penetrate the magnetic field of the trap). In another trap, in contrast to the one described above, grid 4 was connected to the body, whereas a positive potential of 24 V was fed to grid 3, preventing from penetration into the trap the ions of energies below 24 eV (with the uncertainty equal to the sum of the satellite's body potential relative to undisturbed environment and the contact potential difference between the body and the grid 3). At the moving satellite the energy of relative motion of ionospheric ions was under 15 eV, therefore ordinary thermal ions of the upper atmosphere were not registered. In this case the amplifier scale permitted to register positive currents of $3 \cdot 10^5$ to

- 4 -

ster⁻¹

$3 \cdot 10^8$ ion $\text{cm}^{-2} \text{sec}^{-1} \text{V}$ for the isotropic flux and from
 $3 \cdot 10^6$ to $3 \cdot 10^9$ ion $\text{cm}^{-2} \text{sec}^{-1}$ for the anisotropic one.

ELECTRON
DEFLECTION

→ The electron indicator, whose diagram is given in Fig.3, consisted of thin fluorescent screen 5 put on glass plate 6 and covered with aluminium foil sheet 4. Metallized screens 5 with foils of certain indicators were fed with a positive voltage relative to the body accelerating electrons and periodically varying in steps. Besides that, a potential of - 40 V relative to the body was applied to grid 3 placed after grid 2 connected to the body to bar the way of thermal electrons of the ionosphere to the screen. Fluorescence of the screen was registered by photomultiplier 7 whose signal was amplified and applied to the radiotelemetering system with a memory register. The amplifiers were equipped with fine and coarse channels which provided for measuring the intensity within the limits over 3 orders of magnitude.

The indicators responded both to electrons and protons whose ranges exceeded the thickness of the aluminium foil sheet. A small part of soft corpuscles was registered due to accidentally thinned portions of the foil. In addition, electrons which did not penetrate the foils influenced the fluorescent screens by X-ray bremsstrahlung.

Additional accelerating voltage increased penetrating ability of electrons. As a result, our indicators were able to register electrons of small initial energies. For

- 5 -

instance, the indicator with a foil of 0.4 mg cm^{-2} at an additional acceleration of 11 kV was able to register electrons of energies above 40 eV (this threshold is determined by the potential at grid 3 mentioned above).

Electrons of energies from 40 eV to 7 keV could be registered in case the isotropic flux exceeded respectively $2 \cdot 10^8$ and $2 \cdot 10^6$ particle $\text{cm}^{-2} \text{ sec}^{-1} \text{ ster}^{-1}$, i.e. the energy flux beginning from $2 \cdot 10^{-1}$ erg $\text{cm}^{-2} \text{ sec}^{-1} \text{ ster}^{-1}$, for energy 1 keV and about an order of magnitude as low for 40 eV and 7 keV. However at an accelerating voltage of 6 kV the sensitivity for such electrons decreased by more than 2 orders of magnitude. With an increase of initial energy of electrons the ratio of signals at accelerating voltages of 11 and 6 kV decreased. At initial energies of electrons exceeding 20 keV the sensitivity of the indicator described was comparable at all additional voltages. The less the initial energy of electrons was, the deeper the modulation of signals was which permitted to estimate this energy. At satellite COSMOS 5 the same voltages as being applied to the ion trap were used for additional acceleration of electrons. At satellite COSMOS 3 the voltages fed to the indicators were 2.5 times lower than those applied to the trap. At our satellites use was made of indicators with $1.4 \cdot 10^{-3} \text{ cm}^{-2}$ of fluorescent substance $\text{Sr}_3(\text{PO}_4)_2$ [Eu] screened with aluminium foils of $0.4 \cdot 10^{-3}$ and $0.6 \cdot 10^{-3}$ and

- 6 -

1.1.10
-3

$\sqrt{g \text{ cm}^{-2}}$. Only at satellite COSMOS 5 together with the foil of $1.1 \cdot 10^{-3} \text{ g cm}^{-2}$ use was made of fluorescent screen $5.3 \cdot 10^{-3} \text{ g cm}^{-2}$ thick (made of ZnS [Ag]). The comparison of data of the indicators with the foils of different thickness is an additional source of information about the range of particles and, consequently, about their energy. Signals from electrons and protons with ranges exceeding considerably the foil thickness were not modulated when an accelerating voltage was applied. This comparison permitted to distinguish these signals from signals of lower energy electrons.

Due to the spatial anisotropy of charged particle fluxes in the geomagnetic field the rotation of a satellite also causes a typical modulation of a signal registered.

Electrons of approximately 1 meV and of a higher energy penetrate through the walls of the indicator body. Therefore the aperture of the indicators which for electrons of small energy was equal to $\sim 1/12$ steradian increased for hard particles and almost reached a hemisphere. During the rotation of the satellite the modulation of signals due to the anisotropy of such an electron flux decreased and ceased to be deep. This circumstance allows to identify such corpuscles.

Fig.4 represents a pattern of the signal record made by means of one of the indicators of satellite COSMOS 5. The record reveals two types of modulation. One of them is due to the stepped variation of the accelerating voltage and the other is caused by the satellite rotation in anisotropic field of electrons.

- 7 -

Fig.5 represents signal records of the other indicators installed in satellite COSMOS 3.

The axes of these two indicators and the satellite axis of rotation were mutually perpendicular. The axis of rotation lied in a plane perpendicular to the magnetic line of force (See Fig.6). The data records of these indicators have a phase shift equal to 90° and 2 maxima within one period of the satellite rotation. They indicate the intensity distribution according to the value of the pitch angle and achieve their maximum when the pitch angle is equal to 90° .

The signals shown in Fig. 5 were produced by very hard electrons of energies amounting to hundreds of KeV.

The experiments carried out testify to the fact that by means of fluorescent screens and accelerating voltages electrons can be analysed within a rather wide range of energy. If a modulating voltage is applied additionally to grid 3 of the indicator (See Fig.3) then we shall have an instrument registering electrons of any energies beginning from thermal ones.

Electron indicators with fluorescent screens are of little sensitivity of the X-ray bremsstrahlung arising at the expense of very fast electrons absorbed either in the satellite body or in the lower lying atmosphere. This is due to the fact that the fluorescent screens are rather thin.

In time thin aluminium foils are subject to meteoritic erosion. Owing to this fact they become porous and more transparent.

- 8 -

When in the process of the satellite rotation the viewing apertures of the indicators are directed to the Sun, a signal appears which indicates exposure of the photomultipliers. Information pertaining to the satellite orientation relative to the Sun obtained additionally by special indicators permits to distinguish such phenomena and exclude them from analysis of signals received from corpuscles. Shortly after launching the satellites foils, 0.4 and 0.6 mg cm^{-2} thick were found to have increased their transparency by more than an order of magnitude as compared to the results of the tests carried out before the launching. This may have been caused by piercing action of meteoritic dust-suspended in the atmosphere at altitudes of 80 to 200 km or by deformation of the foils when the satellites entered the vacuum. However, afterwards, during the flight in the vacuum the increase of the erosion of these foils was not recognized. Foils 1.1 mg cm^{-2} thick did not reveal any marked signs of erosion at all.

MICRO
NEVORITE
TRANSCEP

GM COUNTER → To facilitate the comparison of the data on the soft corpuscles obtained by means of satellites COSMOS 3 and COSMOS 5 with the data of radiation belts received before with the help of G-M counters, for our satellites we also used such, a counter of the design described below.

A standard halogen G-M counter CTC-5 shielded with 3.4 g cm^{-2} Pb was installed inside the satellite. The elements of the construction created a complicated additional shielding the minimum value of which is about 0.8 g cm^{-2} . Al

- 9 -

in the solid angle of about 2π ster. and approximately up to 25 g cm^{-2} from the other directions.

From the counter the pulses were applied to the chain consisting of 12 triggers with totalizers whose readings were transmitted to the radio-telemetring system. The effectiveness of the counter for γ -radiation of Co^{60} (1.17 and 1.33 mev) reached approximately $2 \cdot 10^{-2}$ counts/quantum and for electrons of 1 meV about $8.6 \cdot 10^{-6}$ counts per electron cm^{-2} . The area of the counter was equal to 4.3 cm^2 . With such a shielding the counter practically does not respond to electrons whose energy is under 400 keV. At higher energies the counter registers X-ray bremsstrahlung with low effectiveness. An electron flux of 1 meV which develops a counting rate of 100 counts/sec is equal to $2.3 \cdot 10^7$ particle $\text{cm}^{-2} \text{ sec}^{-1}$. Electrons whose energy exceeds 10 meV and protons over 50 meV penetrated into the counter. The high counting rate (approximately 10^3 counts/sec) over equatorial regions may have been caused mainly by protons whose energy exceeded 50 meV. Increase of intensity in high latitudes was caused at least partially by the latitudinal effect of cosmic rays. This increase sometimes might be also connected either with solar cosmic rays or with X-ray bremsstrahlung from rather hard electrons. However, the interpretation of the counter's records is not quite of a single meaning.

In the course of the research the values of different voltages feeding the equipment, physical conditions at the satellite, currents of solar batteries etc., were periodically

- 10 -

checked. In flight the electron indicators with fluorescent screens were periodically calibrated by means of a beam of electrons from tritium targets. The beam of electrons was padded by aluminium foil. During the calibration these electrons were accelerated by an additional voltage of 11 KV applied to the circuit between the target and the foil. The analysis of this information showed stability of the equipment used. This stability was specially ensured by the automatic temperature control inside the satellite.

IN FLIGHT CALIBRATION

The subsequent reports contain preliminary data of the information processed. The information about the satellites orientation relative to the Sun and the geomagnetic field are still in the process of computation. The information about the atmospheric retardation of identical satellites COSMOS 3 and COSMOS 5 presents valuable data of the upper atmosphere density in the regions of their perigees.

- 11 -

THE FIGURE CAPTIONS

1. Orientation of Viewing Apertures of Traps and Indicators in Satellites COSMOS 3 and COSMOS 5.
2. Charged Particle Trap Scheme
 - 1) Trap body
 - 2) Metal grids coupled to body
 - 3) Grid fed with voltage of - 40 V
 - 4) Grid fed with variable voltage +0.15; 3; 6; 11 kV
 - 5) Ring collector
 - 6) Permanent magnet
3. Indicator of Electrons Scheme.
 - 1) Indicator body
 - 2) Metal grid coupled to body
 - 3) Grid fed with voltage of - 40 V
 - 4) Aluminium foil 0.4; 0.6 or 1.1 mg cm^{-2} thick
 - 5) Fluorescent screen
 - 6) Glass plate covered with fluorescent ^{lacquer}
 - 7) Photomultiplier
4. On Example of Signals Record of Electrometer
of Indicator Installed in Satellite ^{signals to}
Screen $\text{Sr}_3(\text{PO}_4)_2$ [μ], ^{1.5 mm off axis} ^{thin}
 0.4 mg cm^{-2} thick.
Record shows two types of modulation ^{signals to}
to stepped variation of acceleration ^{signals to}
results from rotation of satellite in ^{signals to}
of radiation.

- 12 -

5. Record of Signals Received in Satellite COSMOS 3 by means of Two Indicators Whose Axes Are Mutually Perpendicular. One of records is presented by continuous line, the other by hatched line. Second indicator has somewhat lower sensitivity. In present case axis of satellite rotation was perpendicular to axes of indicators and magnetic line of force.

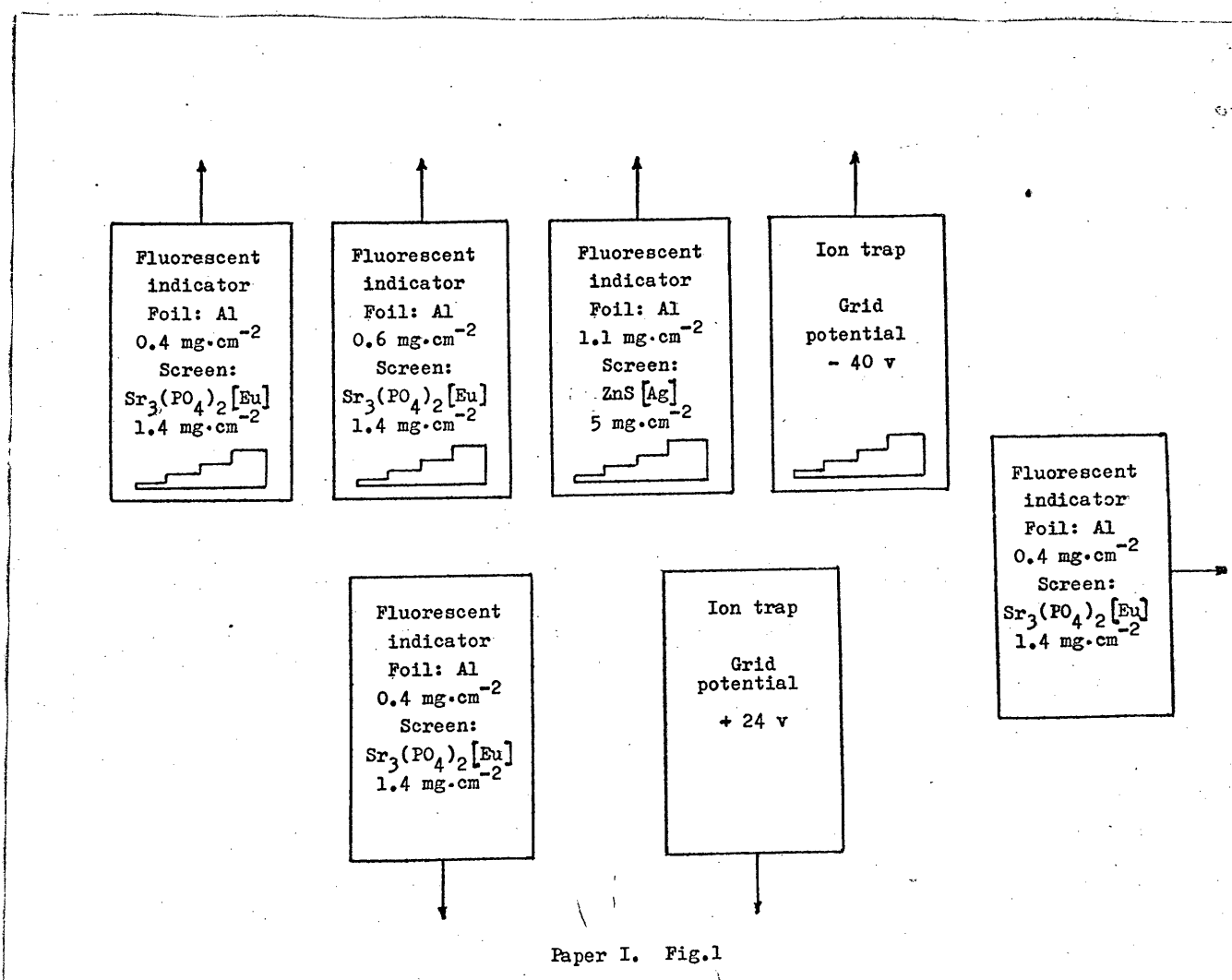
6. Mutual Orientation of Indicators, Axis of Satellite Rotation and Direction of Magnetic Field Vector \vec{B} for the Case Shown in Figure 5.

\vec{M} is the vector of the kinetic moment of satellite rotation;

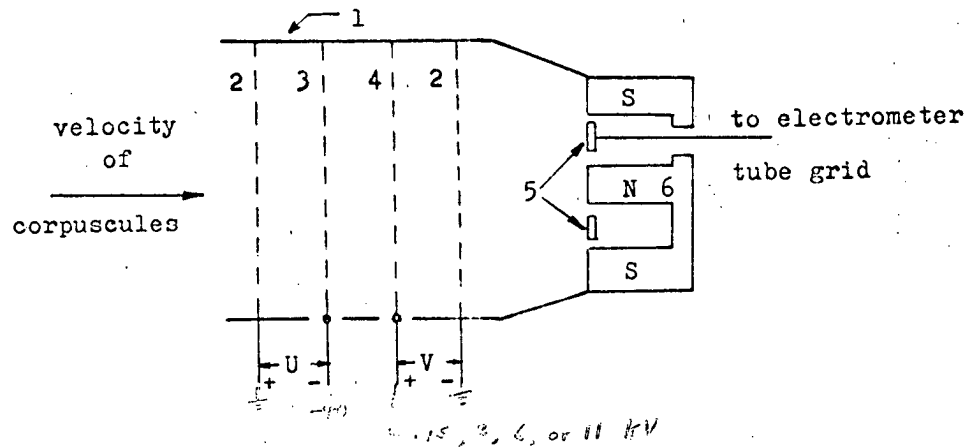
θ_1 and θ_2 are angles of indicators axes with magnetic line of force.

Reference

1. V.I.Krassovsky, Yu.M.Kushnir, G.A.Bordovsky, G.F.Zakharov, Ye.M.Svetlitsky. Detection of Corpuscles by Means of Third Artificial Earth's Satellite. Isk.Sput.Zemli, Ac. Sci.USSR, N 2, pp. 59-60, 1958.
2. V.I.Krassovsky, I.S.Shklovsky, Yu.I.Galperin, Ye.M.Svetlitsky. Detection of Electrons of about 10 keV in Upper Atmosphere by Means of Third Artificial Satellite. Doklady Ac.Sci.USSR, Vol.127, No 1 p.78, 1959.
3. V.I.Krassovsky, I.S.Shklovsky, Yu.I.Galperin, Ye.M.Svetlitsky, Yu.M.Kushnir, G.A.Bordovsky. Detection of Electrons of about 10 keV in Upper Atmosphere. Isk.Sput.Zemli Ac.Sci.USSR, N 6, pp. 113-125, 1961.
4. COSPAR. Information Bulletin, No.12, pp.51-53, 1962.

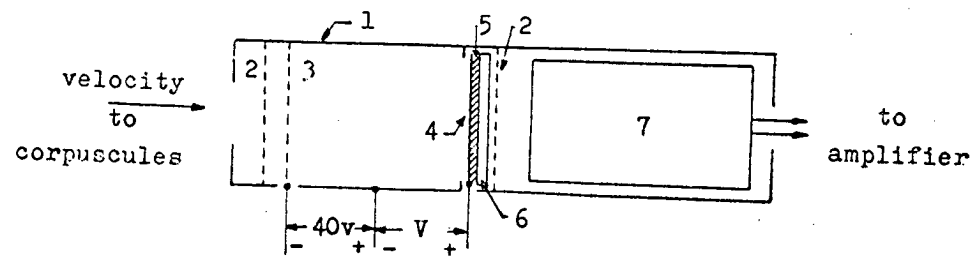


Paper I. Fig.1



1. Aluminium sheath
2. Grids with zero potential
3. Grid with potential - 40 v
4. Grid with modulating high voltage V which is retarding for ions
5. Ring collector
6. Magnet system

Paper I. Fig.2



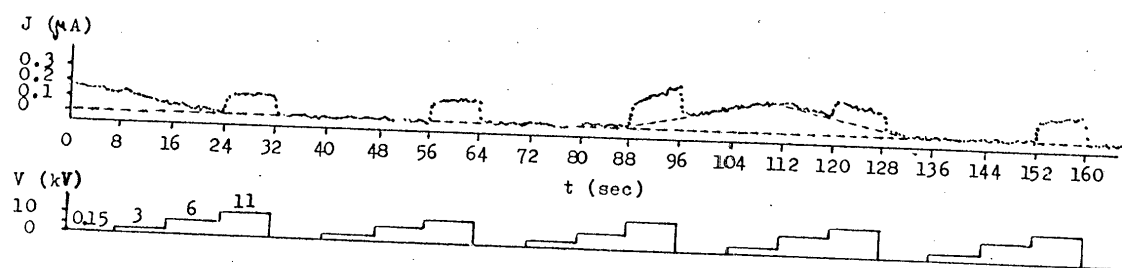
V - modulating high acceleration voltage changing
in stepwise fashion

1. Aluminium sheath
2. Grids with zero potential
3. Grid with potential - 40 v
4. Aluminium foil
5. Fluorescent screen
6. Glass disc carrying the screen
7. Photomultiplier tube

FLUORESCENT INDICATOR. SCHEMATIC DIAGRAM

Paper I. Fig.3

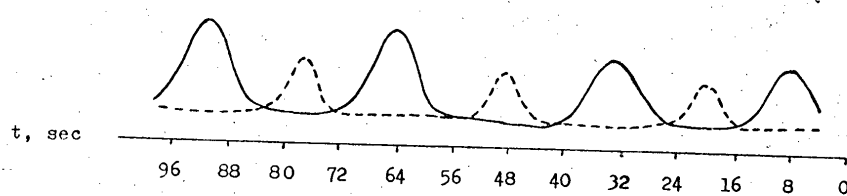
Declassified in Part - Sanitized Copy Approved for Release 2012/12/13 : CIA-RDP80T00246A022400050001-7



Paper I. Fig. 4

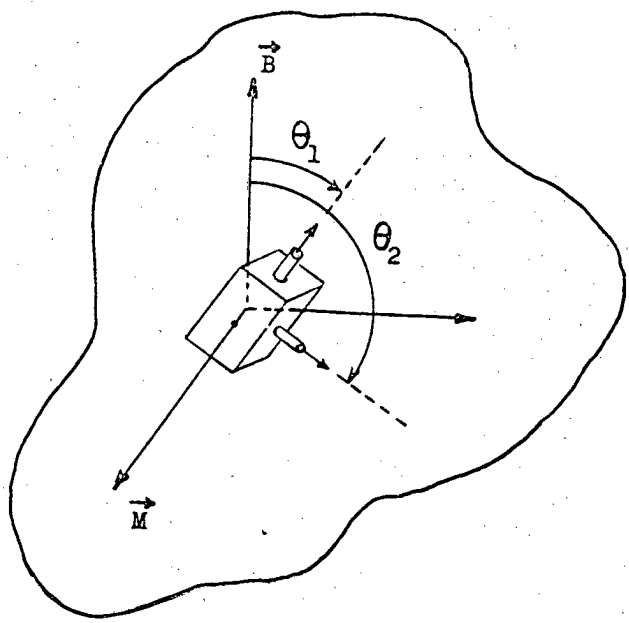
Declassified in Part - Sanitized Copy Approved for Release 2012/12/13 : CIA-RDP80T00246A022400050001-7

Declassified in Part - Sanitized Copy Approved for Release 2012/12/13 : CIA-RDP80T00246A022400050001-7



Paper I. Fig.5

Declassified in Part - Sanitized Copy Approved for Release 2012/12/13 : CIA-RDP80T00246A022400050001-7



Paper I. Fig.6

STAT

UPPER ATMOSPHERE RESEARCH BY USING
ARTIFICIAL EARTH SATELLITES
COSMOS 3 and COSMOS 5 .

2. Soft Corpuscular Radiation

By V.I.Krassovsky, Yu.I.Galperin,
N.V.Jorjio, T.M.Mularchik,
A.D.Bolunova.

+. 1st RESULTS — The fast charged particle traps described in the previous report /1/ were installed in the artificial Earth satellites "COSMOS 3" and "COSMOS 5". They made it possible to record ion fluxes of relatively low energy. Besides, using a range of retarding potentials and account of the effect of the trap magnetic field permit to estimate the energy of the predominant part of ions. The obtained information pertaining to the trap currents indicates that fluxes of positive ions with energies far in excess of the thermal energy are discovered in the upper atmosphere.

The characteristic feature of these ion fluxes is that they are recorded predominantly from one particular direction, i.e. their velocity vector distribution is sharply stretched to one side in the coordinate sistem linked with the satellite. At the same time, the ion flux moving from the opposite direction is either essentially weaker or even lower than the trap sensitivity threshold. The prefered velocity direction of such ions is approximately perpen-

- 2 -

icular to geomagnetic force lines.

The orientation analysis of the COSMOS 3 and COSMOS 5 satellites has not been yet completed; nevertheless, it is already now obvious that the direction from which the above-mentioned ion fluxes are recorded, does not always coincide with the satellite velocity vector and is sometimes at a considerable angle from the latter. When the trap with switched-on stepped retarding voltage was oriented by the velocity vector the ion signal showed no signs of increase, while at the same time the energy of the relative motion of the ionospheric molecular ions might increase up to 15 ev (in the system of coordinates coupled with the satellite and with due allowance for possible contact potential difference between the grid and the vehicle skin and for the potential of the skin relative to the plasma). This vividly manifests that the energy of the particles recorded is of the order of dozen of ev.

The absence of simultaneous signals on the fluorescent - screen indicator shielded with aluminium foil and facing the same direction shows that the range of the ions does not exceed 0.4 mg cm^{-2} and, consequently, their energy (in case of protons) is not over 200 kev. The cumulative data obtained by using the ion traps permit to come to the conclusion that the ion energy apparently may be estimated of the order of tens of ev and only sometimes for some part of the corpuscles attains to several kev. The ion flux usually reached

- 3 -

approximately 10^8 ions $\text{cm}^{-2} \text{ sec}^{-1}$ sterad $^{-1}$ with the maximum recorded values being of the order of 10^9 ions $\text{cm}^{-2} \text{ sec}^{-1}$ sterad $^{-1}$ (in case of the ion flux which is isotropic within the solid angle of 1 steradian).

It is rather interesting that occasionally at the same time with registration of the positive ion signal on the trap, the fluorescent-screen indicator shielded with aluminium foil of 0.4 mg cm^{-2} records the flux of soft electrons from the opposite direction with the energy not exceeding 5 kev. The fact that the trap fails to record such electrons after it turns through 180° due to the satellite rotation, also indicates that their energy is considerably less than 5 kev. If we assume that the energy of the above-mentioned electrons does not exceed approximately 3 kev, then their flux agrees by the order of magnitude with the simultaneous ion flux.

ELECTRIC FIELD ?
The movement of electrons and ions in the opposite directions possibly indicates that a certain electrical field is available in the ionosphere.

It is characteristic that if such a flux was recorded during one satellite revolution, it was usually observed during subsequent revolutions as well within the same range of latitudes, i.e. at the points of orbit specified by the same local solar time. In several cases a more or less sharply outlined region of the ion flux over the equator maintained for at least 9 hours (See Fig.1).

The orbital plans of the satellite gradually turns with

- 4 -

respect to the Earth, so that the moments it passes over a certain geographical region are shifted, for earlier hours in the local solar time. This will make it possible to perform an approximate evaluation of the distribution of the described ion fluxes, depending on the local time. Apparently the ion fluxes possessing the energy far in excess of the thermal energy can appear in any local time.

The above-mentioned ion fluxes were recorded only at low altitudes from 200 to 600 km in the F-region of the ionosphere. Positive ions, as a rule, were recorded at a given satellite revolution for 3 to 15 minutes, i.e. within a range of thousands of kilometres. It is quite possible that the observed ion fluxes with the energies appreciably exceeding the thermal energy, pertain to the system of ionospheric S and L currents. On switching off the stepped positive voltage which generated the retarding potentials, one of the traps recorded the ionospheric ions penetrating through its magnetic field. This resulted in a strong dependence of the signal intensity on the trap orientation with respect to the satellite velocity vector even at great heights.

ELECTRICAL RESULTS -- The fluorescent-screen electron indicators with a variable accelerating potential could record the electrons in a rather broad energy range beginning from 40 ev. Besides, such an indicator can record the ions whose range exceed the foil thickness.

- 5 -

Let us first consider the results pertaining to low-energy electrons (not exceeding 5 to 7 kev) and medium-energy electrons (i.e. of order of 7 to 50 kev). The signal generated by such electrons was appreciably modulated by the accelerating voltage, and the low-energy electrons were recorded practically only by the indicator shielded with foil 0.4 mg cm^{-2} . At the maximum accelerating voltage of 11 kV while the medium-energy electrons were recorded even at lower accelerating voltages. The electrons with energies below 5 kev are recorded rather often, but sporadically. Their energy flux sometimes reaches $0.1 - 1 \text{ erg cm}^{-2} \text{ sec}^{-1} \text{ steradian}^{-1}$ (assuming the electron energy is 5 kev or 1 kev, respectively). At typical values the flux is approximately $0.03 \text{ erg cm}^{-2} \text{ sec}^{-1} \text{ steradian}^{-1}$ if the energy equals 5 kev. The variation of such electron fluxes due to height as well as their anisotropy in the magnetic field greatly differs from similar characteristics of other types of corpuscular radiation available in the atmosphere. Both these interconnected characteristics are highly variable, with the fluxes of such electrons being nearly isotropic on the average and their intensity is slightly dependent on height. The signal generated by the electrons possessing energies lower than 5 kev appear at all the latitudes and even over the equator. The characteristic feature of these electrons is that they are recorded mainly in the illuminated region of the atmosphere. Their intensity on the night portion of the satellite orbit is, as a rule, considerably lower than

- 6 -

that on the day portion of the orbit. Often this corpuscles disappear at all several minutes after the satellite enters the region of the Earth's shadow.

This information was obtained mainly by the use of memory data-storage facility of the satellite when the satellite - borne radio-transmitter used to transmit the telemetrical information was switched off and only the low-power transmitter "Mayiak" was in operation. The nature of the signals detected remained unchanged when the more powerful transmitter was switched on and off. This permits to assume that the electrons recorded were not merely the ordinary thermal electrons of the ionosphere accelerated in the variable fields of the satellite-borne transmitting antennas. It can not be excluded that the satellite moving in the illuminated portion of its orbit also records the photo-electrons originating either in the illuminated region of the ionosphere or emitted from the "Mayiak" transmitter antenna surface which is within the field of view of the fluorescent-screen indicator. However, such an explanation is not valid for the night portion of the orbit.

The medium-energy electrons (approximately 7 to 50 kev) appear mainly at high geomagnetic latitudes and at high altitudes. Their intensity dependence on latitudes is more definite than that of low-energy electrons, and at altitudes below 1000 km they appear only from time to time. No medium-energy

DETECTION
ELECTRONS
NOT
ACCELERATED
BY TRANSMITTER

- 7 -

electrons are recorded at altitudes below 700 km in the South-Atlantic magnetic anomaly. However, in some cases such corpuscles were recorded at low and middle latitudes at approximately 1000 km altitude where their flux amounted to some 10^6 electrons $\text{cm}^{-2} \text{ sec}^{-1}$ steradian $^{-1}$ assuming the electron energy equals 40 kev. As a rule, the anisotropy of such electron fluxes is more distinct as compared to that of low-energy electrons. In addition to the above mentioned distributions of the electron velocity vectors typical for the corpuscles trapped by the geomagnetic field, many cases were recorded when the shape of the anisotropic distribution of the velocity vectors was an evidence of the invasion of considerable electron fraction into the dense atmosphere. This phenomenon first detected in the course of upper atmosphere research by using the artificial Earth satellite "Sputnik-III" in 1958 /2,3,4/ and then confirmed by O'Brien /5,6 and 7/ using the data obtained from satellite "Injun-I" in 1961, may contribute to the energy-balance and ionization of the upper atmosphere /3,4/.

Besides the above-mentioned fluxes of electrons whose signal was to a considerable extent modulated by the variable accelerating voltage, the fluorescent-screen indicators recorded the particles possessing higher energies. Their signal was subject to modulation merely due to the satellite

- 8 -

rotation. The distinct anisotropy of these particles with the maximum intensity at the pitch-angles equal to 90° , and stability of their intensity indicate that the particles have been trapped by the geomagnetic field. The traps recorded negative currents simultaneously and in phase with the signal variations of these particles displayed on the indicators. This leads to the assumption that the fluorescent-screen indicator signals which are not modulated by the stepped accelerating voltage, were generated by the electrons whose energies range from approximately 50 kev up to several hundreds of kev, but not by protons with energies in excess of $200 \div 500$ kev which can also penetrate through the aluminium foils. Now this conclusion will be considered in detail.

The signal ratio of the indicator and the trap at the pitch-angle equal to 90° as calculated from the calibration data and their geometric factors, differs by not more than 40 per cent from the indicator-to-trap signal ratio measured in the South Atlantic geomagnetic anomaly. Now let us assume that the electron flux with energies exceeding 50 kev (lower energies are impossible since no modulation by the accelerating voltage takes place and the sensitivity of the fluorescent-screen indicator with foil 0.4 mg cm^{-2} Al is higher than the trap sensitivity) is added with the flux of protons with energies exceeding $200 \div 500$ kev whose signal displayed on the indicator is commensurable with the signal produced by the electrons of over 50 kev energy or even exceeds

- 9 -

the latter considerably. It is obvious that the indicator signal should markedly increase while the negative current of the trap recording the algebraic sum of electron and ion currents will, on the contrary, decrease. Consequently, their ratio will to a considerable extent increase and will differ from the results obtained in the South Atlantic magnetic anomaly. It should be also taken into account that the fluorosum cont-screen indicator sensitivity to the protons penetrating through the foil, is rather high, i.e. the energy release per one proton with the energy over 200 kev in the fluorescent screen and its light output pmm per unit energy greatly exceeds the similar values obtained per one electron with the energy in excess of 50 kev. Therefore, even a negligible (as compared with the electron flux) flux of protons possessing the energies mentioned above (or the flux of some other ions) would have significantly changed the signal ratio of the two pick-ups. Hence, at altitudes up to 700 km in the South Atlantic magnetic anomaly the proton flux is negligible as compared with the flux of electrons.

Only approximate energy evaluation of these electrons can be made. As has already been stated, their energy exceeds 50 kev, while the omnidirectional flux reaches $5 \cdot 10^7$ particles $\text{cm}^{-2} \text{ sec}^{-1}$. The deep signal modulation with the satellite rotating in the anisotropic radiation field shows that the energy of electrons does not exceed 1 mev. This conclusion is in accord with the fact that the counting rate of the shielded

- 10 -

G-M counter was rather low at the pertinent time intervals (Fig. 3).

ELECTRON
COUNTING RATE
CONTOURS OVER
SOUTH ATLANTIC

→ Figs 4 and 5 show the isolines of electron flux intensity with energies in excess of 50 kev over the South Atlantic magnetic anomaly as measured by using the "COSMOS 3" satellite for the period from April 24 to May 10, 1962. The height of the cross-section surface is approximately 650 km. The values indicated close to each isoline are expressed in the units of the omnidirectional electron flux ($\text{cm}^{-2} \text{ sec}^{-1}$) when multiplied by $6 \cdot 10^4$.

The isolines shown in Fig 4 were obtained by using the records taken during the periods when the magnetic K-index was below 4 while the lines represented in Fig. 5 take into account also the results of measurement taken at $K > 4$.

When taking into account the satellite revolutions measured during the periods with large K-index values, the intensity isolines become more curved and displaced. The observed displacement of the isolines does not necessarily indicate the increase or decrease of the total amount of electrons trapped by the geomagnetic field. It may also be due to the height fluctuations of the surface these particles are drifting over or due to changes in their composition and energy spectrum.

*/ The K-index values are taken from the data obtained by the Moscow station (ISKIRAN). The satellite revolutions at $K > 4$ refer to May 5-6, 1962.

- 11 -

Similar cross-sections plotted by using the data obtained from the shielded G-M counter which records mainly the protons possessing the energies in excess of 50 mev, are illustrated in a separate report /8/. The shape of isolines and the maximum flux intensity regions of these two groups of particles are different.

TIME VARIATIONS → It is rather difficult to distinguish between the space of intensity and time variations (and the results obtained are not always single-valued). For better presentation of the values actually obtained during different satellite revolutions, Figs. 6 and 7 show maximum flux intensity points obtained by using the fluorescent-screen indicator data (blank circles) and the G-M counter data (solid circles) with the altitudes indicated in the graphs in km. Dashed lines refer to the satellite revolutions with $K \geq 4$ (See Fig. 5). Apparently, the relative disposition of corpuscles of different groups varies even from one satellite revolution to another. It is possibly due to certain peculiar characteristics of the South Atlantic geomagnetic anomaly region.

Table I gives some data on the corpuscular radiation intensity at rather low altitudes within the $\pm 49^{\circ}$ latitude. The tabulated data indicate that predominant at low altitudes are not the protons with energies ≥ 50 mev, but some other corpuscular radiation of lower energy.

- 12 -

Sample Fluxes Registered at Particular Locations.

F - omnidirectional number flux in particles $\text{cm}^{-2} \text{sec}^{-1}$;

P - omnidirectional energy flux in erg $\text{cm}^{-2} \text{sec}^{-1}$

Time	Coordinates			Type of particles		
	H	φ	λ	Protons	Electrons $E \sim 100\text{kev}$	Electrons $E \leq 5 \text{ kev}$
	km. degrees	degrees			$E \geq 50 \text{ Mev}$ (assuming (omnidirectional)	(assum- (omni- rectio- nal) isotropic rectio- nal)
3 Mai 1962						distribut- ion and $E = \text{kev}$)
19 h 02 m				num- ber flux		
GMT	1470	47 S	37 W	<u>F</u> 150	<u>$3 \cdot 10^7$</u>	<u>$1 \cdot 10^8$</u>
				ener- gy flux		
				<u>P</u> $1 \cdot 2 \cdot 10^{-2}$	5	0.8
3 Mai 1962				num- ber flux		
19 h 19 m						
GMT	1520	19 S	10 E	<u>F</u> 820	<u>$7 \cdot 10^7$</u>	<u>$2 \cdot 10^8$</u>
				ener- gy flux		
				<u>P</u> $6 \cdot 5 \cdot 10^{-2}$	10	1.6

- 13 -

Captions to Figures

Fig.1. Example of Recording of Soft Positive Ions by Using Artificial Earth Satellite "COSMOS 3" on April 25, 1962. Satellite orbits are shown by dashed lines and regions of recording positive ions - by solid lines. Figures at ends of solid lines indicate altitudes in km. Figures in circle-numbers of satellite revolutions. Shown at the right side are the same regions of positive ion recording, with the longitude transformed into the local time.

Fig.2. Record Pattern Obtained by "COSMOS 5" Satellite by Using Electron Indicator with Foil 0.4 mg cm^{-2} thick. Signal modulation by stepped accelerating voltage is evident.

Fig.3. Pattern of Signals from G-M Counter (solid line) and Electron Indicator (dashed line). Y-axis shows G-M counter counting rate in logarithmic scale. Electron indicator readings are given in arbitrary units. Maximum flux of electrons is $1.5 \cdot 10^6$ electrons $\text{cm}^{-2} \text{ sec}^{-1} \text{ steradian}^{-1}$ in case their energy $E = 50 \text{ kev}$.

Fig.4. Intensity Isolines of Electron Fluxes over South Atlantics for Moments with Low Geomagnetic Activity ($K < 4$). Units are as shown in Fig.5.

- 14 -

Fig. 5. Intensity Isolines of Electron Fluxes over South Atlantics. Intensity values near isolines are expressed in units of $4 \cdot 10^4$ particles $\text{cm}^{-2} \text{ sec}^{-1}$ steradian $^{-1}$ assuming electron energy equals 50 kev.

Figs 6 and 7. Mutual Arrangement of Radiation Intensity Maxima Recorded with G-M Counter (solid circles) and Electron Indicator (blank circles). Each point is accompanied by height value in km of appropriate maximum.

- 15 -

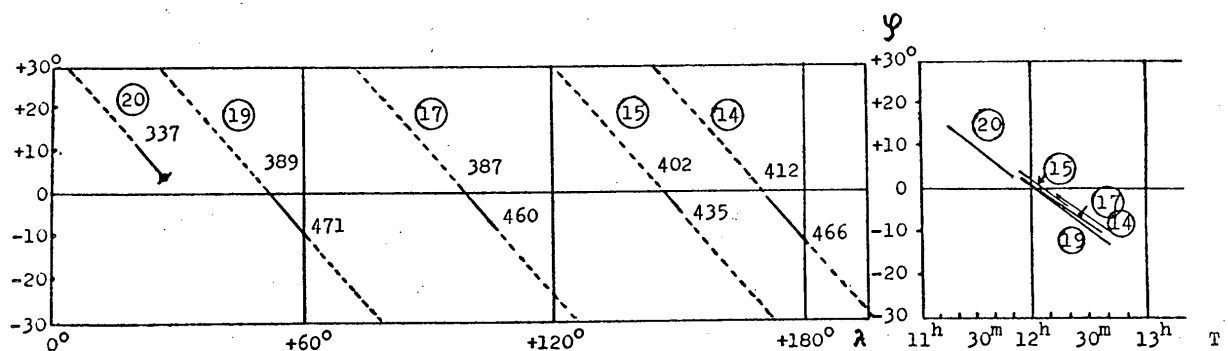
References

1. Upper Atmosphere Research by Using Artificial Earth Satellites COSMOS 3 and COSMOS 5. I.Yu.I.Galperin, V.I.Krassovsky. Equipment.
2. V.I.Krassovsky, Yu.M.Kushnir, G.A.Bordovsky, G.F.Zakharov, S.M.Svetlitsky. Detection of Corpuscles by Using Third Earth Satellite. Isk.Sput.Zemli, N 2, 59-60, 1958. V.I.Krassovsky, Yu.M. Kushnir, G.A.Bordovsky, G.F.Zacharov, S.M.Svetlitsky. Artificial Earth Satellites, 2, Plenum Press, Inc., New York, pp.75-77, 1960.
3. V.I.Krassovsky, I.S.Shklovsky, Yu.I.Galperin, S.M.Svetlitsky. Detection of Electrons with Energy Approximately 10 kev in Upper Atmosphere by Using Third Earth Satellite. Doklad of the Academy of Sciences of the USSR, 127, No.1, 78, 1959.
4. V.I.Krassovsky, I.S.Shklovsky, Yu.I.Galperin, S.M. Svetlitsky, Yu.M. Kushnir, G.A. Bordovsky. Detection of Electrons with Energy Approximately 10 kev in Upper Atmosphere. Isk.Sput.Zemli, N 6, 113-126, 1961. V.I.Krassovsky, I.S.Shklovsky, Yu.I.Galperin, Yu.I.Kushnir, G.A.Bordovsky, 1961, Artificial Earth Satellites, Plenum Press Inc., New York, 137-155, 1961; Plan.Sp.Sci., 9, 27-40, 1962.
5. B.J.O'Brien. Direct Observations of Dumping of Electrons at 1000-kilometer Altitude and High Latitudes. Journ. Geophys.Res., 67, No. 9, 1227-1233, 1962.

- 16 -

6. B.J.O'Brien. Lifetimes of Outer-Zone Electrons and Their Precipitation into the Atmosphere. Journ.Geophys.Res., 67, No.10, 3687-3705, 1962.
7. B.J.O'Brien. Review of Studies of Trapped Radiation with Satellite-Borne Apparatus. Space Sci.Rev., I, No.3, 415-484, 1963.
8. Upper Atmosphere Research by Using Artificial Earth Satellites "COSMOS 3" and "COSMOS 5" 2. V.V.Temny. High-Energy Corpuscles.

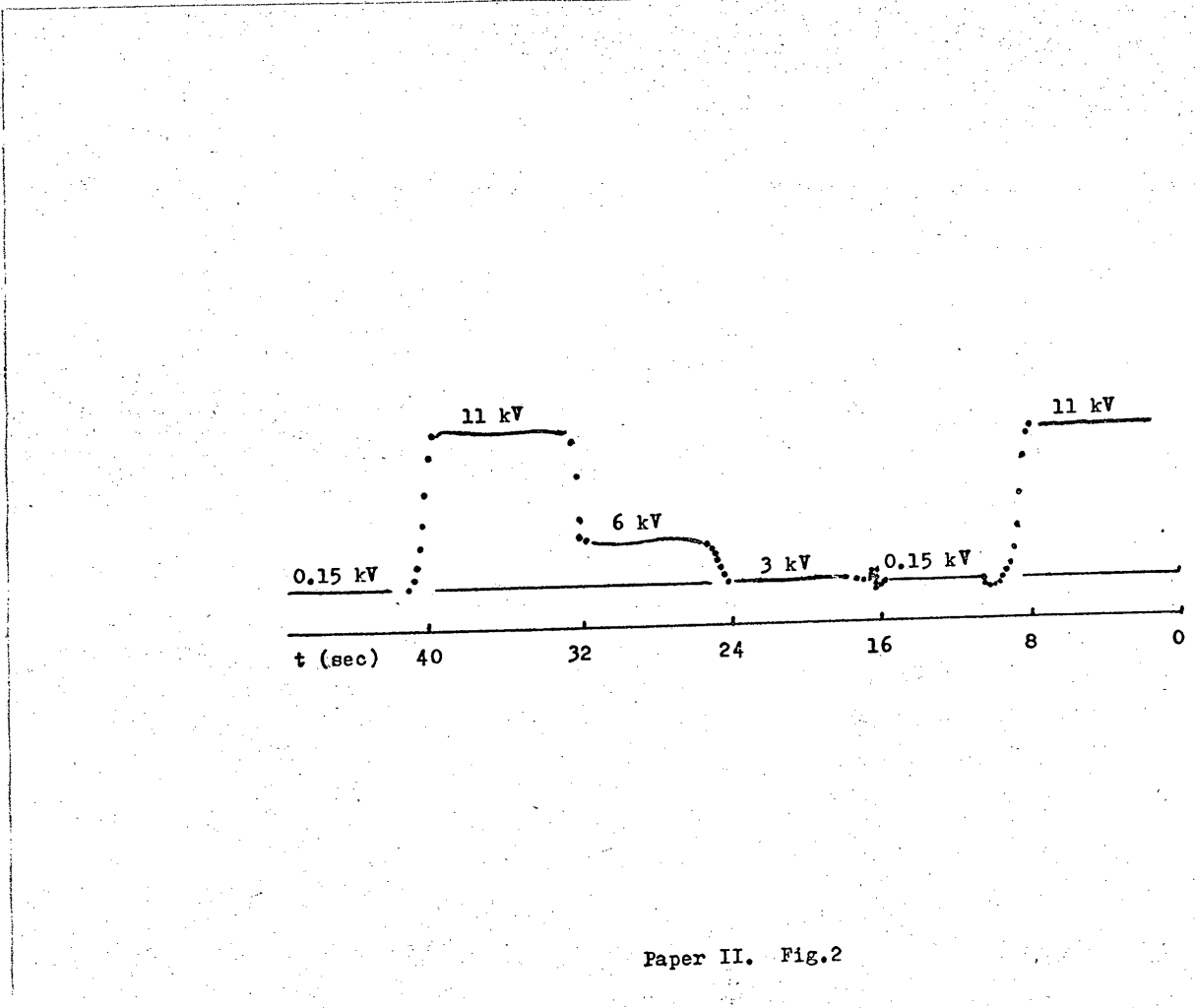
Declassified in Part - Sanitized Copy Approved for Release 2012/12/13 : CIA-RDP80T00246A022400050001-7



Paper II, Fig. 1.

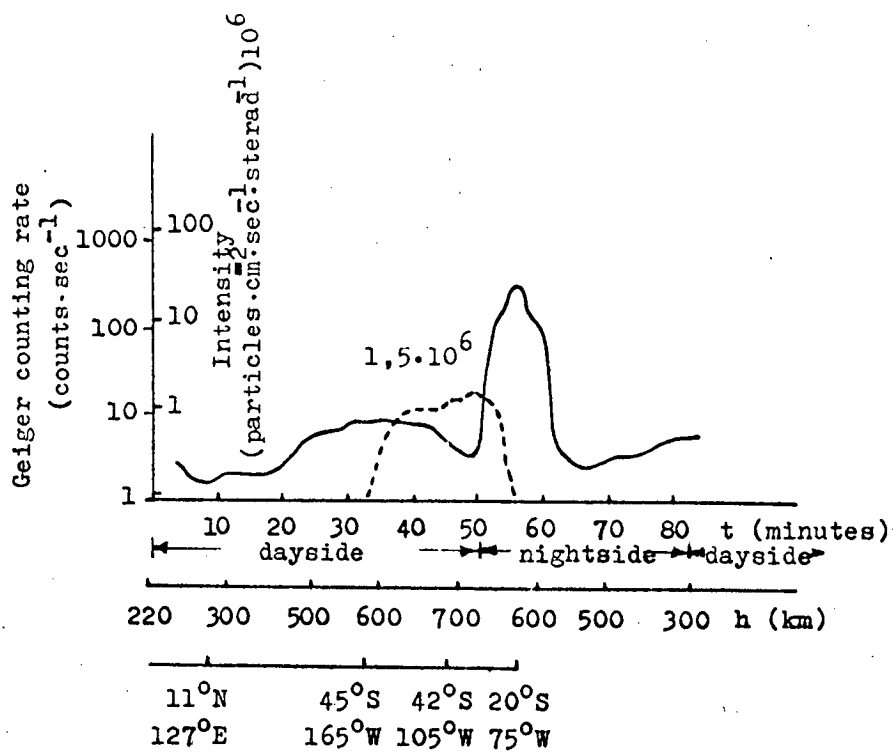
Declassified in Part - Sanitized Copy Approved for Release 2012/12/13 : CIA-RDP80T00246A022400050001-7

Declassified in Part - Sanitized Copy Approved for Release 2012/12/13 : CIA-RDP80T00246A022400050001-7



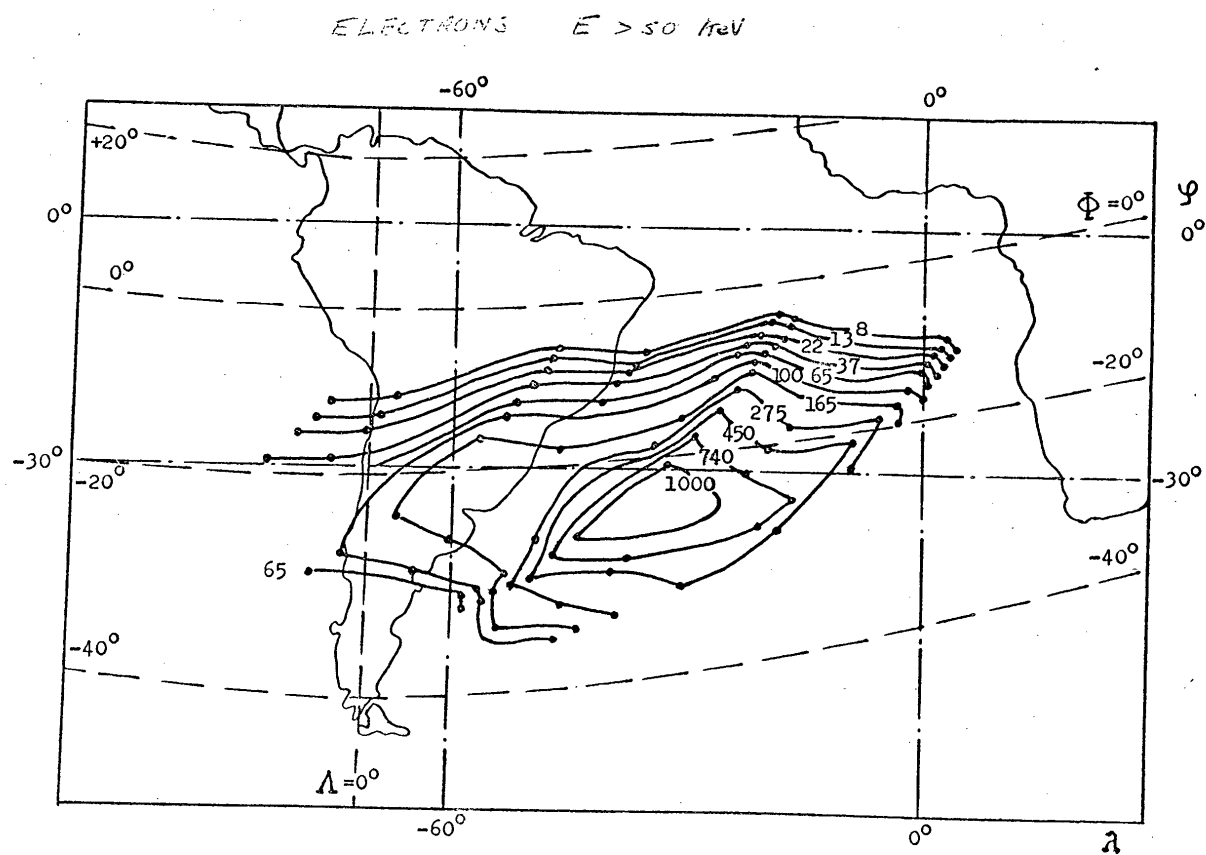
Paper II. Fig.2

Declassified in Part - Sanitized Copy Approved for Release 2012/12/13 : CIA-RDP80T00246A022400050001-7



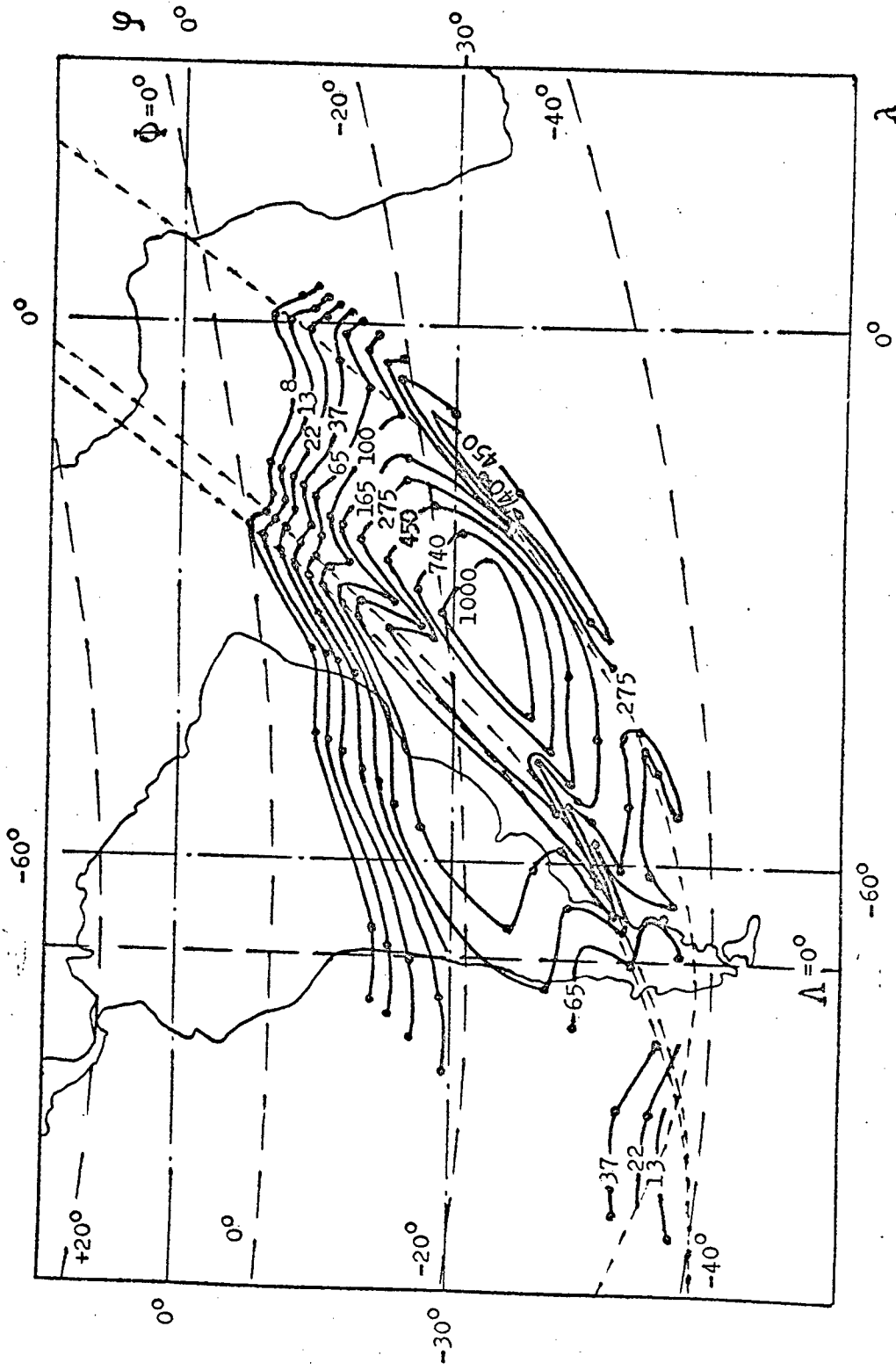
Paper II. Fig.3

Declassified in Part - Sanitized Copy Approved for Release 2012/12/13 : CIA-RDP80T00246A022400050001-7



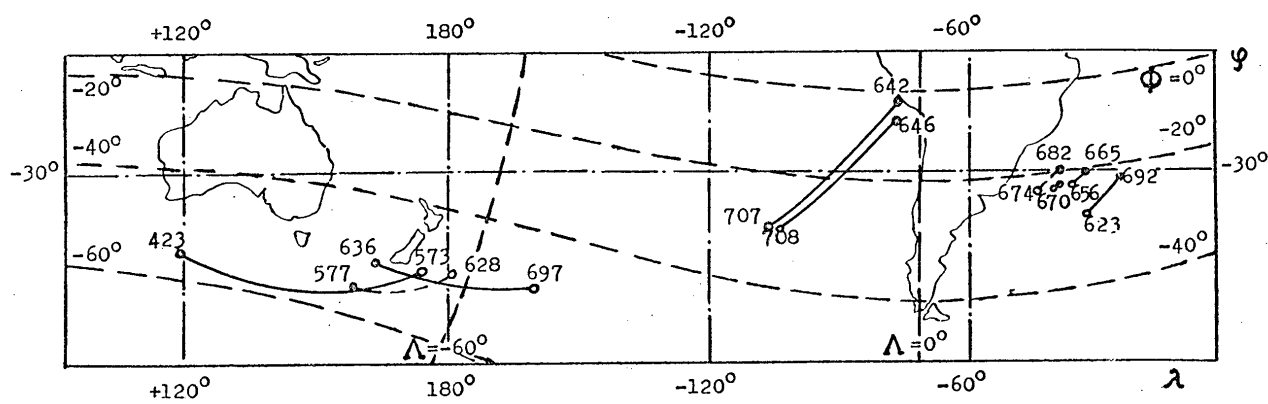
Paper II; Fig. 4

Declassified in Part - Sanitized Copy Approved for Release 2012/12/13 : CIA-RDP80T00246A022400050001-7

ELECTRONS $E > 50 \text{ keV}$ 

Paper II. Fig.

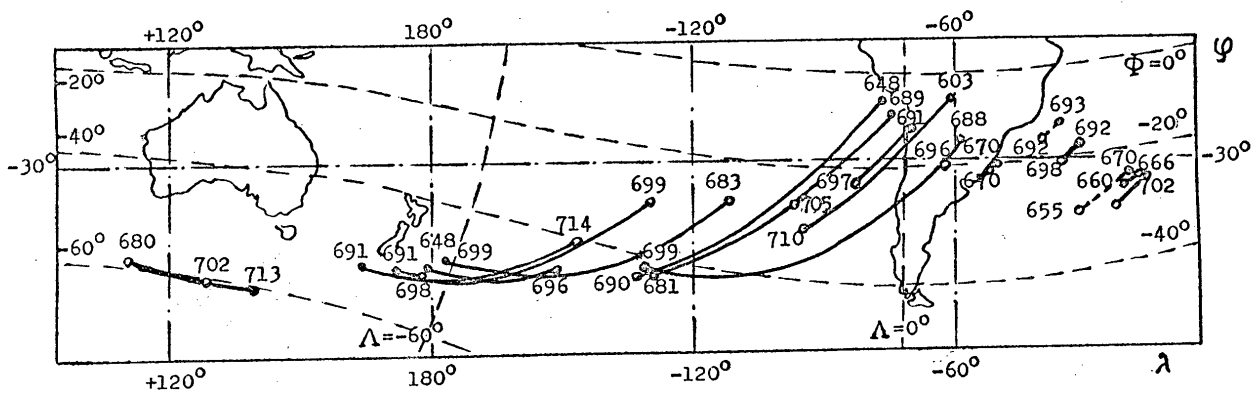
Declassified in Part - Sanitized Copy Approved for Release 2012/12/13 : CIA-RDP80T00246A022400050001-7



Paper II, Fig. 6.

Declassified in Part - Sanitized Copy Approved for Release 2012/12/13 : CIA-RDP80T00246A022400050001-7

Declassified in Part - Sanitized Copy Approved for Release 2012/12/13 : CIA-RDP80T00246A022400050001-7



Paper II, Fig. 7.

Declassified in Part - Sanitized Copy Approved for Release 2012/12/13 : CIA-RDP80T00246A022400050001-7

RESULTS OF INVESTIGATION REACHED BY USING
ARTIFICIAL EARTH SATELLITES
COSMOS 3 and COSMOS 5.

3. High-Energy Corpuscular Radiation

Yu. V. Efimov¹

Institute of Atmospheric Physics of the
USSR Academy of Sciences, Moscow.

The "Cosmos 3" and "Cosmos 5" artificial earth satellites carried gas geiger tubes of CGC-5 type shielded by 3.4 g/cm^2 Pb + 0.8 g/cm^2 Al for recording of penetrating radiation. Such a shielding reduce the number of radiat. types creating significant counting rates.

To evaluate the range of electrons in the composite shield it is convenient to replace it by an aluminium sheet, 5.6 g/cm^2 thick, which possesses an equivalent absorbing power. This value corresponds to the extrapolated range of 10.8 Mev electrons and the 50% transmission thickness for 10 Mev energies. A bremsstrahlung contribution from electrons with energies less than 10.8 Mev is determined using the efficiency curve (Fig.1). The left-hand scale of the Y-axis reads the calculated efficiency of the geiger counter,

ϵ (i.e. the ratio of the counting rate versus to number of electrons incident to 1 cm^{-2}), while X-axis shows the energy in kev. In Fig.1 principal points obtained during laboratory calibration of a similar counter

- 2 -

are also shown. The curve bend within the energy region of 1.5 to 2 Mev demonstrates the growth of the bremsstrahlung intensity for such penetrating through the satellite aluminium shell and are slowed down in the lead shield and other structural elements of the satellite with intermediate Z . The counter efficiency curve may be used for determining the flux of particles $N(E)$ per cm^2 per sec. of energy E which results in a particular counting rate. For example, a flux at which the counting rate equals 500 counts/sec is determined using the right-hand scale of T -axis (Fig.1). Protons penetrate through the same shield beginning from energies of ~ 50 Mev.

The results of counting rate measurements permit distinguishing two regions around the Earth : I - a shell close to the Earth where the counting rate varies from 1.5 counts/sec at the geomagnetic equator to 15-20 counts/sec at geomagnetic invariant latitudes of 60° */; II - region of penetrating radiation with a sharp lower boundary where the counting rate exceeds 25 counts/sec. This region has been identified within latitudes of $\pm 50^\circ$. No systematic growth of the counting rate has been recorded within region I.

*/ Hereafter "geomagnetic invariant latitude" is defined as an angle between the radius-vector of the point in space from the center of the dipole and the equatorial surface (at the same value $|B|$) of the real geomagnetic field computed in [6]. The angle lies in the geomagnetic meridian plane.

- 3 -

(at low counting rates) during the ascent along the line of force, which means that the majority of the particles recorded are not trapped. Let us consider the cosmic ray contribution to the measured counting rate. The primary cosmic ray intensity varies from 8.3×10^{-3} particles $\text{cm}^{-2} \text{ sec}^{-1}$ sterad at geomagnetic equator to 1.5×10^{-1} particles $\text{cm}^{-2} \text{ sec}^{-1}$ sterad at 51° latitude [1]. With a mean counter geometric factor of 25 cm^2 sterad for isotropic radiation assuming no shower formation the counting rate should vary from 0.2 counts/sec to 3.8 counts/sec between the equator and the 51° latitude, which is 5 to 10 times as low as recorded counting rate. Such an excess of the recorded counting rates over the "cosmic ray background" may be due to showers from primary cosmic ray particles formed in the satellite body. A similar counter with 5 g/cm^2 shielding installed in the third Soviet space vehicle /2/ recorded minimum counting rate of 3.2 counts/sec in the equatorial region at similar altitudes, i.e. twice as high as that recorded by the satellites "Cosmos 3" and "Cosmos 5". This may be accounted for by different conditions of shower formation in the satellite body.

Now consider region II where the counting rate grows from 25 counts/sec to 500 counts/sec and up. The recorded radiation is trapped by the geomagnetic field since :

- 1) in most cases it was observed that the counting rate undergoes modulation by a factor of several times with the

- 4 -

satellite rotational half-period due to different shielding (from maximum of about 25 gr/cm^2 to minimum of 4.2 gr/cm^2) as well as due to change of the counter axis orientation with respect to the line of force;

2) radiation intensity varies systematically along the line of force.

Let us consider the composition of the radiation recorded by the counter in this region. Fig.1 shows that the counting rate of 500 counts/sec may be due to 1 Mev electron flux of $1.2 \cdot 10^8 \text{ particles cm}^{-2} \text{ sec}^{-1}$ or by even higher electron fluxes of lower energies. Since fluorescent-screen indicators at that time recorded no such high electron fluxes, it may be concluded that the contribution to the counting rate of 500 counts/sec of the bremsstrahlung from the electrons of less than 1 Mev is significant. Similarly, for creating the same counting rate the monochromatic flux of 3-Mev and six 6-Mev electrons (which still cannot penetrate through the shield into the counter) should be of $4 \times 10^6 \text{ part. cm}^{-2} \text{ sec}^{-1}$ and $10^6 \text{ part. cm}^{-2} \text{ sec}^{-1}$ respectively. Electrons possessing such energies penetrate through the walls of the fluorescent-screen indicators and can be detected. In many cases the fluorescent-screen indicators displayed no signals at the times of the geiger counting rate of 500 counts/sec. Since their detection threshold for electrons of such energies is below $10^4 \text{ part. cm}^{-2} \text{ sec.}$, the above mentioned fluxes would have certainly been detected. It

- 5 -

becomes evident, therefore, that the counting rate is the region where trapped particles are present, is caused mainly by penetrating corpuscles. Since none of the measurements taken as far away as several thousand kilometres from the Earth's surface in latitudes up to 40° recorded electrons possessing such a penetrating power, the conclusion may be drawn that the counter records mainly penetrating protons. From the results obtained by Freden and White /3/ and by Haugle and Kniffen /4/ it may be deduced that within the comparable region of space the trapped proton flux with energy exceeding 50 Mev reaches $40 \text{ part. cm}^{-2} \text{ sec}^{-1}$ sterad. With the counter geometric factor of 25 cm^2 sterad the counting rate should be approximately 1000 counts/sec. which is close to the value recorded.

The lines shown in Fig.2 connect points of equal counting rates obtained at an altitude of about 650 km over the South Atlantic. The shape of the isointensity curves is quite similar to the lines for equal values of the module of total magnetic field at this altitude. /5/

To determine the position of the trapping region boundaries, the points of the counting rates of 25 counts/sec and 500 counts/sec are plotted in coordinates $B - \Phi$, where B - the geomagnetic field vector in gauss and Φ - the latitude of the point defined earlier (Fig.3a). Values of B and Φ have been obtained using the data on the

- 6 -

earth's field harmonic expansion with 512 coefficients /6/. The scattering of experimental points depends to a considerable extent on the error in determining the maximum counting rate at deep modulation due to the satellite rotation. The mean curves have been drawn to describe the obtained distribution. Solid line corresponds to the counting rate of 500 counts/sec, the dashed line - to 25 counts/sec. Then these mean curves are replotted in coordinates $H - \Phi$ (Fig. 3b), where H - minimum height above the Earth's surface which is reached by the mirror point of a particle drifting around the Earth. These minimum heights in the Southern Hemisphere are located approximately along the 60th meridian, western longitude.

Figs 3a and 3b show that the lower boundary of the trapping region at latitudes up to $15^\circ - 20^\circ$ below 500 km is determined by the atmospheric scattering and at higher latitudes it runs along lines of equal values of the magnetic field vector.

It is well known, that when describing the movement of charged particles in a stationary non-uniform magnetic field using three invariants of motion, such as :

μ - magnetic moment, I - longitudinal invariant and Φ - flux invariant, at least the following requirement should be met :

$$\frac{R}{Larm} \frac{/\text{grad } B/}{B} \ll 1$$

- 7 -

where R_{Larm} = particle Larmor radius. This requirement is not met for recorded protons, as this value is of the order of 0.2 for a proton energy of 100 Mev. Therefore, the movement trajectory can hardly be calculated accurately enough using the three invariants mentioned above. Figs 3a and 3b suggest the idea that the particles might drift in the meridional direction along lines of the equal value of $|B|$.

In conclusion the author wishes to express his appreciation to V.I.Krassovsky for guidance and to Yu.I.Galperin for advice and direct assistance.

- 8 -

F i g u r e s

Fig.1. Efficiency Curve of G-M Counter

Points are Results of laboratory calibration.

Fig.2. Lines of Equal Counting Rate at altitude of about
650 km in South Atlantic.

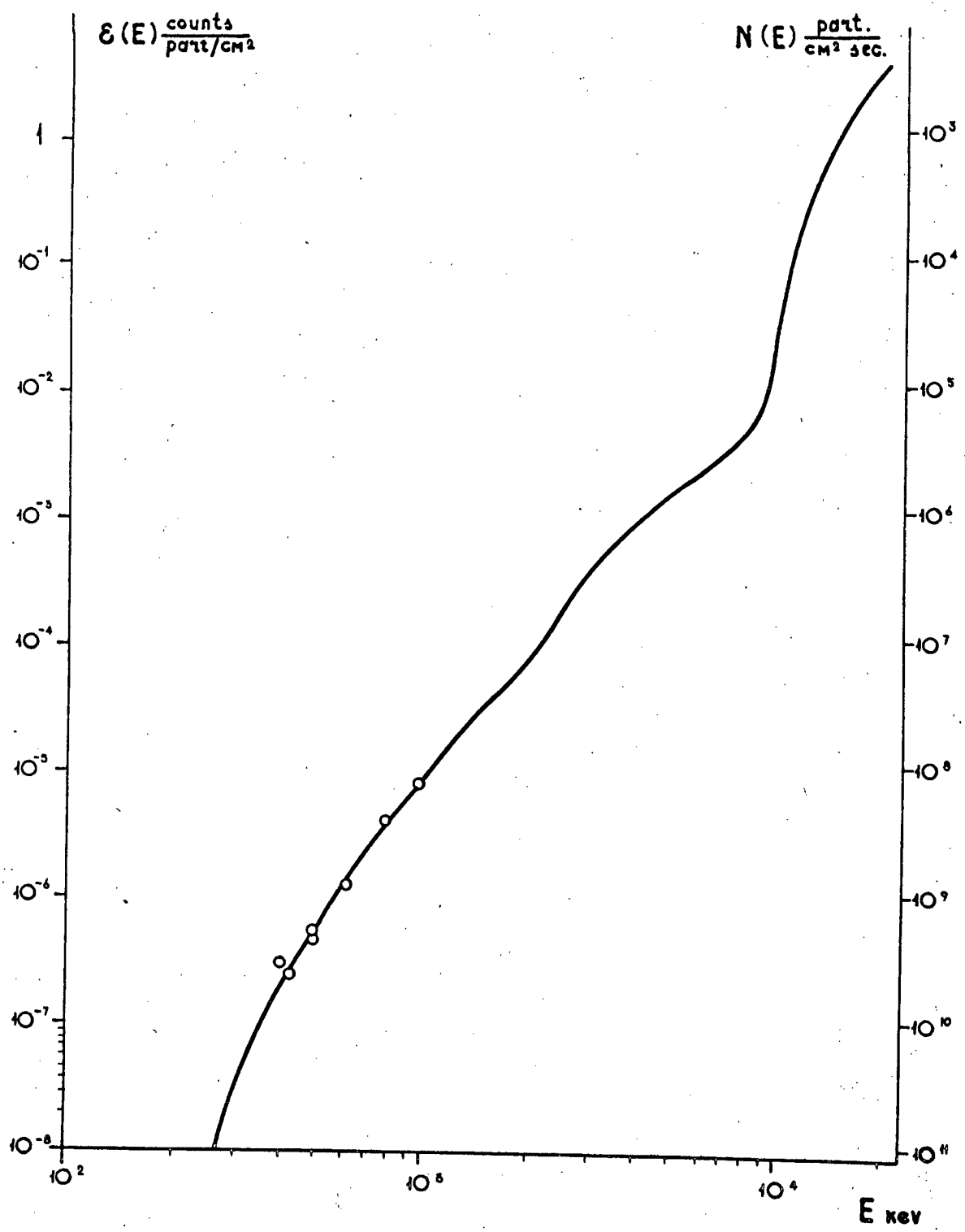
Fig.3. Locations of Equal Counting Rate 25 counts/sec.
and 500 counts/sec in Coordinates:

a) B, ϕ (B - magnetic field vector at the point
of measurement ; ϕ - geomagnetic invariant
latitude (see text) ;

b) H, ϕ (H - minimum altitude above the Earth's
surface in km which is reached by the mirror point
while drifting around the Earth.

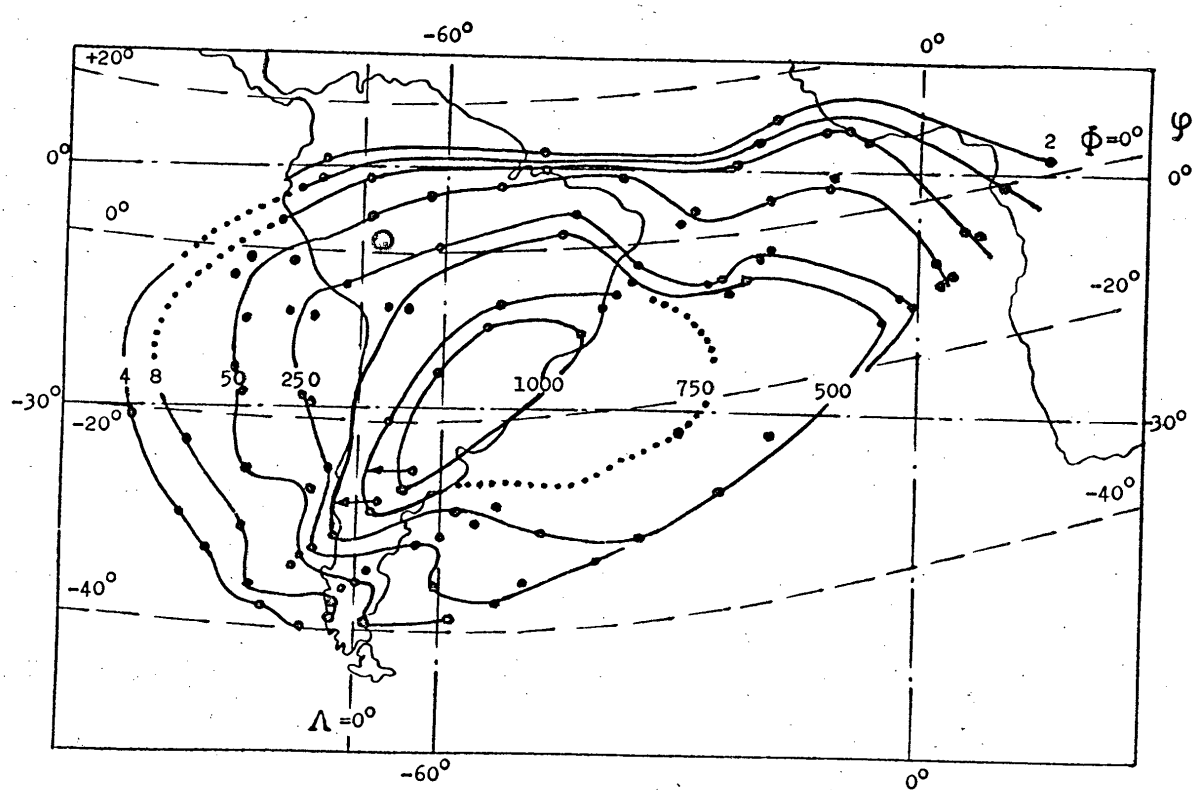
Bibliography

1. A.N.Charakhchian, T.H.Charakhchian. Measurements of Cosmic Ray Intensity in Stratosphere. Journ.of Exper.and Theor.Phys., Vol. 35, No 5, 1958, 1088-1101.
2. I.A.Savenko, V.E.Nesterov, P.I.Shavrin, N.F.Pisarenko. Cosmic Ray Equator from Data Obtained from Third Soviet Earth Satellite Vehicle. Artificial Earth Satellites, issue II, 1961, 30-34.
3. S.C.Freden, R.S. White. In Journ.Geophys., Ref., 65, 1377-1383, 1960.
4. J.E.Naugle, D.A. Kniffen. Flux and Energy Spectra of the Protons in the Inner Van Allen Belt. Phys.Rev.Let., 7, No.1, 3-6, 1961.
5. Handbook of Geophysics, New York, p. 10-12, 1960.
6. D.C.Jensen, R.W. Murray, J.A.Welch. Tables of adiabatic Invariants for Geomagnetic Field 1955. AFSWC-TN-60-8, April 1960, AFSWC-TN-60-19 August 1960.



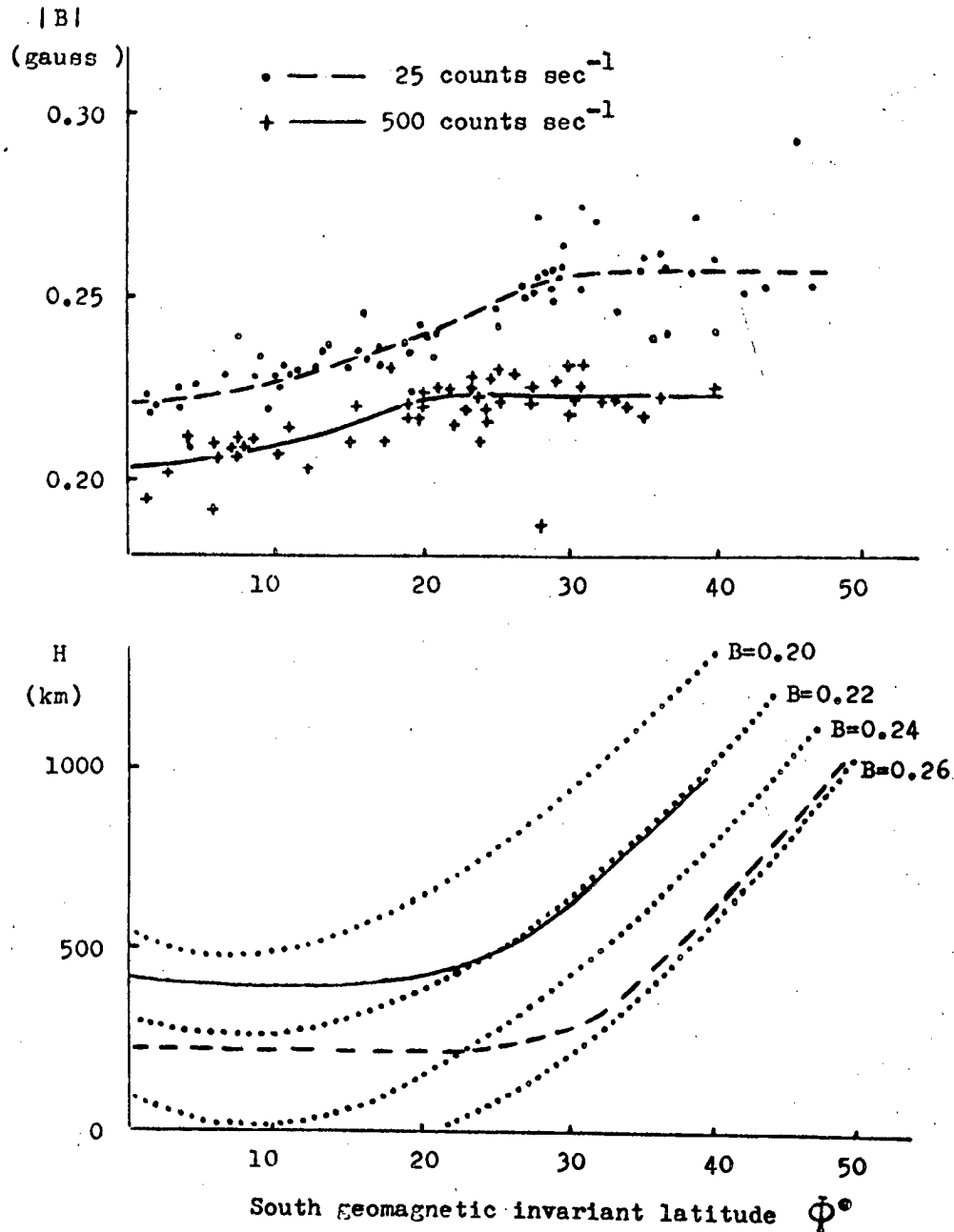
Paper 3. Fig. I .

Declassified in Part - Sanitized Copy Approved for Release 2012/12/13 : CIA-RDP80T00246A022400050001-7



Paper III. Fig.2

Declassified in Part - Sanitized Copy Approved for Release 2012/12/13 : CIA-RDP80T00246A022400050001-7



Paper III. Fig. 3

S.N.Vernov, I.A.Savenko, P.I.Shavrin,
L.V.Tverskaya

THE EARTH AND RADIATION BELTS STRUCTURE AT AN ALTITUDE OF 320 KILOMETRES

Abstract

According to the 2nd Soviet Spaceship-satellite data, the intensity distribution in the radiation belts on the drifts shells at an altitude of 320 km was studied.

The dependence of intensity on longitude, for various values of shell L parameter has been obtained.

The change of intensity as a function of longitude has been discovered along the lines of equal B (B denotes magnetic field intensity).

The connection of intensity with the structure of the real geomagnetic field has been traced. The temporal intensity variations are also discussed.

Analysis of spatial intensity distribution in the radioactive belts at low altitudes is considerably hard to carry out because of quite a number of circumstances. The fact, that the geomagnetic field is not that of a dipole causes an adverse effect at low altitudes. Whereas for the central dipole the equal B line at all longitudes is located at an uniform altitude, this altitude strongly depends on longitude for the real geomagnetic field. By this reason while their longitude drift the particles come to regions of significantly variable atmospheric density. As an example we can point out that the altitude of mirror points in the South hemisphere

- 2 -

varies by more than 1,000 km depending on longitude, while the atmospheric density, according to / 1 /, varies by e times at a distance of 100 km. Since atmospheric density at low altitudes is high the mean particle lifetime, related to the downward diffusion can be shorter than a longitude drift period. This will lead to the appearance of longitude dependence (longitude dependence is understood as a dependence of the intensity along the equal B lines on longitude).

In the presence of the longitude dependence the methods of presenting results in McIlwain's two-dimensional coordinate system B, L / 2 / is naturally inapplicable as in this case different intensities from different longitudes will correspond on the graph to the point with given B, L.

The results obtained at the 2nd Soviet spaceship-satellite / 3 / show planetary intensity distribution registered by luminescent counters at an altitude of 320 km and enable to trace longitude intensity dependence on different drift shells.

To a drift approximation the leading centre of a charged particle moves in a magnetic trap on a surface which consists of the pieces of magnetic force lines and is determined by the conditions of constancy of magnetic moment and of longitudinal invariant

where the integral is taken along a magnetic line of force between the reflection points 1 and 1*, and B_3 is field intensity in mirror points.

Generally speaking, in an asymmetric field the drift sur-

- 3 -

faces of the particles initially located on the same magnetic forcecline may fail to coincide. Ho Ilwain /2/, however, on the basis of spherical analysis data showed that for the actual geomagnetic field this effect is negligible. Consequently there existing surfaces in the geomagnetic field which are formed of magnetic forceclines and which all particles being set on them must independently ca. B_3 drift along. These surfaces can be characterized by the numerical parameter L , which is constant for a given surface. According to the Ho Ilwain relationship of L , I and B_3 in the case of real geomagnetic field is practically the same as in the case of ideal dipole, while processing /treating/ the data of the 2-nd spaceship - satellite L for experimental points were computed proceeding from the values of I and B_3 for real geomagnetic field /4/.

Since the orbit of the satellite was circular /located at an altitude of 320 kms/, we could easily synonymously determine a position of experimental point in the space by presetting drift surface and longitude.

Fig.1 shows the dependence of intensity on longitude for various drift surfaces at an altitude of 320 kms in B Southern Hemisphere. Continuous curve represents $L = 2.6$. The dotted curve shows the dependence of magnetic field intensity on latitude on the same drift surface at an altitude of 320 kms. The region of sudden increase of count anomaly will be discussed later on. Here and further this region of count will be implied under the term "anomaly".

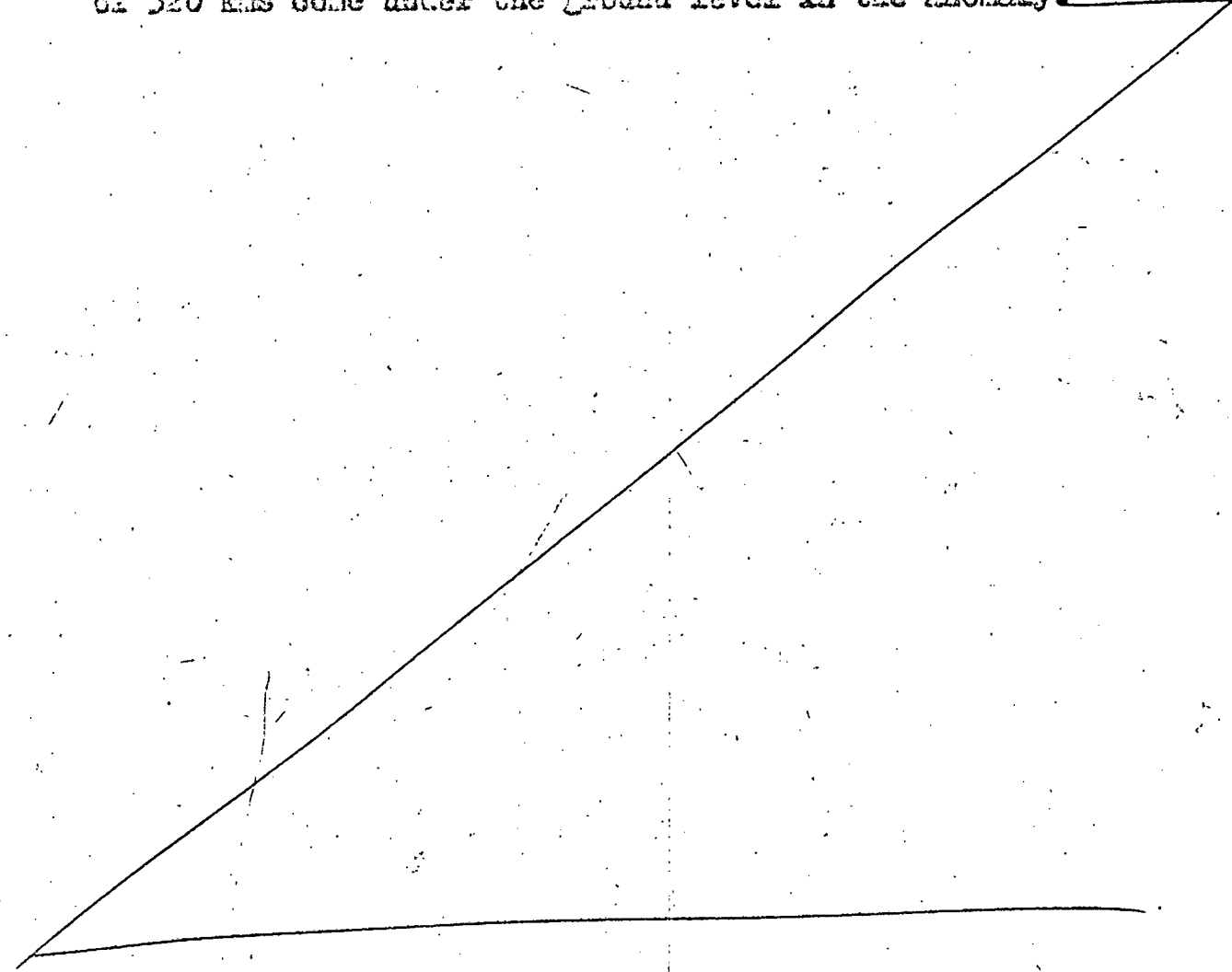
It is easy to note that in the region of longitudes of $260^\circ - 360^\circ$, at the left of the anomaly increased intensity at a level of 40-50 imp. per sq. cm per second is observed. Complete absence of points in which the background was registered should be noted.

The region of longitudes at the right of the anomaly, beginning from $30^\circ - 60^\circ$, presents quite different picture. Here, at the same L points with intensity which practically does not differ from the background /for graph data the background is subtracted/ so these points coincide with the X-axis/ and points with intensity of about 20 imp. per sq.cm per

second arc observed. Thus in this region the mean intensity is considerably lower than at the left.

As it is seen from the shape of the curve dependences of B on longitude for the same drift surface are identical in considerable interval in the regions at the left and at the right, while intensities are different. This indicates to the existence of longitudinal dependence along the lines of equal B . Such result is quite natural and clear. On the fig.2 the continuous curve presents dependence on longitude of one of drift trajectories for $L = 2,5$ in Southern hemisphere. The experimental points which this trajectory passes at an altitude of 320 kms are located at the longitudes of 270° and 76° at the left and at the right of anomaly respectively.

The dash-dott curve 2 shows for comparison drift trajectories of conjugated mirror points in northern hemisphere. It can be seen from fig.2 that the mirror points of particles located at the right and at the left of anomaly at an altitude of 320 kms come under the ground level in the anomaly.



itself. It is natural that on the way out of anomaly intensity at the points at the right at an altitude of 320 km is almost absent and that during the longitude drift particles from high altitudes have time to diffuse to these altitudes.

It is noted that in the region of longitudes at the right of the anomaly the background was practically registered for all L on 5 spires passing at night from the North to the South, and the points with intensity which differed from zero we observed at the same longitudes on 5 other spires passing in the day-time from the South to the North (local time is implied).

It is impossible, however, to speak with confidence about the presence of daily variations since measurements were carried out for only 1 day.

On Fig.1 the points for $L = 2,4-4.5$ are plotted. For all there L intensity at the left remains higher than that at the right, all L at the right having the points with intensity which practically does not differ from the background. The outer belt maximum is on $L = 3.5-4.5$ with the data available one does not succeed in determining it with great accuracy. For $L = 5$ intensity already falls to the same level as for $L = 2.6$

For $L = 2$ only the background is practically registered at the left and right of anomaly. In this sense the transition from the outer to the inner belt can be spoken of.

Table 1 and Fig.3 demonstrate the features of intensity distribution in the anomaly. In Table 1 the intensities I imp. per sq.cm per second and corresponding longitudes

- 6 -

in the region of anomaly for some L are given. On Fig. 3 the dependence curves of B on longitude for various drift surfaces at an altitude of 32 km are plotted. The continuous curve - for $L = 1.3$, dotted curve - for $L = 1.5$, touch-dotted curve - for $L = 2.1$. Increased count in anomaly is naturally registered in the regions of the minimum of these curves. From the data of the Table 1 a noticeable longitude shift of intensity maximum to the right for different L corresponding to the shift of the curves on Fig. 3 is seen.

The inner belt maximum is in interval 1.5-1.6. Thus analysis of intensity distribution along the drift shells shows that a number of regularities exist at low altitudes too and that with change of altitude the gradual intensity change takes place.

Three longitude regions are distinctly notable: peak in anomaly (320° - 50°), low intensity region (60° - 220°) and plateau westward from the anomaly. The connection of intensity distribution in the anomaly with the features of the actual geomagnetic field is traced.

Authors express their acknowledgment to V.N.Erofeeva; L.B.Drozdova; N.M.Trishkina for the carried computations and the design of results.

- 7 -

References

1. F.S. Johnson. J.Geophys.Res. 1960, 65, No.2, pp577-584.
2. Mc Ilwain. J.Geophys.Res. 1961, No.11, p.3681
3. S.N.Vernov, I.A.Savenko, P.I.Shanrin, V.E.Nesterov,
N.F.Pisarenko. Artificial Earth satellites, 1961,
issue 10.

- 8 -

Captions to Figures

Fig.1 Dependence of intensity on longitude for different L at an altitude of 320 km.

X - L = 2.4

◐ - L = 2.6

□ - L = 2.8

○ - L = 3.4

■ - L = 4.5

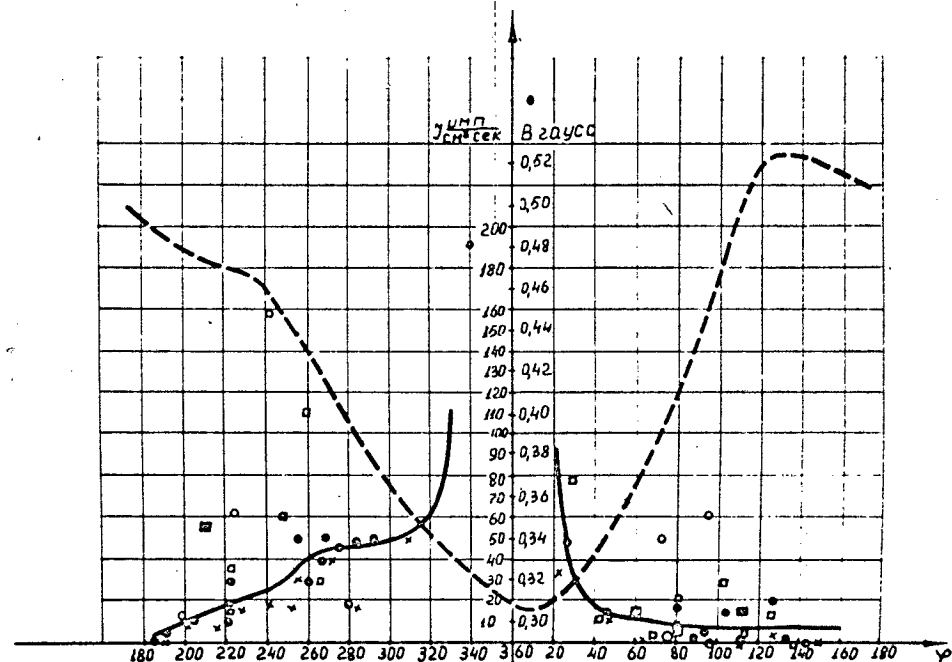
Fig.2 Dependence of altitudes of the vertically conjugated points on longitude in Southern (continuous curve) and Northern (touch-dotted curve) hemisphere.
(B = 0.39, L = 2.6).

Fig.3. Dependence of magnitude of magnetic field B intensity on longitude at an altitude of 320 km for different L.

— L = 1.3

— ▲ — L = 4.6

— · — L = 2.1



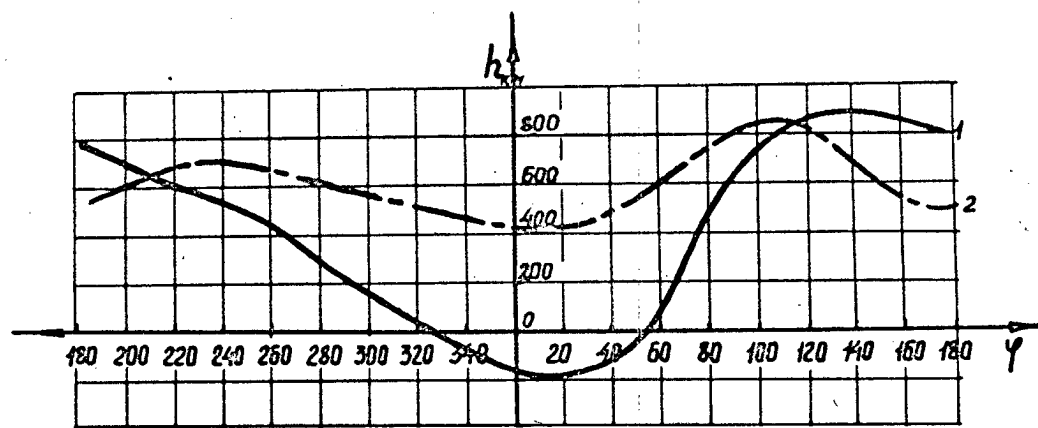


Fig. 2

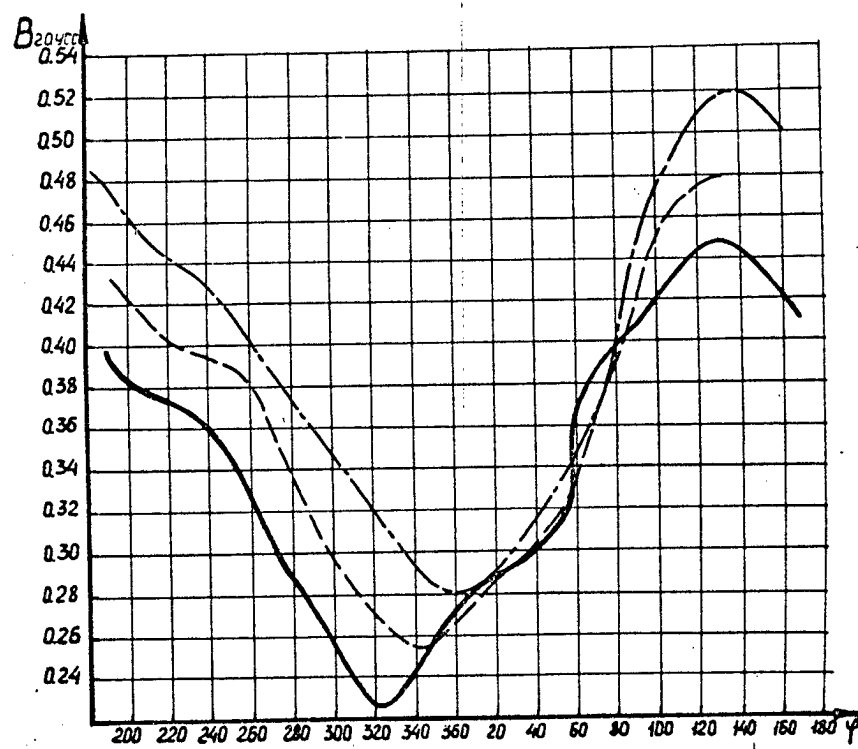


Fig. 3

longitude -

of carts -

	$L = 1.3$				$L = 1.6$				$L = 2.1$				$L = 2.9$			
φ	311	326	349	320	336	353	333	346	359	339	360	16				
J	50	153	16	100	344	110	120	178	85	200	600	300				

Table 1

P.V.VAKULOV, S.N.VENOV, E.B.GORCHAKOV,

Yu.I.JOGACHEV, A.H.CHARAKHCHIAN, T.N.CHARAKHCHIAN

and A.P.CHEBDAYEV

(The USSR Academy of Sciences)

DEPARTMENT OF RADIOACTIVE RAYS.

COSMIC RAYS IN THE STRATOSPHERE AND THEIR
CORRELATION WITH SOLAR ACTIVITY
(1958-1962)

The records of cosmic ray intensity in the stratosphere began in the USSR in connection with the IGY from the middle of 1957 at geomagnetic latitudes 64 degrees (Murmansk) and 51 degrees (Moscow) and since April 1958 at latitude 41 degrees (Simeiz). By the beginning of 1963 at these stations about 4,000 flights of probes-balloons with recording instruments were accomplished.

Threshold energies of primary protons at these latitudes are 0.1, 1.5 and 4.6 Revs, respectively (1).

To record cosmic rays at probes-balloons either a single Geiger counter or a telescope from two Geiger counters were used. Data on the height of flight were determined from readings of a barograph similar to that used on meteorological probes.

The transmission of data on intensity and altitude was carried out through one radio channel. In the use of an instrument with a single counter about 75 per cent of time information about counting rate was transmitted, and information about the height of the flight was transmitted for 25 per cent. In the use of an instrument with a telescope from two counters information about the number of two-fold coincidence was transmitted for about 75 per cent of time and information about the counting rate of a single counter and the height of flight was transmitted for 25 per cent of time. Fig.1 shows the electric scheme of the telescope consisting of two counters. In the case of a single counter the tube L 1 and counter

- 2 -

S, are excluded from the diagram. The signals of the transmitter were recorded by the Earth by means of an ultra short-wave receiver at whose output a sealing circuit with a mechanical counter is switched on. This instrumentation was used for practically every-day measurements of cosmic ray intensity. Extensive data were obtained whose analysis permits us to separate and study different fluctuations of cosmic ray intensity observed in the stratosphere can be divided into two types:

Comparatively rare cases of anomalously great increase of cosmic ray intensity belong to the first type of fluctuation. These increases are observed mainly at polar latitudes where radiation intensity grow as compared to usual one by tens, hundreds and less often by thousands and more times. Such cases of anomalous intensity increase which correspond to the appearance of solar comic rays in years of high solar activity are observed several times a year.

Fluctuations of the intensity of cosmic rays of Galactic origin belong to the second type. They are more gradual in character and their amplitudes are smaller. Fluctuations of this type includes:

a) 27-day cosmic ray intensity. These variations have an amplitude of five-ten per cent and are caused by active regions on the Sun --flocculi existing during several revolutions of the sun about its axis.

b) Sudden decreases of cosmic ray intensity during magnetic storms: Forbush-decreases. During Forbush-decreases the cosmic ray intensity sometimes falls by 30-40 per cent.

- 3 -

c) Secular variations of cosmic ray intensity connected with 11-year solar cycle. At the change of solar activity cosmic ray intensity changes approximately two-fold.

The present report deals with the results of stratospheric measurements of cosmic rays on the basis of which effects connected with bursts of solar cosmic rays, secular cosmic ray intensity variations as well as 27-day cosmic ray intensity variations are investigated.

1. Solar Cosmic Ray Bursts

Bursts of solar cosmic rays in the stratosphere were recorded for the first time in the USSR and independently in the USA in 1958. In the USSR flights of probes-balloons were made in the region of Murmansk and in the USA in the region of Minneapolis and Fort Churchill. According to the date of measurements the stratosphere in the region of Murmansk primary cosmic radiation intensity exceeded the normal level approximately by 2,500 times, on March 3, 1958, and by 40 times on March 17 and July 8, 1958 (2), (3). In 1959 during the flare the increases of cosmic radiation intensity by 200,800 and 2,800 times were recorded on July 10, July 15 and July 17, respectively.

The duration of different bursts varies from a few hours to a few days (4). At large distances from the Earth the solar cosmic ray burst was for the first time recorded during the flight of Sputnik III on July 7, 1959 (5).

In total from 1958 to September 1961 twenty six solar cosmic ray bursts are described in the literature. Twenty

thereof. There were conducted several flights of balloons equipped by instruments and their total weight, which was equivalent to one ton, on July 7, 1958 (5).

During last years the interest for the investigation of solar cosmic radiation bursts has sharply increased which led to a considerable increase of the number of the flights of probes-balloons with instrumentation recording radiation in the upper atmosphere. For instance, the liftings of instruments by large polyethylene envelopes (5-10 metres³) increased from 27 in 1957 to 206 in 1960 in the USA (Winckler's group).

Winckler for the first time successfully exposed photo-nuclear emulsions during solar cosmic ray bursts at high altitudes in the stratosphere (May 12, 1959) and by this method he obtained direct data on the spectrum of particle charges in the burst (6). From these experiments it follows that the main part of particles in the burst is protons. Subsequently this method of the investigation of bursts was widely used in the USA not only on balloons, but also in measurements on geophysical rockets (7).

Investigation of solar cosmic ray bursts is of great interest for knowledge of processes taking place in the Sun's interior and in connection with the general problem of cosmic ray generation. In addition to this investigation of those flares is necessary from the practical point of view for the correct selection of the protection of instrumentation and crews of space ships against radiation.

The problem of radiation protection of cosmonauts from

- 5 -

radiation in the period of solar cosmic ray bursts during flights in interplanetary space can be solved in principle on the basis of the data available on duration, intensity and energy spectrum of particles in bursts.

Basing on this data one can say that an essential and in a number of cases excessive increase of the weight of space ships is needed at the expense of shielding against radiations.

Therefore, for space flights in the near future it is very important to find methods of prediction of solar cosmic ray bursts and of establishing the main regularities of their distribution in interplanetary space. For a successful solution of this new problem it is necessary to conduct complex and systematic investigation of solar activity by astronomical, radio astronomical and other methods at simultaneous continuous recording of cosmic radiation intensity at different points of circumterrestrial outer space, particularly, outside the limits of the Earth's magnetosphere.

1. Cosmic Ray Bursts in the Stratosphere and Correlated Phenomena

Solar ray bursts in the stratosphere usually begin approximately in 1-10 hours after the beginning of chromospheric flares and last from a few hours to a few days (4). In 20-30 hours after the chromospheric burst geomagnetic storms and aurorae begin. By the beginning of magnetic storms or a little bit later a sudden decrease is observed of cosmic ray intensity recorded near sea level and also in the stratosphere at middle latitudes (the Forbush decrease).

- 6 -

Not all cosmic ray bursts in the stratosphere correlate with magnetic storms and Forbush decrease. This correlation is maximum when the chromospheric flare which caused the cosmic ray burst occurs in the region of the central meridian of the solar disk.

Soon after the beginning of the chromospheric flare solar radio emission sharply increases accompanied by ionospheric disturbances. Then a period of space radio emission absorption in polar regions (8), (9) begins.

The latter phenomenon is connected with the arrival of solar protons with energies in the main lower than 100 Mevs (8), (10).

As a rule, cosmic ray bursts are accompanied by the radio emission burst of type IV.

2. Investigation of the Proton Energy

Spectrum in Bursts

Investigation of the energy spectrum was made by the method of measurements of proton absorption in the stratosphere (4), (11).

In a quiet period cosmic ray intensity depending on height has the maximum in the stratosphere at altitudes of 18-22 km. At further increase of height the intensity falls. During bursts the cosmic ray intensity in the stratosphere at high latitudes has no maximum, it continuously increases with the increase of height (see Fig.2). Subtracting from the measured number of particles at different heights during the burst the corresponding data before burst

it is possible to plot the so-called absorption curve — the dependence of the number of recorded particles on the pressure in the stratosphere. During bursts more frequent measurements occur, in a number of cases each 3-4 hours. This permits to obtain information about time variations of the intensity and the primary radiation spectrum. Graphs in Fig.3 illustrate the shape of absorption curves obtained during some measurements according to bursts on May 4 and September 3, 1960. Along the ordinate the number of double coincidences is given, along the abscissa pressure in grams per square centimetre is given. Data on the intensity of radiation beyond the atmosphere were obtained by extrapolation of absorption curves for the pressure of 5 g/cm^2 which corresponds the path of protons with energies of 90 Mevs.

As far as absorption curves obtained at different periods of the burst are concerned their inclinations differ little. Therefore, it can be said that slopes of energy spectra do not change considerably with time. Besides, they are close for different bursts which testifies to the universal character of the formation of the solar cosmic ray proton energy spectrum (12).

The constancy of the spectrum is difficult to explain from the point of view of its formation during the burst. It is most probable that the spectrum is produced in the process of the outlet of particles from the magnetic trap into which they are injected after acceleration. The kind of the energy spectrum obtained at this supposition (13) agrees well with the data of our experiments.

- 8 -

The problem of the constancy of the energy spectrum is very important and, therefore, other possibilities of its explanation should be considered. It is not excluded that cosmic rays are generated not in one, single region, but in a few independent regions of the chromospheric flare. If the number of such regions is sufficiently great, then at differences in energy spectra connected with conditions of acceleration of protons in separate regions of the chromospheric flare the energy spectrum observed by the complex of many sources will be averaged and identical for different bursts. But the amplitude of cosmic ray bursts can differ by many times depending on the number and power of sources.

A unique interpretation of the constancy of the energy spectrum of protons generated by the Sun for different bursts is, in our opinion, of great theoretical interest.

The data shown in Fig.3 were obtained during flares which were not followed by geomagnetic storms and Forbush-decreases or before the beginning of geomagnetic storms and Forbush decrease.

Fig.4 shows the same dependencies, but obtained in bursts during the period of geomagnetic storms and Forbush-decrease, (Data on May 12, July 12, July 15, 1959). For this cases the slopes of straight lines drawn through experimental points also differ little. The conclusion on the universality of energy spectra for different bursts can be drawn here too, though the steepness of the particle energy spectrum in the bursts followed by magnetic storms and Forbush-decreases are much higher than in the first case.

- 9 -

Two kinds of the spectrum: a relatively slightly sloping spectrum before a magnetic storm and a steep one during a magnetic storm for the same burst were observed by us for the first time during experiments on July 11-12, 1959 (4). Later the same result was obtained during the burst on November 15, 1960 (14) and also in the USA on November 12, 1960 over Minneapolis during the flare on November 15, 1960 (15) which led to the conclusion that the increase of the steepness of the proton spectrum during magnetic storm is followed by a considerable increase of the intensity of recorded protons (14).

Averaged (according to the date of different bursts) proton integral spectra are given in Fig.5 (12). The intensity of primary protons in relative units is given along ordinate, and proton kinetic energy in Mevs is given along abscissa. Spectrum 4 with the exponent $\chi=5.5$ is given from the data of measurements during Forbush-decreases. Spectra 1,2 and 3 correspond to the results of measurements obtained in the absence of Forbush-decrease. The difference in curves 1,2 and 3 is the following: curve 1 corresponds to scaling of the height of the point of measurements to proton energy with ionization losses taken into account (the same refers to curve 4). Curve 2 is the same as curve 1, but proton absorption in nuclear collisions in the air is taken into account. Curve 3 as curve 2 is obtained with approximate consideration of proton diffusion time in interplanetary space depending on their velocity. Thus the following conclusion can be made: energy spectra of the protons of solar cosmic rays differ considerably before and during Forbush-decreases.

- 10 -

In the first case the exponent of the integral spectrum
 $\gamma = 2$, in the second case $\gamma = 5$.

3. Interpretation of the Energy Spectrum

Softening During Forbush-Decrease

It is common knowledge that Forbush-decrease effects correlate with magnetic storms. The commencement of magnetic storms is associated with the arrival to the Earth of solar corpuscular streams ejected during the chromospheric flare. There are several interesting approaches to the theoretical description of the phenomenon of the Forbush-decrease (Elliot, Dorman, Parker, Ehrent, Stepanyan and others). But for our purpose it is sufficient to point out the essence of the problem. According to Alfvén corpuscular streams from the Sun-solar plasma streams-carry "frozen in" electromagnetic fields which shielding the Earth cause a decrease of primary cosmic ray intensity.

Protons of solar cosmic rays arrive to the Earth earlier than corpuscular streams from the chromospheric flare which caused the solar cosmic ray burst. Hence, by the moment of the arrival of corpuscular streams to the Earth, space around the Sun, at least within the limits of a few Astronomical Units, is filled with solar cosmic rays. The fact of the proton energy spectrum softening during the Forbush-decrease can be explained only by the supposition on a new proton source connected with the corpuscular stream of the chromospheric flare. The following picture can be imagined:

- 11 -

A part of cosmic ray protons produced during the chromospheric flare leaves the Sun and soon comes to the Earth. For them the energy spectrum has an exponent $\gamma \sim 2.0$. The other part of protons being trapped by corpuscular streams magnetic clouds cannot leave freely the Sun. For energies of protons produced by the Sun the strengths of magnetic fields frozen in corpuscular streams are considerable (This follows directly from the decrease of the intensity of cosmic rays of galactic origin). Therefore, particles trapped by magnetic clouds of corpuscular streams in the process of their production cannot rapidly diffuse and leave the streams. These particles are carried away into interplanetary space together with corpuscular streams. They are recorded when the Earth is inside these corpuscular streams. Hence, one can say that the spectrum with the steep slope ($\gamma \sim 5.0$) gives an energy distribution of protons localized and transported in the corpuscular stream of the chromospheric flare. Thus, we come to the conception on the existence of peculiar magnetic traps of fast protons in the corpuscular stream of the chromospheric flare which spreads in interplanetary space (4), (11), (12), (14).

4. Production of Large and Low Energy Cosmic Rays on the Sun

At sea level bursts of solar cosmic rays are recorded which consist particles of sufficiently large energies (about 3-5 Revs). In the stratosphere particles with an energy of hundreds of Mevs are recorded. Does the correlation of intensities of particles in bursts recorded in the

- 12 -

stratosphere and at sea level exist? In other words, does the particle energy spectrum retain at solar cosmic rays bursts in the energy interval from 10^8 to $3 \div 5 \cdot 10^9$ ev/ μ . In table 1 data are given on the bursts in the stratosphere and at sea level. As is evident from the table, there is no correlation between measurements at sea level and in the stratosphere.

- 13 -

TABLE I

The Date of the Chromospheric Burst		Measurements in the Stratosphere	Measurements at Sea Level (in per cent).
March 17, 1958	10 h 25m	35	< 2
July 7, 1958	0 h 58m	40	< 1
May 11, 1959	20 h 55m	40	< 1
July 10, 1959	02 h	200	< 1
July 14, 1959	04 h	200	< 1
July 16, 1960	21 h	2,800	5
May 4, 1960	10 h 15m	35	10
September 3, 1960	00 h 40m	70	3
November 12, 1960	13 h 22m	1,200	150
November 15, 1960	02 h 07m	500	80
November 20, 1960		7	5
July 18, 1961	09 h 30m	140	12
July 20, 1961	15 h 50m	13	3

Fig.6 shows proton energy spectra from terrestrial and stratospheric data on May 4, 1960, and November 15, 1960. From the figure it is evident that particle spectra in the low energy region are equal for both bursts and in the high energy region they differ greatly.

Thus, the negative answer should be given to the question on the rotation of the solar proton spectrum in the wide energy interval.

- 14 -

5. Primary Protons Intensities as a Function of Time

Having carried out measurements in the stratosphere during the different periods of the burst we could plot the temporal dependence of primary proton intensity in bursts $N_p(t)$ according to data of absorption curves and their extrapolation. $N_p(t)$ values obtained during measurements on May 4-5 and September 3-5, 1956, are given in Fig.7. $t=0$ is assumed for the beginning of the corresponding chromospheric flares.

Errors for the data in Fig.7 are in the main connected with the extrapolation of the results of measurements (up to the pressure of 5 g/cm^2). For the majority of points these errors are about 20-30 per cent. Great duration of the flare in May is mainly due to the gently sloping section of curve 2.

It is interesting to compare values $N_p(t)$ obtained in the stratosphere for primary protons with energies more than 0.1 Bev with the data for the flare on February 23, 1956, obtained for primary protons with much higher energies (3-4 Bevs). From Fig.7 is evident that the decrease rate of the high-energy proton intensity is approximately five times higher than the decrease rate for low-energy particles.

6. Diffusion of Solar Cosmic Ray Protons in Interplanetary Space

The above mentioned measurements of large solar cosmic ray bursts, for instance, the burst on February 23, 1956, permitted the determination of the dependence of additional

- 15 -

radiation intensity on time. This dependence in a wide time internal following the burst maximum was described well by the law $t^{-3/2}$.

The intensity of additional radiation by this time became sufficiently isotropic. On the basis of the solution of the diffusion equation free-path lengths and strengths of magnetic fields were found which lead to scattering of high-energy protons observed during solar flares at sea level 3 ± 5 Bev μ — see Table 2 (16), (17).

During investigation of the time dependence of solar proton intensity in the stratosphere free-path lengths and strengths of magnetic fields ensuring scattering and diffusion of protons with the energy 0.1 Bev were determined. In Fig.8 theoretical and experimental dependences of intensity variations on time are given. The best coincidence of experimental and theoretical curves is obtained at the diffusion coefficient equal to $D = 5.5 \cdot 10^{21} \text{ cm}^2$ per sec. In Table 2 the free-path length in this case and the strength of magnetic fields are given.

TABLE 2

Proton Energy	Proton Pulses ($\text{cm}^{20} \text{sec}^{-1}$)	($\text{cm}^4 \text{m}$)	H (Gauss)
3-5 Bev μ	$5 \cdot 10^9 \text{ ev}/\mu/\text{c}$	$2.7 \cdot 10^{22}$	$2.7 \cdot 10^{12}$ $6.2 \cdot 10^{-6}$
0.1 Bev μ	$5 \cdot 10^8 \text{ ev}/\mu/\text{c}$	$5.5 \cdot 10^{21}$	$1.1 \cdot 10^{12}$ $1.5 \cdot 10^{-6}$

Assuming the power law of the diffusion coefficient on proton pulse $D(p) \sim p^\alpha$ we obtain $\alpha \sim 0.7$. Approximately the same dependence $D(p)$ follows for the proton energy interval 5-15 Bevs from comparison of data of a neutron monitor and an ionization chamber during the burst on February 25, 1956.

As evident from Fig.8, two experimental points for the beginning of the burst strongly differ from data of calculated line for $t=0$ and agree better with the curve for $t=0.3$. However, it is impossible to make a conclusion that cosmic ray production delayed as compared to the commencement of the chromospheric flare. Such a conclusion is difficult to make since the data of the calculations of curves are not sufficiently accurate. This inaccuracy is connected mainly with the supposition on the constancy of the diffusion coefficient in space. Actually one should believe that the value of the diffusion coefficient is greater than mean one in space closer to the Sun and lower beyond the Earth's orbit. Therefore, qualitatively one can understand why the data of the experiment for the beginning of the flare's development lie below the calculated line for $t=0$. If a reasonable assumption is made that for the initial section of the curve the effective diffusion coefficient is higher than the mean one by thirty-fourty per cent, then it is possible to describe experimental data for $t=0$.

As evident from Fig.8 for large values of t the results of the experiment lie below the calculated straight line. Such result also can be explained on the basis of the assumption that the value for space beyond the Earth's orbit is

- 17 -

lower than the average value. Therefore, one can say that on May 4 if the delay of low energy cosmic rays production took place, as compared to the beginning of the chromospheric flare, it was less than 20 minutes.

7. On Bursts of Cosmic Rays Generated on the
Reverse Side of the Solar Disk. The Sun's
Radial Magnetic Fields

Chromospheric flares in the process of which cosmic rays are produced should occur equally frequently on the visible and on the reverse sides of the Sun. Investigations of the cases of cosmic ray production on the reverse side of the Sun will make it possible to obtain additional data on the structure of electromagnetic fields in interplanetary space.

If propagation of solar protons in interplanetary space is of a diffusive character, in one-two hours after cosmic ray production on the Sun radiation into space will be isotropic and conditions for records of protons of cosmic rays near the Earth produced on the visible and reverse sides of the Sun will be close. In this case solar cosmic ray bursts produced on the reverse side of the Sun should be recorded in the stratosphere.

We attempted to separate from recorded cosmic ray bursts in the stratosphere those bursts which might be due to chromospheric flares occurring on the back side of the Sun. For this purpose out of 26 cosmic ray bursts known to us we separated those bursts which were undoubtedly caused

- 13 -

by chromospheric flares on the visible side of the solar disk (18).

It is known that many cases of cosmic ray bursts in the stratosphere are accompanied by geophysical and radio astrophysical phenomena: magnetic storms, ionospheric disturbances, auroras, Forbush effects, cosmic radio emission absorption in the polar cap, etc. Magnetic storms, auroras and Forbush-decreases are associated with the arrival to Earth of corpuscular streams ejected by the Sun during chromospheric flares. The direction of motion of corpuscular streams is almost radial. Therefore, corpuscular streams of chromospheric flares occurring only on the visible side of the solar disk come to Earth. Hence the cosmic ray bursts in the stratosphere accompanied by a Forbush-decrease, magnetic storms and auroras can be accounted for by chromospheric flares on the visible side of the solar disk. In addition it is known that chromospheric flares producing cosmic ray bursts in the majority of cases give radio emission of type IV. Therefore, if a cosmic ray burst was preceded by a chromospheric burst accompanied by radio emission of type IV it can be believed that the cosmic ray burst was caused by this chromospheric flare.

The cosmic ray bursts selected according to these signs are listed in the first part of Table 3 where the date of the burst and primary proton intensity are indicated. It is very probable that 17 cosmic ray bursts mentioned in the table are produced by chromospheric flares on the visible part of the solar disk.

- 19 -

TABLE 3

The Order Number	The Date	The Maximum Recorded ← Increase
1.	March 17, 1958	35
2.	March 26, 1958	15
3.	July 8, 1958	40
4.	August 22, 1958	10
5.	August 26, 1958	2
6.	May 11, 1959	40
7.	July 10, 1959	200
8.	July 15, 1959	800
9.	July 17, 1959	2,000
10.	April 1, 1960	4
11.	May 4, 1960	35
12.	September 3, 1960	70
13.	November 12, 1960	70
14.	November 15, 1960	500
15.	July 12, 1961	10
16.	July 19, 1961	140
17.	July 20, 1961	10
<hr/>		
1.	March 3, 1958	2,500
2.	October 3, 1958	2
3.	July 9, 1959	2
4.	April 28, 1960	2
5.	April 29, 1960	2

- 20 -

6.	May 12, 1960	3
7.	May 13, 1960	5
8.	November 21, 1960	7
9.	May 9, 1961	5

In the second part of the table solar cosmic ray bursts are given which cannot be explained with definite certainty by chromospheric flares on the visible side of the disk, though some of them were preceded by chromospheric flares. The flare on March 3, 1959, was preceded by a chromospheric flare on March 1 at 3 hours 14 min (the importance of the flare is 5). There is no information about radio emission burst of type IV. However, it is known that from March 3 (6 hours) to March 8 (18 hours) an auroral display was observed in Ushuaia. Therefore it is quite possible that this burst also was caused by a chromospheric flare on the visible side of the Sun.

The magnitudes of cosmic ray burst amplitudes in the first and second parts of the table differ. With the exception of March 3, the amplitudes of the bursts in the second part of the Table appear mainly two orders of magnitude lower than those in the first part.

Thus, it is possible that in the stratosphere solar cosmic ray bursts produced on the reverse side of the Sun's disk, but with much lower amplitudes are recorded. This result testifies to the predominant direction of the motion of protons from the side of the Sun on which cosmic rays were produced. However, this conclusion will not contradict con-

- 21 -

options on the diffusive propagation of solar cosmic rays if one supposes that apart from magnetic inhomogeneities there are also radial solar magnetic fields in interplanetary space. If the strengths of radial magnetic fields and fields of inhomogeneities do not differ greatly one can expect anisotropically diffuse proton propagation on the side of the Sun on which cosmic ray burst occurred. Most probably these fields are of a stationary character. This result agrees with the conclusion made for the first time by Vitkevich on the existence of radial magnetic fields of the Sun based on radio astronomical data on propagation of electron inhomogeneities in space of the solar supercorona (19).

III. Secular Cosmic Ray Intensity Variations

It is well known that cosmic ray intensity undergoes secular variations associated with the 11-year solar cycle (20). During the period of high solar activity cosmic ray intensity falls and for the period of the minimum it increases. The amplitude of variations in the mu-meson component at sea level is approximately 5 per cent, and in the nucleonic component it is 20 per cent. Variations of the nucleonic component on the Earth are due to modulation of primary cosmic radiation in the region of their energies mainly higher than 5 Bevs. Variations of the mu-meson component are caused by the primary component of much higher energies. The data on variations of the intensity of primary radiation with particle energies lower than 5 Bev can be obtained by measurements in the stratosphere. The cosmic ray intensity at high altitudes in the stratosphere at northern latitudes during the period of

- 22 -

the solar activity maximum is about two times lower than in the period of the minimum (21). The results described below are based on the great number of measurements. They enabled us for the first time to obtain continuous data on the secular variations of cosmic ray intensity in the stratosphere at a latitude in the region beyond the Polar Circle and simultaneously at lower latitudes. The results of more than three thousand measurements obtained by means of a single Co gas counter have been analyzed.

2. Secular Variations of Integral

Intensity

at 41, 51 and 61 Degrees of the Geomagnetic Latitude

Data of average values of the maximum intensity of particles in the stratosphere are considered at latitudes of 61°, 51 and 41 degrees situated at depths of about 50, 60 and 70 g/cm², respectively. Those results which were obtained during cosmic ray intensity bursts in the stratosphere and those which were distorted by radiations of radio-active clouds from atomic explosions in the atmosphere have not been treated. However, the number of such cases was small as compared to the total number of measurements.

Fig.9 gives mean monthly values of the cosmic ray intensity maximum at three latitudes. The number of particles N_{max} cm⁻² sec⁻¹ is given along the ordinate and time t, sec, along the abscissa.

Points in the figure correspond to mean values of measurements for more than 10 flights per month in 1957-1958

and since 1959 for 15 flights and more. Such frequency of measurements during the time of observations in the region of the intensity maximum of about 8 minutes gives a statistical error of measurements of about 0.25 per cent. As a result of each measurement corrections are made which take into account the difference in the efficiency of counters (22).

From the figure is evident that there are many irregular cosmic ray intensity fluctuations which in the majority of cases correlate at different latitudes. The correlation of data is especially high for latitudes 51 and 64 degrees. At a latitude of 41 degrees the secular variation of cosmic ray intensity (except results referring to the second half of 1958) correlate well with the data of ground measurements of the neutron monitor at Deep River (23). Some fluctuations are caused by magnetic storms and Forbush-decreases in the stratosphere which followed them (24). Such, for instance, are data for September 1957, March, April and July 1958, May and July 1959, April and November 1960, July 1961 and others.

However, against the background of irregular fluctuations one can see the general increase of cosmic ray intensity. It is the greater, the higher is the latitude of the place of observations. The intensity of cosmic rays at the end of 1961 at a latitude of 64 degrees increased by approximately 40 per cent and at a latitude of 51 degrees by 25 per cent as compared to 1957. For a latitude of 41 degrees this increase was less than 10 per cent as compared to 1958. From this it follows that the cosmic ray intensity increase in the stratosphere took part predominantly at the expense of

primary particles with energies lower than 4.6 Bev.

As evident from Fig.8, the increase of the number of particles with time at latitudes of 51 and 64 degrees does not take place continuously. In the period from July, 1957, during approximately two days, i.e. to the end of 1960, it remained almost constant. But in January-February 1961 a sharp increase of the cosmic ray intensity level is recorded, and in November of the same year this level again sharply increases. Thus secular variations of cosmic ray intensity in the stratosphere in the considered period are of a stepwise, leaplike character. Below we shall consider how this correlates with the change of solar activity.

9. Secular Variations for the Difference

of the Number of Particles

Fig.10 shows the differences of the number of particles ΔN^{64-41° and ΔN^{51-41° obtained as a result of subtraction from the measured number of particles at latitudes 64 and 51 degrees of the number of particles for latitude 41° . These differences are given for flights coinciding in time at corresponding latitudes (about 60 per cent of the total number of particles). Secular variations for the difference of the number of particles are due to secular variations of the intensity of primary cosmic rays with particle energies from 0.1 to 4.6 and from 1.5 to 4.6 Bev. Let us note that about 70 per cent of the number of primary particles have energies lower than 4.6 Bev.

As evident from Fig.10, stepwise variation is characteristic also of the difference of the number of particles.

- 25 -

Besides two steps displaying for total intensity one more stage is here displayed for February and March 1959.

According to Fig.10 $\Delta N^{51-41^{\circ}}$ in December 1958 increased as compared with 1958 by approximately 60 per cent, and

$\Delta N^{64-41^{\circ}}$ by almost 100 per cent. At the same time the increase for the total number of particles recorded at latitude 51° for the same time interval is almost 20 per cent. It is natural that the increase in the primary component intensity for the considered period is higher.

10. Correlation with Solar Activity

Solar cosmic ray events, cosmic-ray intensity decreased during magnetic storms correlate with solar chromospheric flares, and secular variations correlate with the 11-year molar cycle.

In Fig.11 along the ordinate are given average values of the maximum of the number of particles at latitude 51° — solid dots, the scale is on the left, average monthly values of the sun-spots number are indicated by crosses, the scale on the right is a logarithmic scale. The data on Forbush-decreases which had amplitudes more than 3 per cent and lasted more than three days (according to the neutron monitor in Deep River) are given along the abscissa by squares.

In Fig.10 it is not difficult to note that there is a definitely expressed correlation between cosmic-ray data and the sun-spots number. With the exception of the period from July 1957 to the middle of 1958 about which we shall say below, the secular variation of the sun-spots number and cosmic-ray intensity is almost identical. The stepwise

- 26 -

character of the cosmic ray intensity growth in 1961 about which it was said above turns to be characteristic for the sun-spots number. Steps in secular variation for R refer approximately to the same time as for cosmic rays.

The revealed character of closed correlation of cosmic ray intensity with the number of solar spots is unexpected, in particular, in the part which refers to a logarithmic correlation between cosmic ray intensity and the number R. It turns out that the effect of the change in sun-spots number on cosmic ray intensity is the greater, the lower is the R-phenomenon which now it is difficult to interpret.

In conclusion let us dwell upon the data which refer to the period from July 1957 to the middle of 1958 (Fig.11). In this time interval the correlation between the sun-spots number and cosmic ray intensity is violated. But, as is evident from the figure, this period is characterized by rather frequent cases of the Forbush-decrease. In some cases several individual Forbush-decreases imposed on each other. These frequent decreases are probably the main cause of the violation of correlation between cosmic ray intensity and sun-spots number which is clearly seen since the middle of 1958.

III. 27-day Variations of Cosmic Radiation

Intensity

As a result of the experiments at sea level and at mountain heights the existence is established of 27-day cosmic ray variations connected with the Sun's revolution about its own axis. It was also shown that 27-day cosmic ray intensity

- 27 -

variation is noticeably expressed in the years of solar activity maximum and is weakly expressed during the years of solar activity minimum.

Investigation of variations of 27-day periodicity according to data of measurements at low altitudes is a complicated problem. In this case variations are to a considerable extent masked by different meteorological effects. Inaccurate consideration of corrections connected with the changes in the temperature and pressure of the atmosphere leads to errors commensurable with variations of cosmic rays of extra-atmospheric origin. More direct data on primary cosmic ray variations can be obtained in experiments at high altitudes where these variations are mainly of extra-atmospheric origin.

Systematic observations in the stratosphere have resulted in the establishment of stable variations in the period from July 1957 to February 1958. In successive years 27-day variations of cosmic ray intensity were absent or were expressed weakly. So, in the period from February 1 to July 1, 1958, the amplitude of the 27-day variation in the stratosphere decreased almost by five times.

To reveal 27-day variations, the values of intensity referring to the maximum of cosmic ray absorption curve were used. The time of the instrument's stay at a height of the maximum was about 10 minutes which ensured statistical accuracy of measurements of about 1 per cent.

The recorded intensities in the maximum were then treated by the method of periodograms. Fig.12 gives periodograms for the period from July 1, 1957, to February 1, 1958. In the region of 27-28 days a sharply expressed maximum is

seen in the periodogram. The straight line in Fig.12 shows the average level of amplitudes during accidental distribution of the data of measurements in the stratosphere. Thus in this period a 27-day cosmic ray variation with the amplitude of 5.5 0.6 per cent was observed in the stratosphere. In this figure periodograms are given for the neutron monitor at latitude 52° and for K-index. From the figure is evident that data of stratospheric measurements and neutron monitor correlate well between themselves, and there is no correlation between 27-day variations of cosmic ray intensity and the K-index.

Fig.13 gives deviations (in per cent) of the intensity from the average value as a function of time. The data for the neutron monitor and ionization chamber are increased in accordance with the ratio of their amplitudes to the amplitude of intensity variation in the stratosphere. This figure shows that the shape of a 27-day wave for different cosmic ray components coincides in phase with the accuracy of 1-2 days and is close to a sinusoid. This sinusoid is shown in the figure by a dashed line.

At present it is assumed that the modulation of cosmic ray intensity is caused by corpuscular streams from the active regions of the Sun. If a 27-day variation can be really explained by cosmic ray modulation by solar corpuscular streams, then the cosmic ray intensity minimum should be preceded by the passage of the active regions of the Sun through the central meridian. The time delay of the intensity minimum with respect to the time of the passage of active

- 29 -

regions through the central meridian for a period from July 1, 1957, to February 1, 1958, turned to be equal to about 20 days. It follows from such a delay that the velocities of the motion of corpuscular streams from stable regions on the Sun are on the order of 10^7 cm/sec. The closeness of the shape of the wave to a sinusoid shows that streams responsible for 27-day cosmic ray variations are not narrow.

Radiation Investigations During "Mars 1" and
"Lunik 4" Flight.

The Mars 1 probe carried instrumentation for investigations of cosmic rays in interplanetary space and of the Earth's radiation belts at the section of its flight trajectory near the Earth. This instrumentation consisted of two scintillation counters and two gas discharge counters. One of the scintillation counters situated inside the probe had a cylindrical crystal Na I with the diameter 20 mm and height 20 mm. By means of this counter the measurement was made of total ionization produced by radiation in the crystal as well as the counting of the number of cases when in the crystal energy is released above the prescribed one, namely, above 30 Kev and higher 2.5 Mev.

The second scintillation counter with a cylindrical crystal CsI 20 mm in diameter and 3 mm in height was installed outside the probe's container. The crystal of this counter on the side of free space in a solid angle of about 3 steradians was covered by a thin aluminium foil of about 2.2 mg/cm^2 . In other directions the crystal and photomultiplier were covered by the aluminium layer with the thickness of about 1 g/cm^2 .

This scintillation counter recorded total energy released by radiation in the crystal and the number of particles which released in the crystal energy higher than 30 Kev. Electrons of energy 70--80 Kev and protons of energy 500 Kev can be such particles.

Geiger counters (the working length is 50 mm, the diameter is 10 mm) were installed inside the probe.

Measurements of ionization and counting rate of scintillation and gas discharge counters were carried out by the same methods as on previous Soviet Sputniks and Luniks (25).

On Lunik 4 launched on April 4, 1963, a gas discharge counter (the length 50 mm, the diameter 10 mm) was installed for the study of radiation. The counter was installed inside the probe near its shell under the layer of the material of about 1 g/cm^2 . The counter was strongly shielded ($\geq 10 \text{ g/cm}^2$ of the material) from other sides. By means of this counter continuous measurements of cosmic radiation intensity were conducted with the transmission to Earth of the total number of counts between radio contacts. For 24 hours of measurements a statistical accuracy of about 0.07 per cent was ensured. The accuracy of counts number measurements and time measurements is several times higher.

During flight of the Mars 1 probe the dependence of cosmic ray intensity on the increase of distances from the Sun up to 1.24 AU (Astronomical Unit) was investigated.

- 31 -

Results of measurements of cosmic ray intensity using a Geiger counter, ionization and the I threshold of the inner scintillation counter of the Mars 1 probe are given in Fig.14.

For the calculation of time intensity variations investigation of the cosmic ray intensity level in the stratosphere at latitudes 64° (in Murmansk) has been conducted.

Fig.I5 gives counting rates of a single Geiger counter in the intensity maximum (the height 50 g/cm^2) for the period from November 1, 1962, to January 31, 1963.

As evident from the figure, no considerable cosmic ray intensity variations on the Earth were observed and introduction of corrections for these variations will not change the values of cosmic radiation intensity recorded by the Mars I probe at the increase of distances from the Sun.

Within the limits of errors of measurements (about 2--3 per cent) the intensity of cosmic primary radiation at the increase of distances from the Earth by 1.25 AU remains constant.

The dependence of cosmic ray intensity on distance towards the Sun was investigated during flights of American space probes Pioneer 5 and Mariner 2. Pioneer 5 was launched in March 1960 and approached the Sun up to a distance of 0.9 AU. Some decrease of intensity was noted which, however, lay within the limits of errors (26). At the end of 1962 the space probe Mariner II flew in the vicinity of Venus approaching the Sun up to 0.7 AU. No intensity change was detected at the approach to the Sun (27).

Thus in a year close to the solar activity minimum near the orbit of the Earth at distances of 40 million kilometres in the direction from the Sun and to the Sun cosmic radiation intensity remains constant with an accuracy of a few per cent.

In 1959 during flight of Soviet Luniks the most precise data were obtained on the primary cosmic radiation stream beyond the Earth's magnetosphere and on the mean ionizing

- 22 -

power of cosmic radiation particles (28). Let us remind that the cosmic ray stream in 1959 was $I = 1.98 \pm 0.1$ part / $\text{cm}^2 \text{ sec}$. with the mean ionizing power 2.5 times higher than the minimum one.

In 1963 during flights of Mars I and Lunik 4 probes data on cosmic rays are obtained which can be compared with the data of 1959.

In Table 3 cosmic ray streams recorded by Geiger counters aboard "Mars I", "Lunik 4" and other Soviet space probes are given averaged over the total flight time.

Table 4

The Date of Launching	The Place of the Counter Location	The Stream $\text{x}/(\text{cm}^{-2} \text{ sec}^{-1})$
January 2, 1959	Inside the container (without shield)	2.3 ± 0.1
September 12, 1959	Inside the container (in the shield of 3 mm lead and 1 mm aluminium)	2.46 ± 0.1
September 12, 1959	Outside the container at distance of 30 cm (in the shield of 3 mm lead and 1 mm aluminium)	2.0 ± 0.1

$\text{x}/$ The error is due to uncertainty of geometrical dimensions of the counters operational volume.

October 4, 1959	On the shell of the container (in the shield of 3 mm lead and 1mm aluminium)	2.12 ± 0.1
November 2, 1962	Inside the container (without shield)	4.45 ± 0.1
April 2, 1963	Inside the container (without shield)	4.45 ± 0.1

Conditions of shielding of inner counters on space probes on the Mars 1 probe and Lunik IV, are approximately the same. Thus, the cosmic ray particle stream in 1963 exceeds the particle stream in 1959 almost two-fold.

Scintillation counters of space probes and Mars 1 probe had somewhat different characteristics from the point of view of the recording of ionization produced by radiation in the crystal.

The data obtained show that in 1963 the average ionizing power of primary cosmic radiation particles did not increase as compared to 1959.

The complex of data on cosmic ray intensity change from 1959 to 1963 in the stratosphere at latitudes 41°, 51° and 64°, beyond the Earth's magnetosphere and the conclusion on the absence of the increase of the average ionizing power of cosmic ray particles have made it possible to estimate the average energy of particles added in 1963 as compared to 1959. Table 5 gives the ratio of the cosmic radiation intensity and the mean ^{specific ionization} ~~ionizing power~~ in 1963 as

Table 5

The Place of Measurements	In the Intensity Maximum in the Stratosphere			At a Distance of 100,000-700,000 km from the Earth	
	$\lambda = 41^\circ$	$\lambda = 51^\circ$	$\lambda = 54^\circ$	The Stream	Specific Ionization
The Ratio of Intensity in 1953 to the Intensity in 1959	I.I	I.25	I.45	I.95	≤ 1.0

Such a change of the number of particles at different latitudes can be caused by additional particles of sufficiently high energy ($i=5$ Bev) with the spectrum close to the primary cosmic radiation spectrum.

In Fig. I6 data are given obtained during the entire time of the work of space probe Lunik 4. The average value of the counter's counting rate is 19.157 ± 0.005 counts per second. Maximum deviations from the average value are ± 2.5 per cent at the accuracy of each measurement of about ± 0.1 per cent. In the process of flight the voltage of power supply of instrumentation was kept stable with high accuracy. The change of the intensity due to temperature fluctuation inside the probe was for this time less than 0.5 per cent. We do not see other instrumentation causes of

intensity change and we consider that recorded intensity fluctuations are actual.

In the same figure results of measurements of cosmic radiation intensity in the stratosphere in the region of Murmansk are given for the same period of time.

The change of intensity in Murmansk is not correlated with the change of intensity recorded by Lunik 4. From this one can conclude that intensity fluctuations recorded during Lunik 4 flight are due to particles with energies which are not recorded in the maximum of the absorption curve in Murmansk (the height 50 g/cm²), i.e. with energies $1 \text{--} 2$ Bev. In any case one can state that the spectrum of particles causing the recorded intensity variations is softer than the spectrum of particles responsible for 11-year changes in cosmic ray intensity.

During flights in interplanetary space of spare probes "Lunik 3", "Pioneer 5", "Mariner 2" and "Mars 1" time intensity variations with the amplitude of a few per cent were recorded. Therefore, the unexpected one is not a value of the change of intensity recorded by Lunik 4, but the gradual character of this variation. In a year close to solar activity maximum during flight of Lunik 3 intensity changes were leapwise in character and correlated well with terrestrial intensity variations (with the counting rate of a neutron monitor). It is not excluded that during the period of the solar activity minimum the sporadic processes on the Sun leading to sharp fluctuations of cosmic rays intensity take place

rarely or do not occur at all, and the change of magnetic situation in circumterrestrial outer space due to temporal change of the character of the solar wind begins to play part. In this case the periodicity of the change of magnetic situation in interplanetary space may be associated with the time of corpuscular stream propagation in the solar system, i.e. with the time on the order of 5--10 days. The periodicity of such scale has been observed by Lunik 4.

The records of radiation in the Earth's radiation belts was made during the flight of the Mars 1 probe from the Earth. Fig.17 gives radiation intensities depending on a distance from the Earth's centre. First of all the small extent of radiation belts draws one's attention. This is explained by the fact that the trajectory of the Mars 1 probe strongly differed from the trajectories of the first Soviet Luniks which crossed the outer radiation belt near the equator. During flight near the equator the Mars 1 probe crossed the inner belt and then on its path away from the Earth it crossed the outer radiation belt at high geomagnetic latitudes.

The most surprising is the absolutely identical character of the curves recorded by different counters. So, curve V showing the intensity of electrons with energy 70--80 Kev (or protons with energy 500 Kev.) is absolutely the same as the curve of the counting rate of a gas discharge counter which efficiently records electrons with energy 8 Mev (or protons with energy 50 Mev.) During this flight

-38-

and before it no considerable geomagnetic field disturbances were recorded. The passage of the outer boundary of the outer belt by the Mars 1 probe was near the local midnight.

Due to different flight trajectories of lunar probes and Mars 1 it is very difficult to compare the states of the belts in 1963 and 1959. Fig.18 gives values of energy releases in NaI crystals for Lunik 2 and the Mars 1 probe as a function of the L value characterizing the given magnetic shell (29). It is clear from the figure that the character of the outer boundary of the outer radiation belt differs for Lunik 2 and Mars 1 probe. Lunik 2 left the outer belt near the equatorial plane, but the Mars 1 probe did this at high latitudes. If it is assumed that the state of belts for the time elapsed from September 1959 to November 1962 did not change one can make a conclusion on the presence of sharper boundary of the outer radiation belt at high latitudes than near the equatorial plane. In other words, at large L trapped particles with low reflection points are absent. However, it is the most probable that the change of the shape of the outer radiation belt should be ascribed to temporal variations detected for the first time during flight of Soviet space probes (28) and investigated in detail during flight of the American satellite Explorer 7 (30).

It is not excluded that this coolution in the shape and dislocation of the belt's boundary is associated with the difference in local time of the passage of the belt's boundary. This effect was for the first time revealed during

-39-

flights of the American satellite Injun I by means of a counter which recorded electrons with energy > 40 Kev (31).

It turned out that at low altitudes of the satellite's flight (about 1,000 km) at local midday the boundary's belt lies at higher geomagnetic latitudes than at local midnight. Table 6 gives the moments of the passage (local time) of the boundary of the outer radiation belt and the parameter of the boundary magnetic shell according to the data of Soviet lunar rockets and Soviet Venus I and Mars I probes. The magnetic shell during the crossing of which the energy release in the crystal exceeded 10 times the energy release from cosmic rays was taken for the boundary of the belt.

Table 6

	The Local Time of the Passage of the Belt's Boundary	L		
		The Date	Hours	Minutes
Lunik I	Jan. 3, 1959	6	30	6.7
Lunik II	Sept. 12, 1959	20	30	6.5
Lunik III	Oct. 4, 1959	14	30	-
The Venus I Probe	Febr. 12, 1961	14	50	6.1
The Mars I Probe	Nov. 2, 1962	21	30	6.0

-40-

After the emergence from the Earth's radiation belts all the penetrating radiation detectors of Mars 1 probe record almost constant radiation intensity which, however, considerably differs from primary cosmic radiation.

In Table 7 the values are listed of recorded particle streams and energy by all detectors after coming out of the radiation belt.

Table 7

Detectors	The Inner Scintillation Counter		The Outer Scintillation Counter		Geiger Counter
	Ionization	The Threshold 30 kev	The Threshold 2 Mev	Ionization	
Energy Release and Counting Rate	$8 \cdot 10^8$ ev/sec	$2 \cdot 5 \cdot 10^3$ puls/sec	20 puls/sec	10^{10} ev/sec	$4 \cdot 10^3$ puls/sec
					30 Puls/sec

Mean energy released in the crystal per one count of the outer scintillation counter is about 2 Mev/count. The counting rate of the gas discharge counter is about 10^3 times lower than that of the scintillation counters for the threshold of about 30 kev. This indicates that the recorded radiation constitute electrons with energies of about 2 Mev

-41-

directly recorded by outer and inner scintillation counters and for bremsstrahlung by a Geiger counter (The Geiger counter had larger shielding than the crystal of the inner scintillation counter).

Since the stream of recorded electrons turned to be very stable in time it is natural to suppose that they are the decay product of long-living radioactive nuclei.^{x/} The irradiation of Mars 1 probe by the protons of the inner belt leads to the appearance of induced radioactivity. On the other hand, radioactive nuclei formed in the atmosphere as a result of nuclear explosions over Johnson Island carried out not long before Mars I flight might accumulate at the surface of the Mars 1 probe. However, the estimate of the number of radioactive nuclei produced during these effects shows that they are not enough for the explanation of the observed counting rates of radiation detectors of Mars 1 probe.

Therefore, it is probable that the observed effect is caused by the appearance of energetic electrons of unknown origin in the vicinity of the Earth.

^{x/}

For 1 hour of measurements the radiation intensity decreased lower than by 5 per cent.

- 42 -

REFERENCES

1. J.J.Quenby and C.J.Wenk, *Izv. Akad. Nauk SSSR, Ser. Fiz.*, 7, 1961.
2. N.P.Rymko, V.F.Tulinov and A.N.Charakhchyan,
The Journal of Experimental and Technical Physics,
USSR, 36, 1687, 1952.
3. A.N.Charakhchyan, V.F.Tulinov, T.N.Charakhchyan,
Geomagnetism and Astronony, 1, 150, 1961.
4. A.N.Charakhchyan, V.F.Tulinov, and T.N.Charakhchyan,
J.E.T.Ph., 39, 249, 1960.
5. E.V.Gorchakov and G.A.Bazilcvskaya,
Artificial Earth Satellites, Vol.8, 84, 1960.
6. J.R.Winckler, and P.D.Bhavsar, *J.Geophys.Res.*, 65, 9,
2637, 1960.
7. L.P.David, and K.W.Ogilvie, *J.Geophys.Res.*,
67, 5, 1962.
8. A.S.Besprozvannaya, and V.M.Driatskiy,
Investigations of the Ionosphere (a collection of papers),
5,7 the Publishing House of the USSR Academy of Sciences,
1960.
9. N.I.Fedyakin, *Investigations of the Ionosphere*, 5, 20,
1960.
10. G.C.Reid, and H.Leinbach, *J.Geophys.Res.*, 64, 1081,
1959.
11. A.N.Charakhchyan, V.F.Tulinov and T.N.Charakhchyan,
J.E.T.Ph., 38, 1031, 1960.
12. A.N.Charakhchyan, V.F.Tulinov and T.N.Charakhchyan,
J.E.T.Ph., 41, 735, 1961.

- 43 -

13. S.I.Syrovatsky, Problems of Magnetic Hydrodynamics and Plasma Dynamics, The Publishing House of the Latvian Academy of Sciences, 1961.
14. A.N.Charakhchyan, V.F.Tulinov, and T.N.Charakhchyan, Geomagnetism and Aeronomy, 1, 494, 1961.
15. E.P.Ney, and W.A.Stein, J.Geophys.Res., 67, 2087, 1962.
16. P.Meyer, E.N.Parker, and J.A.Simpson, Phys.Rev., 104, 768, 1956.
17. C.J.Dorman, Nuevo Cimento, 8, 391, 1953.
18. A.N.Charakhchyan, and T.N.Charakhchyan, Geomagnetism and Aeronomy, 2, 829, 1962.
19. V.V.Vitkevich, Dissertation for a Doctor's Degree, Physical Institute of the USSR Academy of Sciences, 1962.
20. Physics of Elementary Particles and Cosmic Rays, pp.318-321, Moscow, 1960.
21. Physics of Elementary Particles and Cosmic Rays, pp.282-287, Moscow, 1960.
22. S.N.Vernov, V.F.Tulinov, and A.N.Charakhchyan, Dokl. Akad.Nauk,SSSR, 122, 5, 1958.
23. The Second World Centre of Data, Neutron Monitor Deep River.
24. S.N.Vernov, B.E.Samosudov, V.F.Tulinov, A.N.Charakhchyan, and T.N.Charakhchyan, Proc.Intern.Conf.Cosmic Rays, Vol.IV, p.49, The Publishing House of the USSR Academy of Sciences, 1960.

- 44 -

25. P.V.Vokulov, N.N.Goryunov, Yu.I.Logachev, and E.N. Sosnovets, Geomagnetism and Aeronomy, 1, 880, 1961.
26. C.Y.Pan, P.Meyer, and J.A.Simpson, Phys.Rev.Letters, 5, 272, 1960.
27. NASA Press Conference on February 1963 on the Results of Mariner II Flight.
28. S.N.Vernov, A.E.Chudakov, P.U.Vokulov, Yu.I.Logachev, and A.G.Nikolayev, Dokl. Akad.Nauk SSSR, 150, 517, 1960.
29. C.B.McMillain, J.Geophys.Res., 66, 3681, 1961.
30. S.Forbush, G.Pizzella, and D.Venkatesan, J.Geophys. Res., 67, 10, 3651, 1962.
31. B.J.O'Brien, J.Geophys.Res., 68, 4, 989, 1963.

- 45 -

Figure Captions

Fig.1 A diagram of a radiosonde.

Fig.2 Altitude Intensity variation in the absence of bursts and during solar cosmic ray bursts.

Fig.3. The solar cosmic ray absorption spectrum before the commencement (or in the absence) of a magnetic storm and a Forbush-decrease.

1. Sept. 3, 1960,	the start of the instrument	07 h 00 m
2. Sept. 4, 1960	"	11 h 56 m
3. May 4, 1960	"	15 h 00 m
4. May 4, 1960	"	10 h 20 m

Fig. 4., The solar cosmic ray absorption spectrum during geomagnetic storms and Forbush-decreases.

1. May 12, 1960,	the start of the instrument	12 h 00 m
2. July 12, 1960	"	11 h 45 m
3. July 15, 1960	"	12 h 00 m

Fig.5. Solar proton energy integral spectra.

1. The averaged spectrum according to data of measurements in the absence of a magnetic storm and a Forbush-decrease. Transition from the absorption spectrum is made with only ionization losses taken into account.

2. The same as 1, but with the account of proton absorption and nuclear collisions in the atmosphere.

3. Obtained from curve 2 with an approximated account of proton diffusion time as a function of the velocity of protons.

- 46 -

4. The averaged spectrum according to the results of measurements during magnetic storms and Forbush-decreases.

Fig.6. Integral energy proton spectra according to the complex of the results of measurements in the stratosphere and near sea level.

I — the burst on May 4, 1960

II — the burst on November 15, 1960.

Fig.7. Proton intensity as a function of time according to the data in the stratosphere.

I — the burst on May 4, 1960.

II — the burst on September 3, 1960.

III — data near sea level basdd on the burst on February 23, 1956.

Fig.8. Primary proton intensity as a function of time. Solid lines show calculation as the diffusion coefficient $5.5 \cdot 10^{21} \text{ cm}^2 \text{ sec}^{-1}$ for $t_0 = 0, 0.2, 0.4$.

○ — data on the event on May 4, 1960.

□ — data on the event on September 3, 1960.

Fig.9. Mean monthly values of cosmic ray intensity in the stratosphere from July 1957 to July 1962.

Fig.10. Differences of mean monthly values of cosmic ray intensity.

I — the intensity difference at latitudes 64° and 41°

II — the intensity difference at latitudes 51° and 41°

Fig.11. X — mean monthly values of cosmic ray intensity at latitude 51° .

○ — mean monthly total sun-spots numbers R.

- 47 -

Fig.12. Periodograms according to results of measurements of cosmic ray intensity during the period from July 1, 1957, to February 1, 1958.

- 1 — for the stratosphere at latitude 51°
- 2 — for a neutron monitor at latitude 52°
- 3 — for the K-index.

Fig.13. The shape of the wave of 27-day intensity variations for the period from July 1, 1957, to February 1, 1958.

- 1 — for the stratosphere at latitude 51° .
- 2 — for a neutron monitor at latitude 54° .
- 3 — for an ionization chamber at latitude 51° .
- 4 — for a neutron monitor at latitude 26°
- 5 — for a neutron monitor at latitude 0° .

Fig.14. Cosmic ray intensity during Mars 1 probe flight depending on the distance from the Sun.

- 1 — according to a Geiger counter,
- 2 — ionization of the inner scintillation counter.
- 3 — according to the threshold 30 kev of the inner scintillation counter.

Fig.15. Counting rates of Geiger counters on Mars 1 probe in the stratosphere at latitude 64° (Murmansk) as a function of time.

Fig.16. Geiger counters* counting rate during Lunik 4 and balloon flights in the stratosphere at latitude 64° (Murmansk) for the period from April 1 to April 15, 1963.

- 48 -

Fig.17. Radiation intensity during Mars 1 probe flight through the Earth's radiation belts depending on the distance from the Earth's centre.

1 — energy release per second in the crystal of the outer scintillation counter.

2 — energy release per second in the crystal of the inner scintillation counter.

3 — counting rate of the outer scintillation counter.

4 — counting rate of the inner scintillation counter according to the threshold of 30 kev.

5 — counting rate of a Geiger counter.

6 — counting rate of the inner scintillation counter according to the threshold 2.5 Mev.

Fig.18. Energy release in crystals of inner scintillation counters for the Mars 1 probe and Lunik II as a function of L.

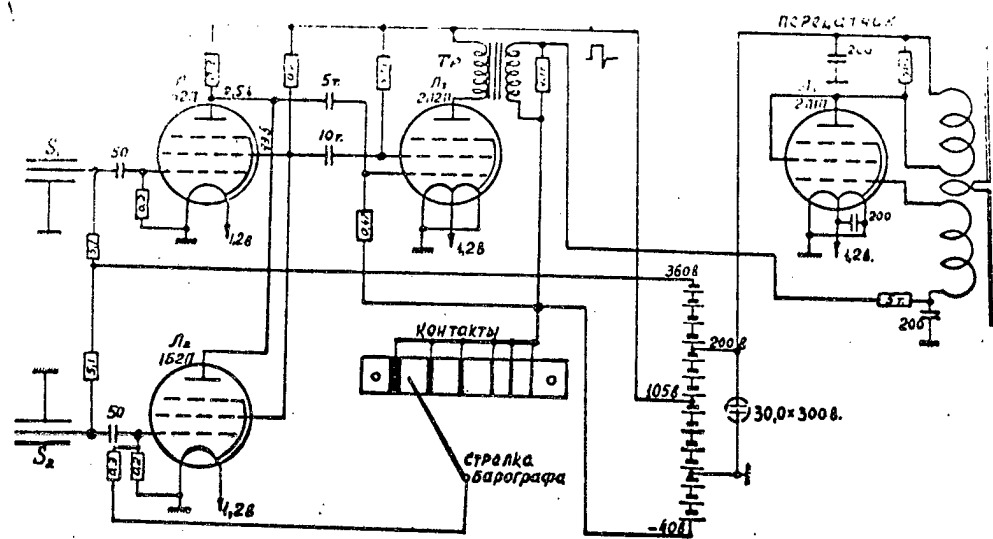


Fig. 1

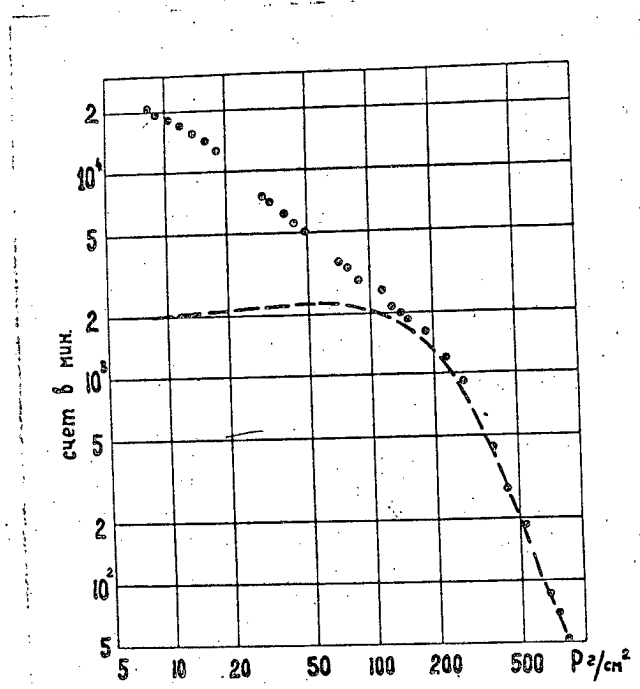


Fig. 2

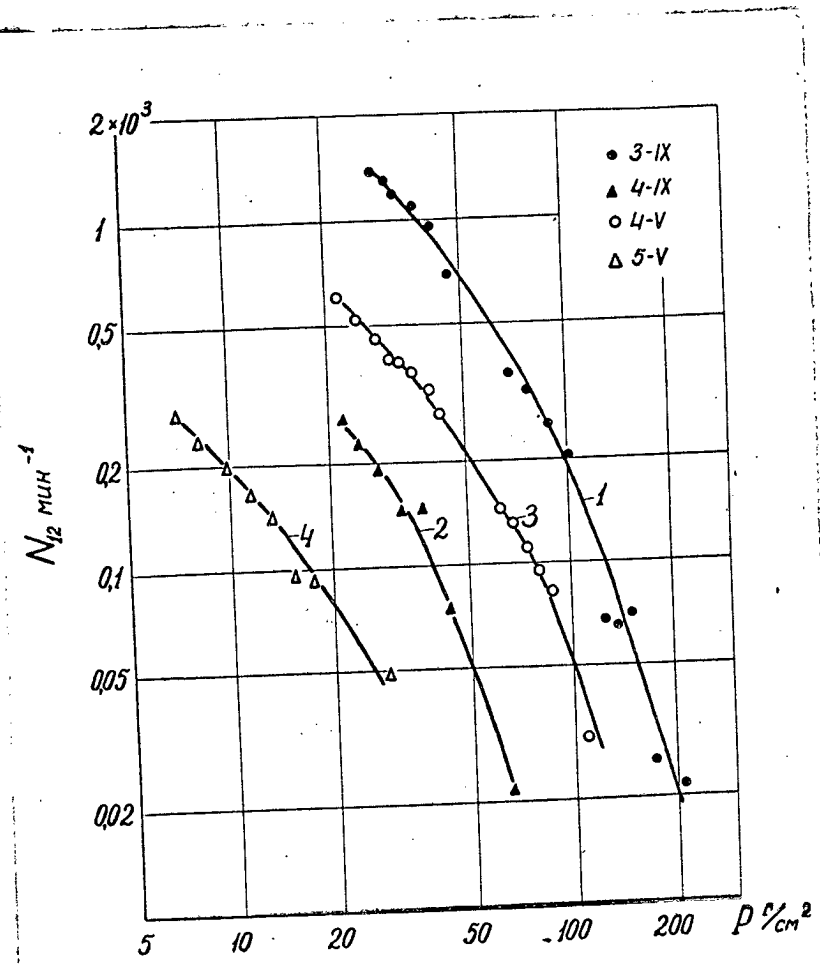


Fig. 3

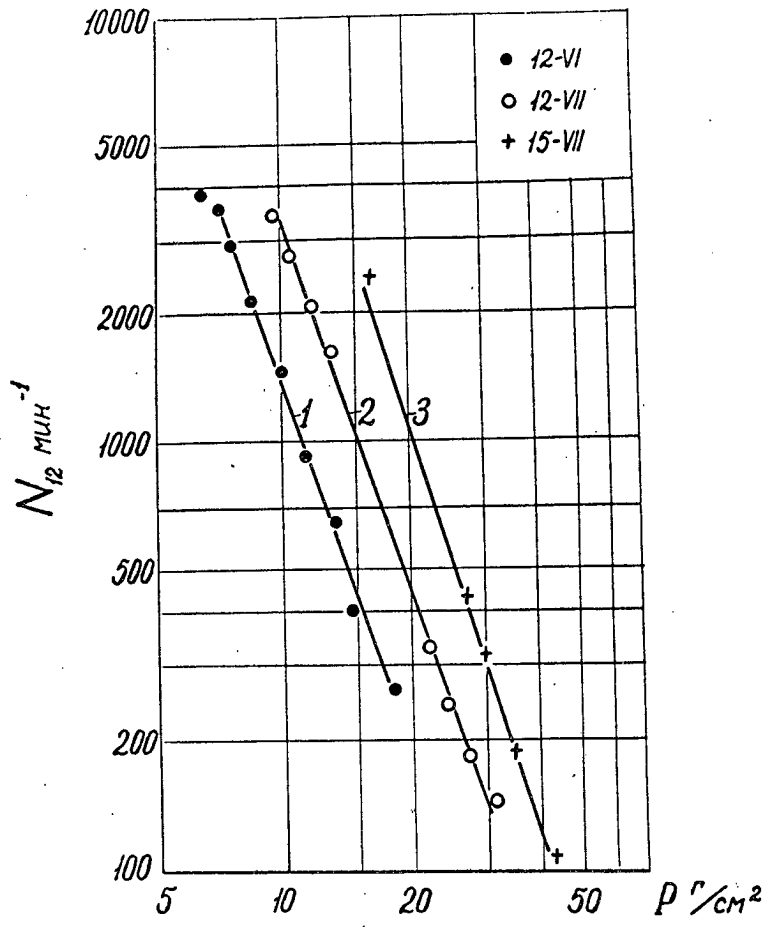


Fig. 4

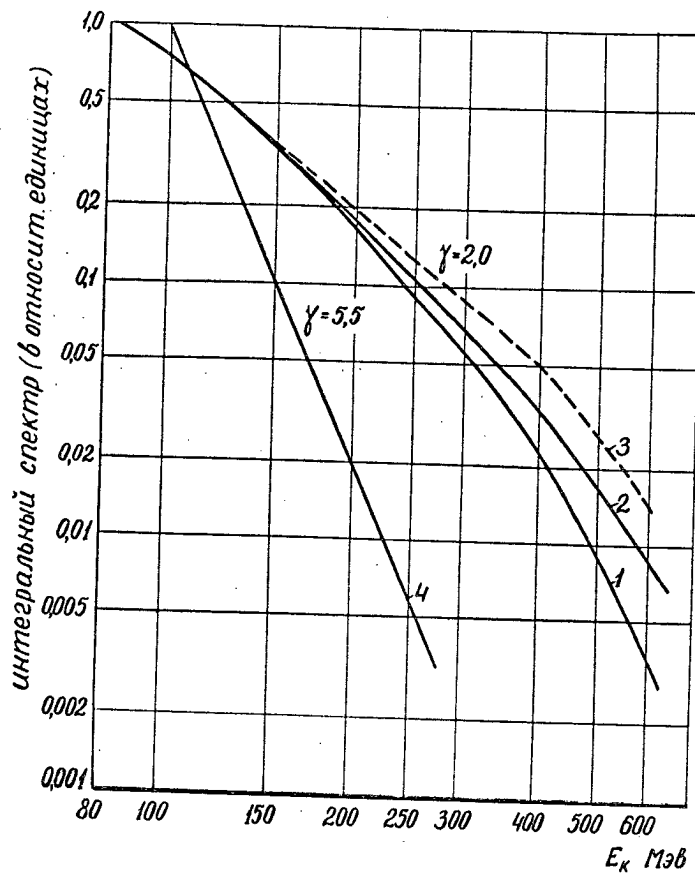


Fig. 5

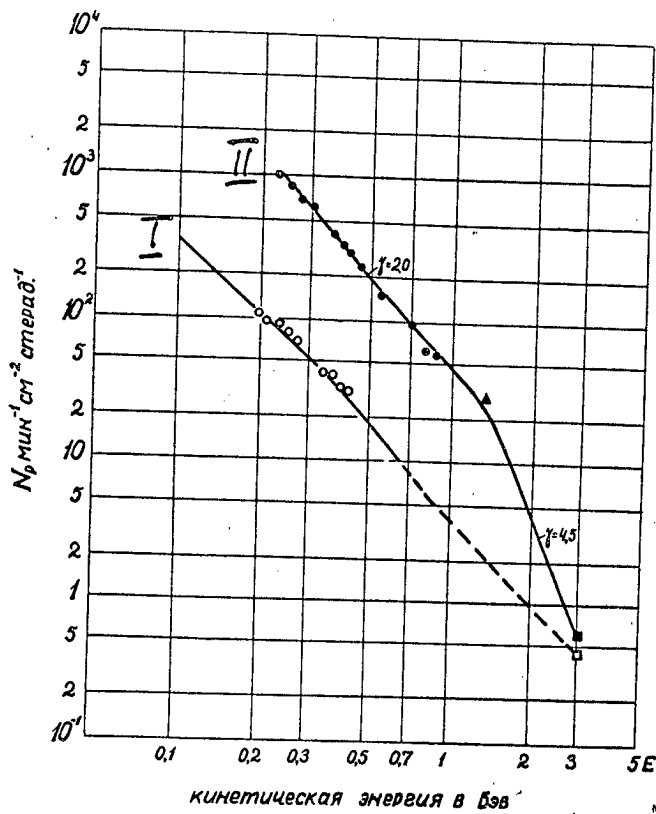


Fig- 6

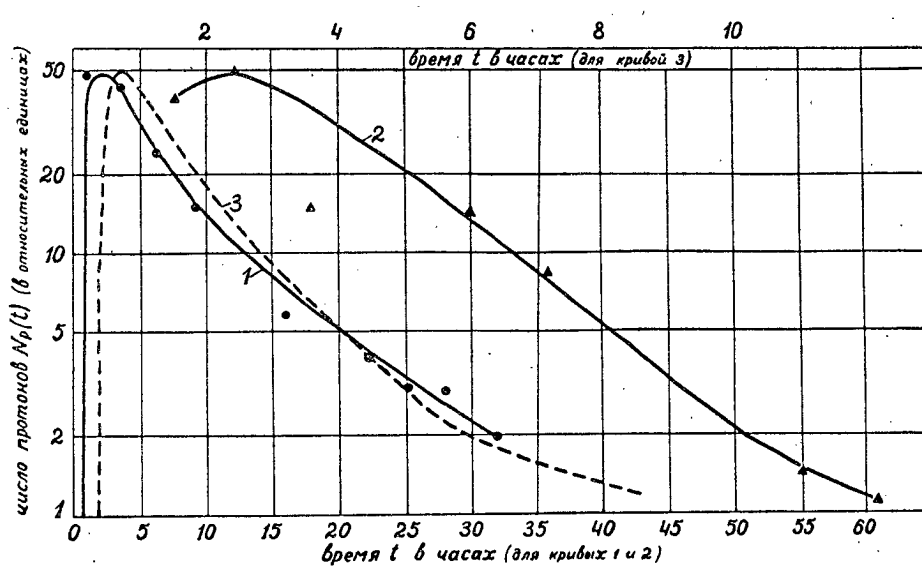


Fig. 7

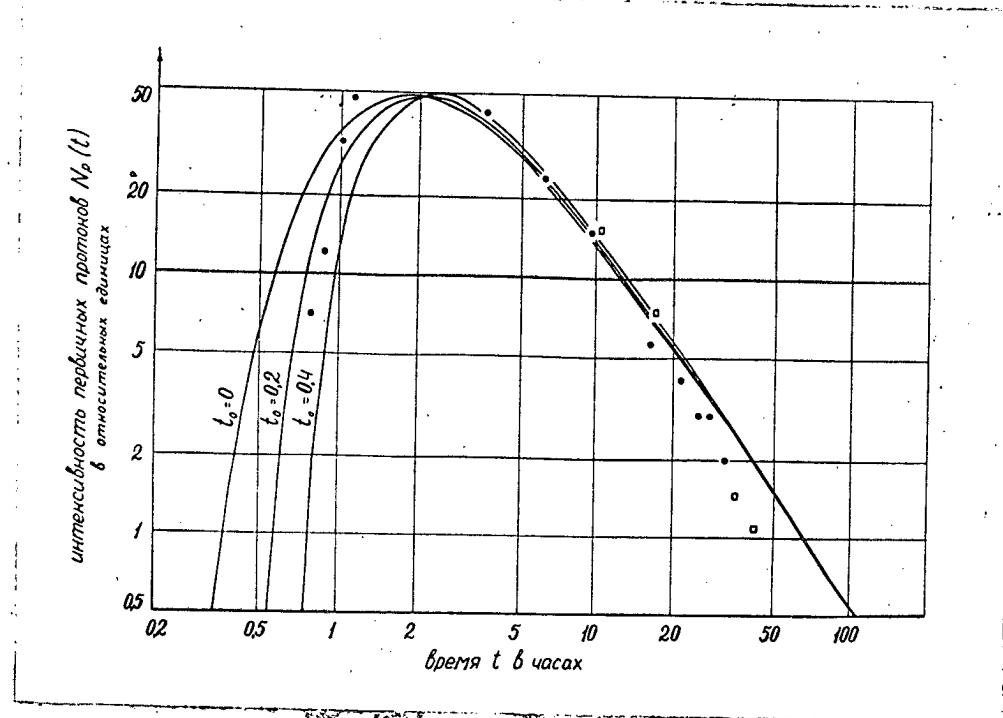


Fig. 8

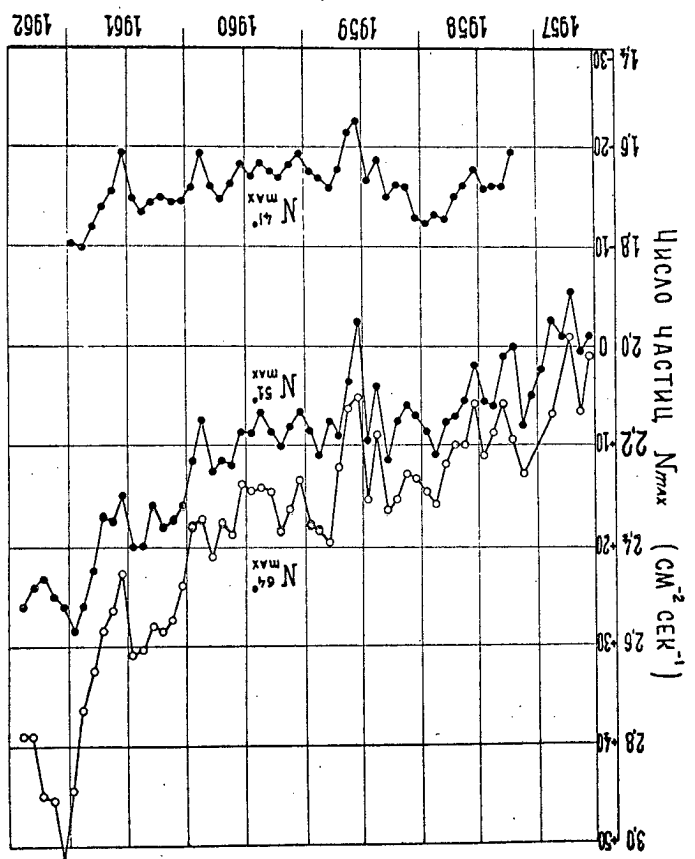


Fig. 9

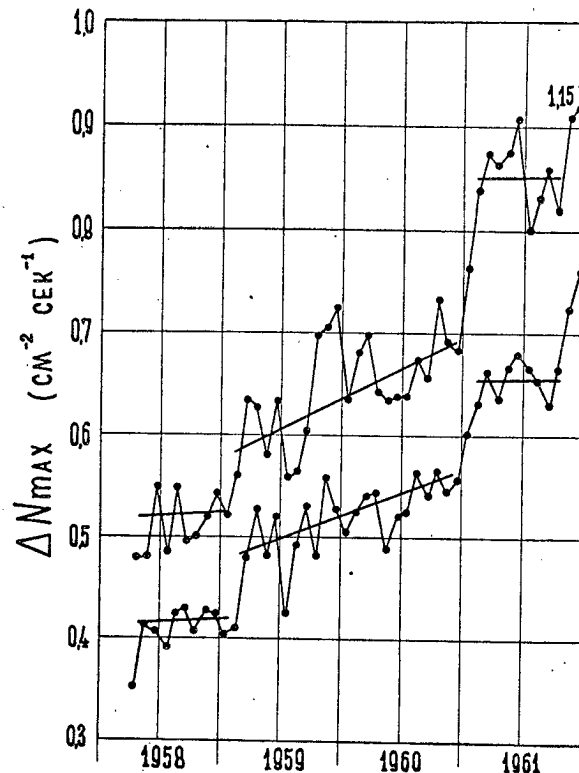


Fig. 10

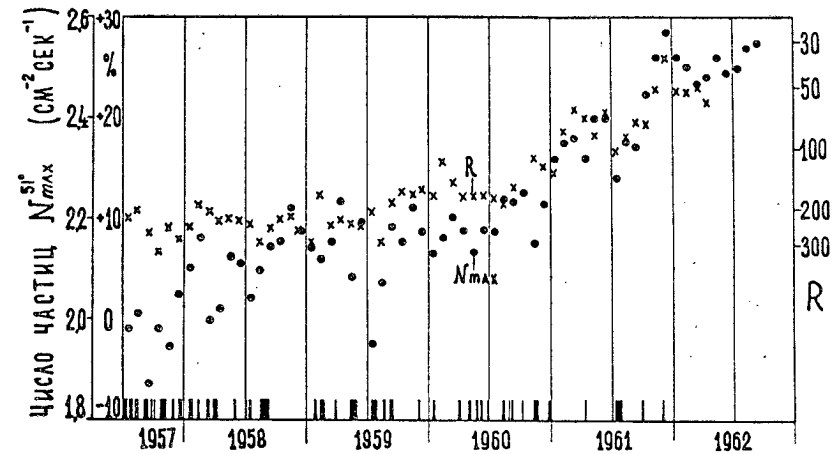


Fig. 11

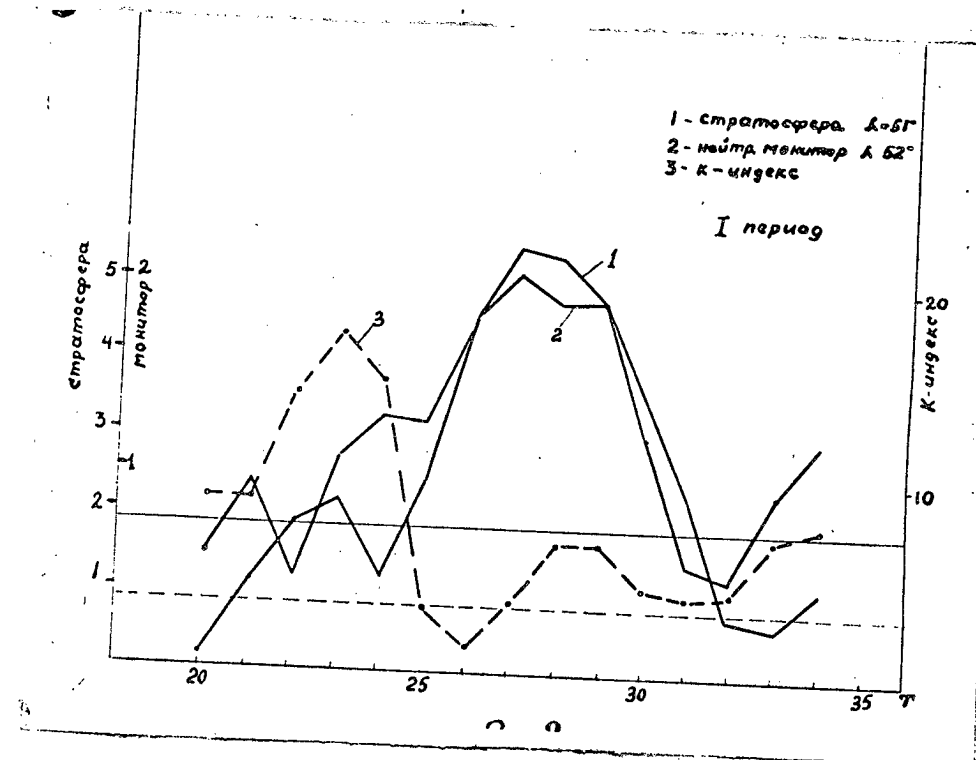


Fig. 12

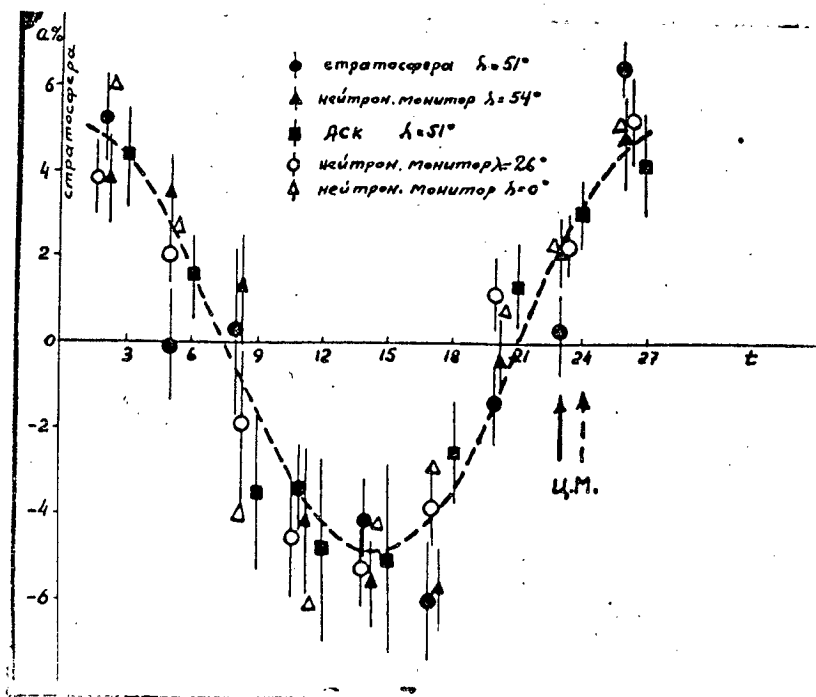
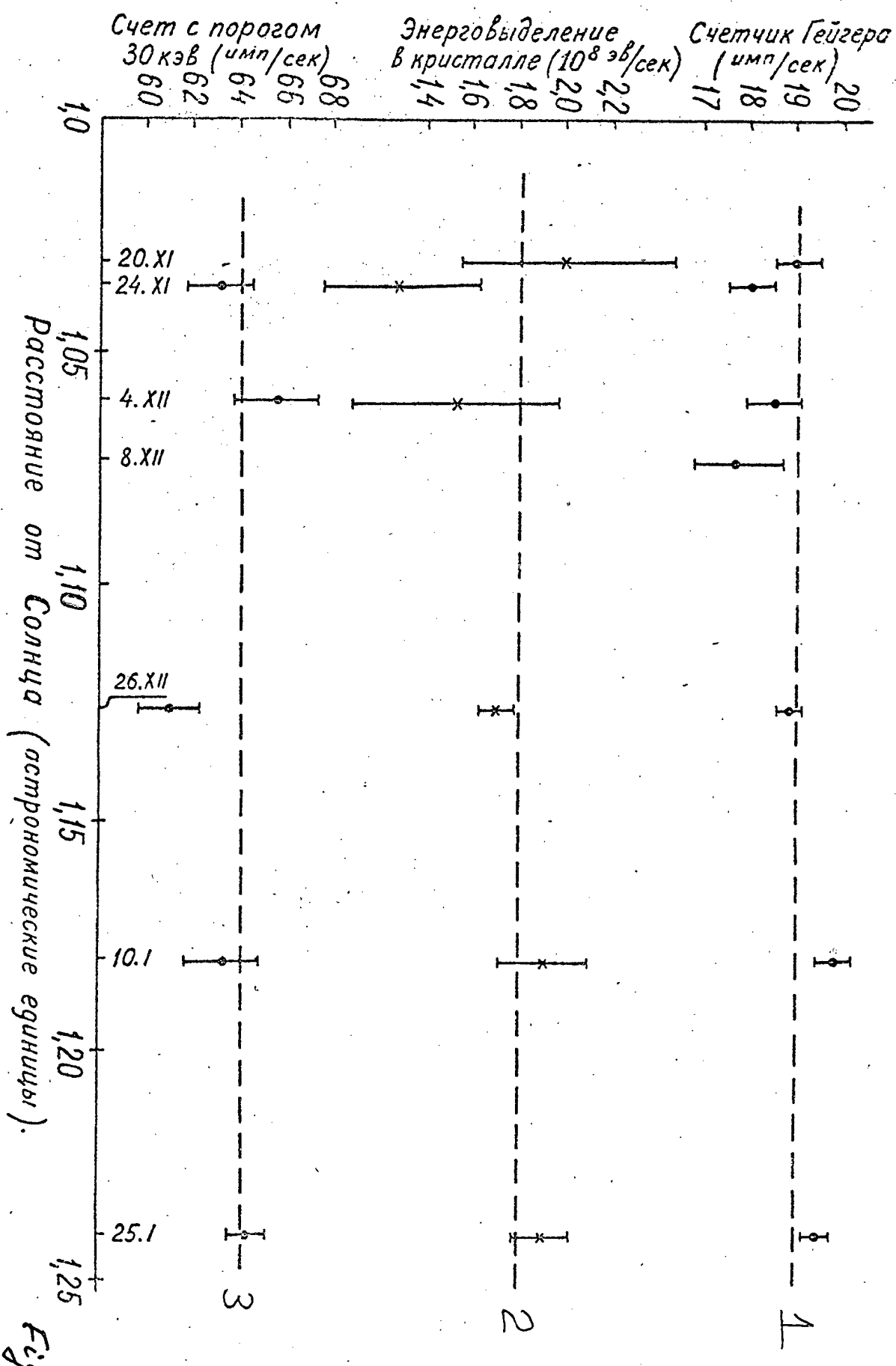


Fig. 13



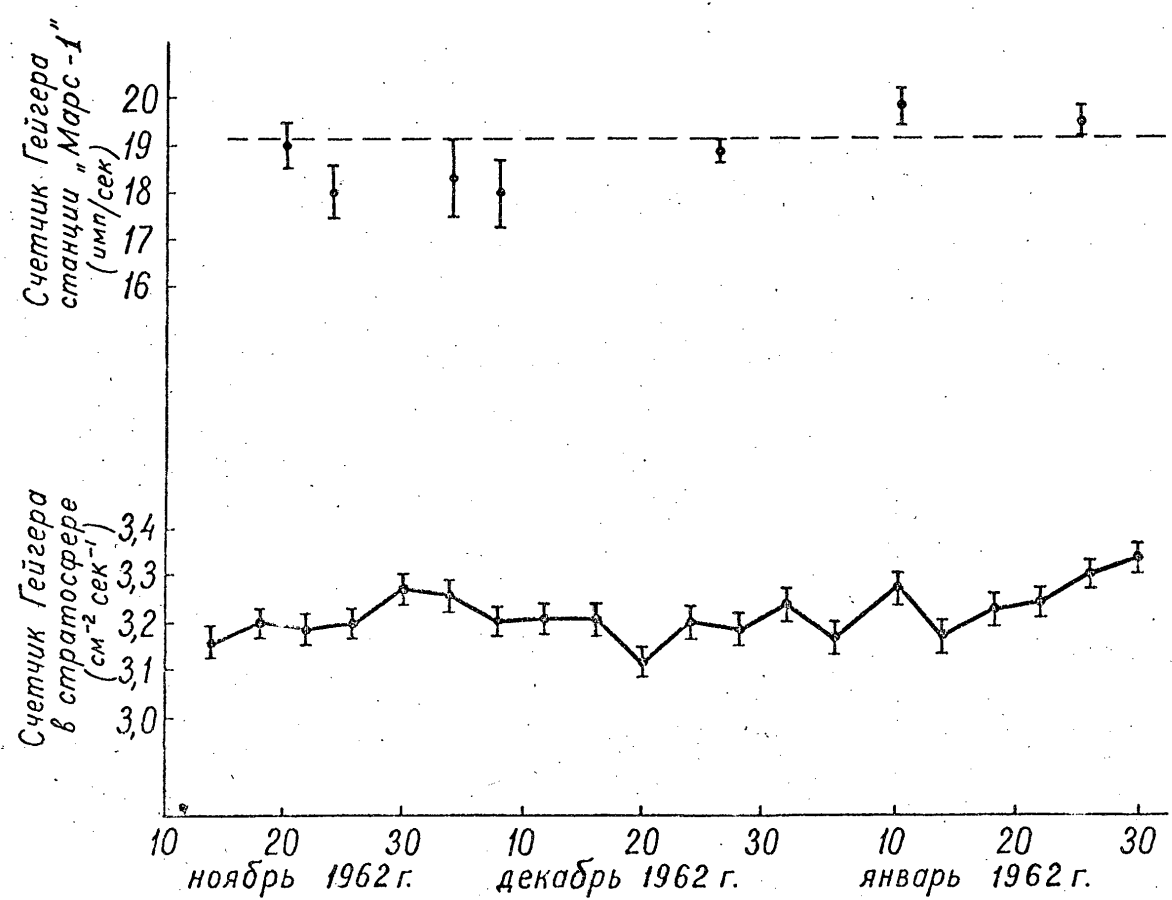


Fig. 15

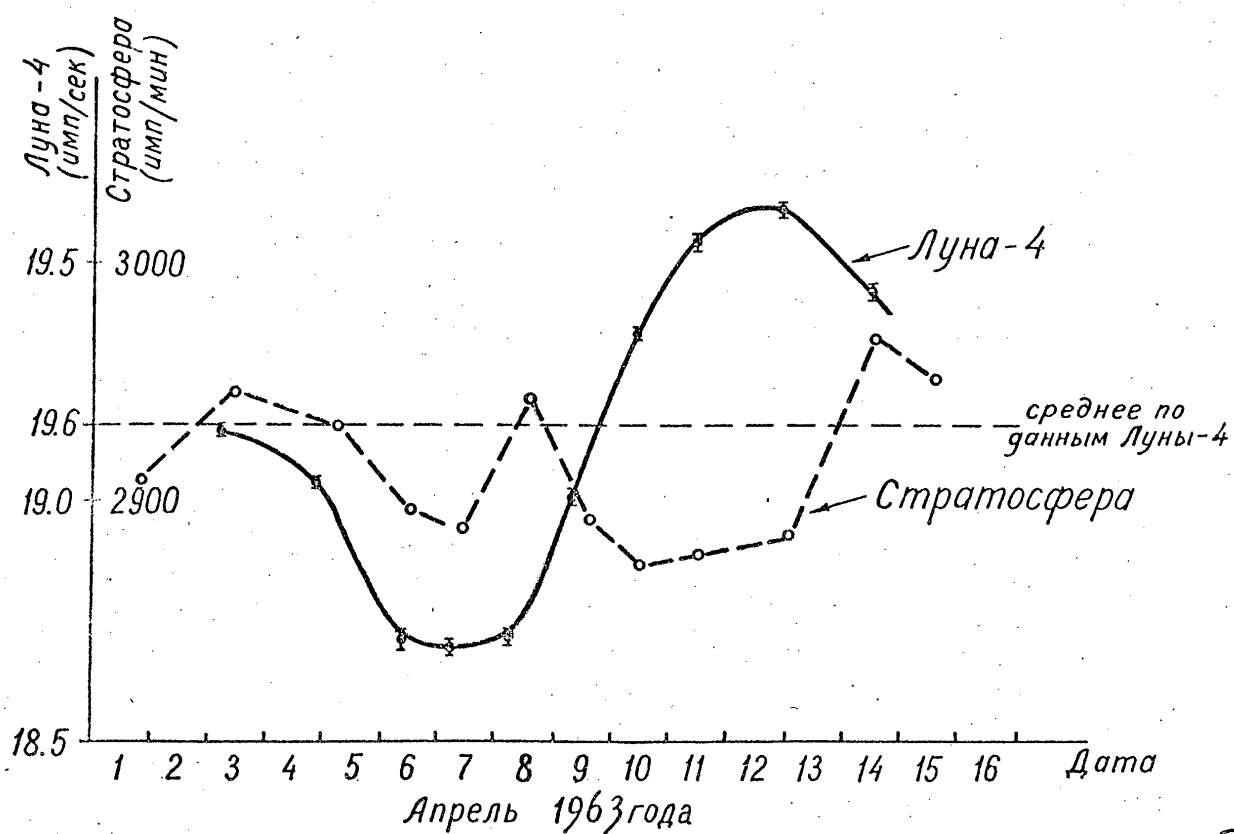


Fig. 16

Declassified in Part - Sanitized Copy Approved for Release 2012/12/13 : CIA-RDP80T00246A022400050001-7

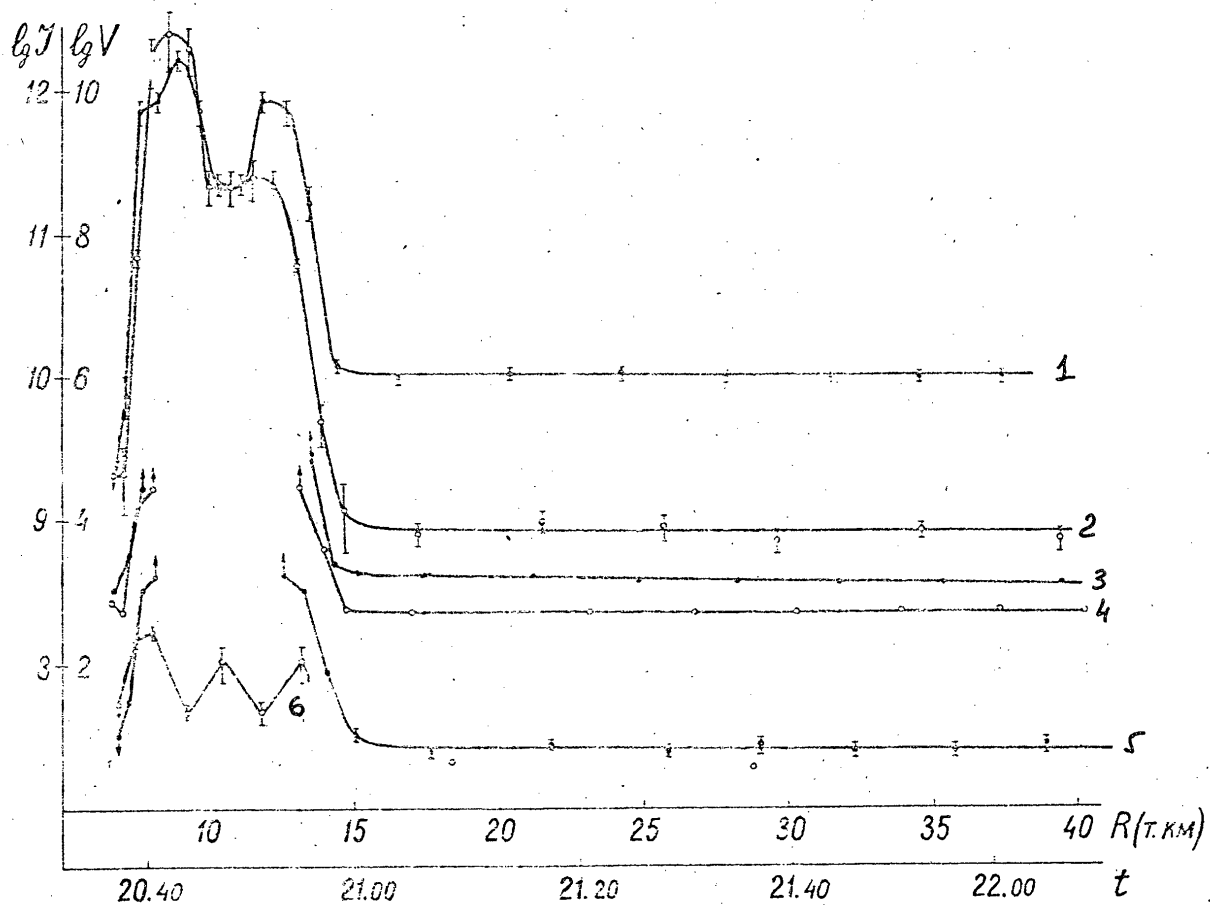


Fig. 17

Declassified in Part - Sanitized Copy Approved for Release 2012/12/13 : CIA-RDP80T00246A022400050001-7

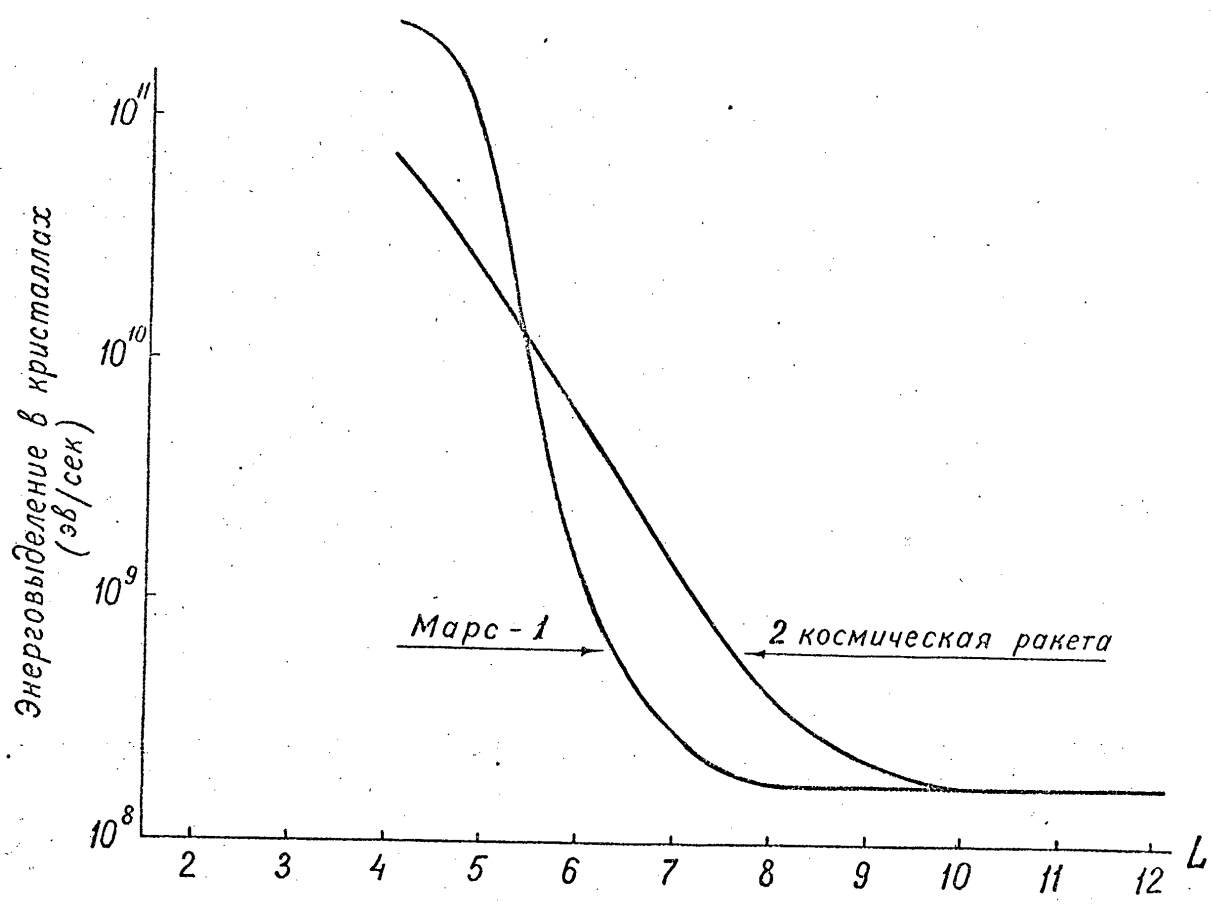


Fig. 18